

# Integrability and Chaotic Behavior in Mechanical Billiard Systems

Zur Erlangung des akademischen Grades eines

DOKTORS DER NATURWISSENSCHAFTEN

von der KIT-Fakultät für Mathematik des  
Karlsruher Instituts für Technologie (KIT)  
genehmigte

Dissertation

von

Airi Takeuchi

Tag der mündlichen Prüfung: 21.07.2022

Referent: Prof. Dr. Michael Plum  
Korreferent: Prof. Dr. Urs Frauenfelder





# Abstract

This thesis is devoted to the study of mathematical billiards in the presence of non-constant potentials and their integrability and chaotic behavior.

Classical examples of integrable billiards are free billiards in circles and ellipses. In the presence of specific potentials (such as Kepler potential and harmonic (Hooke) potential), there are various known integrable billiard systems. These integrable examples have been found independently in different contexts. In Chapter 2, we illustrate how some of these integrable billiard systems are related to each other by conformal transformations. As an application, we obtain infinitely many billiard systems defined in central force problems which are integrable on a particular energy level. We then explain that the classical Hooke-Kepler correspondence extends to the correspondence between integrable Hooke and Kepler billiards. As a result, we show that any focused conic sections give rise to integrable Kepler billiards which give new examples of integrable Kepler billiards. The conformal transformation technique is applied to Stark-type problems and Euler's two-center problem and provides new examples of integrable mechanical billiards.

In Chapter 3 we show that integrable Kepler and Hooke billiard systems on the plane have the corresponding integrable billiard systems on surfaces of constant curvatures. We also establish the integrability of a class of billiard systems defined in the Lagrangian problem, which is the superposition of two Kepler problems and a Hooke problem, on the sphere, in the plane, and in the hyperbolic plane. These results are obtained by the method of projective dynamics and projective billiards.

A toy model of billiard systems with a central force problem in the plane and with a line as the reflection wall was proposed by L. Boltzmann to illustrate his ergodic hypothesis. Later, it has been found that not all such systems are ergodic, and it becomes a question whether some of such systems are ergodic. In Chapter 4, we compute the billiard mappings of Boltzmann's billiard systems, and we present some numerical studies on their chaotic behavior and ergodicity. We found some numerical evidence suggesting that some of these systems might be ergodic.



# Acknowledgement

First of all, I would like to express my greatest gratitude to my doctoral supervisor, Prof. Dr. Michael Plum for accepting me as a Ph.D. student and for many discussions, guidance, trust, and encouragements. He always respects my interests and gives me opportunities to study various topics and to attend and organize mathematical activities.

I would also like to thank Prof. Dr. Urs Frauenfelder from the University of Augsburg for valuable suggestions on my research and for accepting to be a reviewer of this thesis.

I would like to acknowledge PD Dr. Lei Zhao from the University of Augsburg for the chance to work on projects which largely contribute to this thesis. He always takes time to address my questions and problems and gave me precise advices. I am also very excited to start working as a postdoc in Augsburg with him.

I would also like to acknowledge Dr. Kaori Nagato-Plum for supporting my doctoral life in all aspects and for always being helpful.

I am also grateful to Prof. Dr. Alain Albouy from Paris Observatory for his precise comments on my research.

I also thank the IANA group members: In particular, Julia, Fatima, Zihui, Kevin, Jonathan, Sebastian, Lukas, Elias, Simon, Björn, Xian for making my time in the office and at lunch more enjoyable, Marion for helping me with various things such as complicated paperworks, and Wolfgang for organizing group events such as Christmas party, hiking, and running.

I am also thankful to Masason foundation for financial support through years and for the opportunity to meet with experts in many fields.

And to my family in Japan, thank you so much for caring me far away from home. Your presence always gives me comfort and stability.

Finally, I would like to express my heartfelt thanks to my partner, Halil, who has supported my life in Germany from the beginning. Thank you for always offering me tea and snacks while I am doing math until midnight.



# Contents

<b>1</b>	<b>Introduction</b>	<b>11</b>
1.1	A bit of Mechanics . . . . .	11
1.1.1	Natural Mechanical Systems . . . . .	11
1.1.2	Hamiltonian Mechanics . . . . .	13
1.1.3	Integrable Mechanical Systems . . . . .	15
1.1.4	Examples of Integrable Mechanical Systems . . . . .	16
1.1.5	Solution Curves for Kepler Problem in the Plane . . . . .	19
1.1.6	Levi-Civita Regularization . . . . .	21
1.2	A bit of Billiards . . . . .	21
1.2.1	Law of Reflections . . . . .	22
1.2.2	Integrable Billiards . . . . .	22
1.2.3	Free Elliptic Billiards . . . . .	25
1.2.4	Chaotic Billiards . . . . .	27
1.3	Boltzmann's Billiards . . . . .	31
1.4	New Integrable Mechanical Billiards by Conformal Transformations . . . . .	32
1.5	Projective Integrable Mechanical Billiards . . . . .	33
1.6	Comparison of Projective and Conformal Approaches . . . . .	35
1.7	Further Questions . . . . .	35
1.8	Structure of this Thesis . . . . .	37
<b>2</b>	<b>Conformal Transformation on Integrable Mechanical Billiards (joint with L. Zhao)</b>	<b>39</b>
2.1	Preliminaries . . . . .	39
2.1.1	General Setting of Mechanical Billiard Systems . . . . .	39
2.1.2	Known Examples of Integrable Mechanical Billiard Systems . . . . .	41
2.1.3	Purpose of this Chapter . . . . .	42
2.2	Conformal Transformations and Mechanical Billiards . . . . .	43
2.2.1	Duality between Integrable Mechanical Billiards . . . . .	43
2.2.2	Mechanical Billiards from Free Billiards . . . . .	48

2.3	Hooke, Kepler Billiards and their Dualities . . . . .	53
2.3.1	Integrable Hooke Billiards . . . . .	53
2.3.2	Integrable Kepler Billiards . . . . .	57
2.3.3	From Hooke/Kepler Billiards to Free Billiards . . . . .	61
2.3.4	Conjectures related to the Birkhoff Conjecture . . . . .	62
2.4	Integrable Stark-type Billiards . . . . .	62
2.4.1	Separability and Integrability of Stark-type Billiards . . . . .	62
2.4.2	Examples of Stark-type Billiard Systems . . . . .	64
2.5	Integrable Mechanical Billiards of Two-center Problem . . . . .	65
2.A	Integrability of Conic Section Boundaries of Free Planar billiards . . . . .	70
2.B	Invariance of Transformed Jauchimsthal First Integral . . . . .	72
2.C	Invariance of Gallavotti-Jauslin's First Integral . . . . .	74
<b>3</b>	<b>Projective Integrable Mechanical Billiards (joint with L. Zhao)</b> . . . . .	<b>77</b>
3.1	Preliminaries . . . . .	77
3.2	Principles of Projective Dynamics . . . . .	80
3.3	Projective Properties of the Hooke, Kepler and Lagrange Problems . . . . .	81
3.3.1	The Hemisphere-Plane Projection . . . . .	82
3.3.2	Projective Properties of the Hooke and Kepler Problems . . . . .	83
3.3.3	The Lagrange Problems in the Plane and on the Sphere . . . . .	87
3.4	Integrable Lagrange Billiards . . . . .	91
3.4.1	Billiard Correspondence at Confocal Conic Sections . . . . .	91
3.4.2	Integrability of Lagrange Billiards with Confocal Conic Section Reflection Walls . . . . .	95
3.4.3	Subcases of Integrable Lagrange Billiards . . . . .	95
3.5	The Plane-Hyperboloid Projection and integrable Lagrange Billiards in the Hyperbolic Plane . . . . .	97
3.5.1	The Hyperboloid-Plane Projection . . . . .	97
3.5.2	Projective Properties of the Hooke and Kepler Problems in the Hyperbolic Plane . . . . .	98
3.5.3	The Lagrange Problems in the Plane and in the Hyperbolic Plane . . . . .	99
3.5.4	Integrable Lagrange Billiards in the Hyperbolic Plane . . . . .	100
3.5.5	Proof of Theorem 7 in the Hyperbolic Case and the Subcases . . . . .	100
3.6	The Complex Square Mapping and Hooke-Kepler Correspondence in the Hyperbolic Space and on the Sphere . . . . .	100

---

<b>4 Boltzmann's Billiard Systems</b>	<b>107</b>
4.1 New Canonical Coordinates for Central Force Problem . . . . .	107
4.2 Symplectic Property of the Billiard Mapping . . . . .	110
4.3 Computation of the Billiard Mapping . . . . .	112
4.3.1 Solutions for the Central Force Problem: Kepler Problem with Centrifugal Force . . . . .	112
4.3.2 Computation of General Boltzmann's Billiard Mapping	118
4.3.3 Solutions for the Central Force Problem: Cotes' Spiral Case . . . . .	120
4.3.4 Computation of the Billiard Mapping: Cotes' Spiral Case	121
4.4 Numerical Results of Boltzmann's Billiard Trajectories . . . . .	123
4.5 Koopman Operator and Eigenvalue Problem . . . . .	123
4.5.1 Approximation of Koopman Eigenvalue Problem with Galerkin Method . . . . .	126
4.5.2 Discussion on Ergodicity based on Numerical Results .	134



# Chapter 1

## Introduction

### 1.1 A bit of Mechanics

#### 1.1.1 Natural Mechanical Systems

A natural mechanical system  $(M, g, U)$  is defined on a  $N$ -dimensional Riemannian manifold  $(M, g)$  equipped with a smooth force function  $U : M \rightarrow \mathbb{R}$ . Such a system determines the motion of a particle on a manifold. The motion of the particle is governed by the second-order *Newton's equations*

$$\nabla_{\dot{q}}\dot{q} = \nabla_g U(q), \quad q \in M,$$

in which  $\nabla$  is the Levi-Civita connection associated to the Riemannian metric  $g$ . Recall that the Levi-Civita connection is a linear connection

$$\nabla : (X, Y) \mapsto \nabla_X Y$$

where  $X$  and  $Y$  are vector fields on  $M$ , which is torsion-free and preserves the Riemannian metric *i.e.*,

$$\nabla_X Y - \nabla_Y X = [X, Y]$$

and

$$Z(g(X, Y)) = g(\nabla_Z X, Y) + g(X, \nabla_Z Y)$$

for any vector fields  $X, Y, Z$  on  $M$ . When a force function  $U$  is constant, the particle on  $M$  moves freely. We call such cases free motion. When  $U$  is non-constant, natural mechanical systems show various different dynamical behavior depending on  $U$ .

The kinetic energy of the system is a real-valued function on  $TM$  defined as

$$K(q, v) = \frac{1}{2}g_q(v, v),$$

where  $(q, v) \in TM$ . The total energy of the particle located at  $q \in M$  with the velocity  $v$  is given by the combination of the kinetic energy  $K$  and the potential  $V := -U$  i.e.,

$$E = K + V = \frac{1}{2}g(v, v) - U(q), \quad q \in M, \quad v \in T_qM.$$

The energy  $E$  is preserved along the trajectories of the particle on  $M$ . Indeed, one can see from the Newton's equations that

$$\frac{dE}{dt} = \mathcal{L}_{\dot{q}}E = \mathcal{L}_{\dot{q}} \left( \frac{1}{2}g_q(\dot{q}, \dot{q}) - U(q) \right) = g_q(\nabla_{\dot{q}}\dot{q}, \dot{q}) - dU(\dot{q}) = 0.$$

The Lagrangian of a system  $(M, g, U)$  is defined as

$$L := K - V = \frac{1}{2}g_q(v, v) + U(q)$$

and using the Lagrangian, the Newton's equations are transformed into a new form:

$$\frac{d}{dt} \left( \frac{\partial L}{\partial v_i} \right) - \frac{\partial L}{\partial q_i} = 0.$$

which are called the *Euler-Lagrange equations* of the system.

**Remark 1.** For a natural mechanical system with a force function  $U$  on the Euclidean space  $\mathbb{R}^N$  with the standard flat, Euclidean metric. The Newton's equation is nothing else than

$$\ddot{q} = \nabla U(q),$$

where  $\ddot{q}$  is the second time derivative of  $q(t)$ . The corresponding kinetic energy is given by

$$K := \frac{\|\dot{q}\|^2}{2},$$

where  $\|\cdot\|$  is the standard Euclidean norm, thus the total energy is obtained as

$$E = K + V = \frac{\|\dot{q}\|^2}{2} - U(q).$$

In most of our applications, the configuration space is (an open subset of)  $\mathbb{R}^2$  equipped with the standard flat metric. Physically, this models motions of a particle moving in the plane.

### 1.1.2 Hamiltonian Mechanics

We now introduce the coordinates  $(p, q)$ , where  $q = (q_1, \dots, q_N)$  is a base point in  $M$  and  $p = (p_1, \dots, p_N)$  is a generalized momentum which is defined via the Lagrangian  $L$  as

$$p_i := \frac{\partial L}{\partial \dot{q}_i}$$

and is a cotangent vector. We will now describe systems in these coordinates  $(p, q)$  and express them in the Hamiltonian formalism.

In the Hamiltonian formalism, the system is naturally expressed in the language of symplectic geometry. A symplectic manifold is a pair of a smooth manifold  $M$  and a closed and non-degenerate differential 2-form  $\omega$  on  $M$  *i.e.* for  $X \in T_q M$  if  $\omega(X, Y) = 0$  for all  $Y \in T_q M$  then  $X = 0$ . From this condition on  $\omega$ , a symplectic manifold  $(M, \omega)$  is necessarily even-dimensional. As a phase space, we consider a cotangent bundle of  $M$  which is a union of cotangent spaces  $\bigcup_{q \in M} T_q^* M$ . When  $M$  is a smooth  $N$ -dimensional manifold, its cotangent bundle  $T^*M$  is a smooth  $2N$ -dimensional manifold. Additionally, the cotangent bundle  $T^*M$  has the natural symplectic structure which is given in the local coordinates  $(p, q)$  as

$$\omega = dp \wedge dq = \sum_{i=1}^N dp_i \wedge dq_i.$$

Let  $H$  be a smooth function on  $T^*M$ , and there is a vector field  $X_H$  satisfying  $\omega(X_H, \cdot) = dH(\cdot)$ . We call such a vector field  $X_H$  the Hamiltonian vector field. Assume that the vector field  $X_H$  gives a 1-parameter group of diffeomorphism  $\gamma^t : T^*M \rightarrow T^*M$  such that

$$\left. \frac{d}{dt} \right|_{t=0} \gamma^t = X_H.$$

We call such a group  $\gamma^t$  the Hamiltonian phase flow. The following theorem says that a Hamiltonian flow  $\gamma^t$  preserves the symplectic structure:

**Theorem.** *Let  $\gamma_t$  be a Hamiltonian flow on  $(T^*M, \omega)$ , then*

$$(\gamma^t)^* \omega = \omega.$$

For the proof, see [3, Chapter 8] for example. In the case of  $M = \mathbb{R}$  thus  $T^*M = \mathbb{R}^2$ , this theorem equivalently says that a Hamiltonian flow preserves area and is commonly referred to as *Liouville's theorem*.

The Poisson bracket  $\{F, G\}$  of smooth functions  $F, G$  on  $T^*M$  is defined as the derivative of the function  $F$  in the direction of the phase flow with the Hamiltonian function  $G$ :

$$\{F, G\} = \left. \frac{d}{dt} \right|_{t=0} F(\gamma_G^t) = \omega(X_F, X_G).$$

The Poisson bracket has the following properties:

- (skew-symmetry)  $\{F, G\} = -\{G, F\}$
- (bilinearity)  $\{aF + bG, H\} = a\{F, H\} + b\{G, H\}$ ,  
 $\{F, aG + bH\} = a\{F, G\} + b\{F, H\}$ ,  $a, b \in \mathbb{R}$
- (Leibniz rule)  $\{FG, H\} = \{F, H\}G + F\{G, H\}$
- (Jacobi identity)  $\{F, \{G, H\}\} + \{G, \{H, F\}\} + \{H, \{F, G\}\} = 0$ .

These properties directly follow from the definition. See for example [12] for the proof.

**Remark 2.** When the phase space is a  $2N$ -dimensional Euclidean space  $\mathbb{R}^{2N}$  with the standard symplectic form  $\omega = \sum_{i=1}^N dp_i \wedge dq_i$ . The Hamiltonian vector field associated to a Hamiltonian function  $H$  is given by

$$X_H = \sum_{i=1}^N \left( \frac{\partial H}{\partial p_i} \frac{\partial}{\partial q_i} - \frac{\partial H}{\partial q_i} \frac{\partial}{\partial p_i} \right)$$

whose phase flow  $\gamma^t = (p(t), q(t))$  is governed by the equations

$$\dot{q} = \frac{\partial H}{\partial p}, \quad \dot{p} = -\frac{\partial H}{\partial q},$$

which are called Hamilton's equations. A Poisson bracket has the following form:

$$\{F, G\} = \sum_{k=1}^N \left( \frac{\partial F}{\partial q_k} \frac{\partial G}{\partial p_k} - \frac{\partial F}{\partial p_k} \frac{\partial G}{\partial q_k} \right).$$

Using this, Hamilton's equations can be rewritten into

$$\dot{q} = \{q, H\}, \quad \dot{p} = \{p, H\}.$$

More generally, the time derivative of a function  $F \in C^\infty(T^*M)$  is given by  $\{F, H\}$ , since

$$\frac{dF(p(t), q(t))}{dt} = \sum_{k=1}^N \left( \frac{\partial F}{\partial q_k} \frac{\partial q_k}{\partial t} + \frac{\partial F}{\partial p_k} \frac{\partial p_k}{\partial t} \right) = \sum_{k=1}^N \left( \frac{\partial F}{\partial q_k} \frac{\partial H}{\partial p_k} - \frac{\partial F}{\partial p_k} \frac{\partial H}{\partial q_k} \right) = \{F, H\}.$$

### 1.1.3 Integrable Mechanical Systems

For natural mechanical systems  $(M, g, U)$ , we call the function which gives the total energy the Hamiltonian  $H$  and is represented as follows:

$$H = \frac{1}{2}g_q^*(p, p) - U(q), \quad (p, q) \in T^*M,$$

where  $g_q^*$  is the co-metric on the cotangent space  $T_q^*M$  induced from the metric  $g$  on  $M$ .

**Remark 3.** For a natural mechanical system with the force function  $U$  on the Euclidean space  $\mathbb{R}^N$  with the standard Euclidean metric, its Hamiltonian is simply given by

$$H = \frac{\|p\|^2}{2} - U(q),$$

where  $\|\cdot\|$  is the standard Euclidean norm.

A function  $F$  on  $T^*M$  is a constant along the Hamiltonian phase flow  $\gamma_H^t$  if and only if the Poisson bracket  $\{H, F\} = 0$ . We call such functions first integrals of the system.

**Definition 1.** When  $M$  has dimension  $N$ , an natural mechanical system  $(M, g, U)$  is integrable if there exist  $N$  first integrals  $\{F_i\}_{i=1}^N$  including its own energy  $H$ , which are mutually functional independent and in involution i.e.

$$\{F_i, F_j\} = 0$$

for  $1 \leq i, j \leq N$ .

The following theorem on integrable mechanical systems plays an important role in perturbation theory.

**Theorem** (Liouville-Arnold theorem). Let  $(M, g, U)$  be  $N$ -dimensional integrable natural mechanical system and let  $F_1, \dots, F_N$  be its  $N$ -independent first integrals in involution. Set a level set of functions

$$M_f := \{(p, q) \mid F_i = f_i, i = 1, \dots, N\},$$

for  $f := (f_1, \dots, f_N) \in \mathbb{R}^N$ . If  $M_f$  is compact and connected, then

- $M_f$  is diffeomorphic to an  $N$ -dimensional torus.
- There exists angular coordinates  $\phi = (\phi_1, \phi_2, \dots, \phi_N)$  such that along the Hamiltonian flow

$$\frac{d\phi}{dt} = c,$$

where  $c = (c_1, c_2, \dots, c_N) \in \mathbb{R}^N$ .

- *There exist  $N$  functions of  $F_1, \dots, F_N$  denoted by  $I = (I_1, \dots, I_N)$  and called action coordinates, such that the variables  $(I, \phi)$  are symplectic coordinates.*

The proof of this theorem can be found in [3]. This theorem says that there exists canonical transformation to action-angle coordinates in which the transformed Hamiltonian is dependent only on the action coordinates being first integrals, and the angle coordinates evolve linearly in time. These coordinates are useful when we describe perturbed integrable systems. Namely, the *Kolmogorov-Arnold-Moser (KAM) theorem* states that when the integrable system is subjected to a small perturbation, some invariant tori are deformed and remain to be invariant under some condition. There exist many excellent tutorials on KAM theory, see for example, [44], [18], [13].

### 1.1.4 Examples of Integrable Mechanical Systems

We here introduce important examples of integrable mechanical systems.

Any one-dimensional natural mechanical system is integrable since its energy is a first integral.

Any central force problem in the two-dimensional plane with the Euclidean metric  $(\mathbb{R}^2, g_{flat})$  is integrable since its angular momentum  $C := q_1 p_2 - q_2 p_1$  which is clearly independent of the energy is preserved along the trajectories. Indeed, it is straightforward to see that

$$\begin{aligned}
 \{C, H\} &= \{C, K + V\} \\
 &= \{C, K\} - \{C, U\} \\
 &= \frac{\partial C}{\partial q_1} \frac{\partial K}{\partial p_1} + \frac{\partial C}{\partial q_2} \frac{\partial K}{\partial p_2} + \frac{\partial C}{\partial p_1} \frac{\partial U}{\partial q_1} + \frac{\partial C}{\partial p_2} \frac{\partial U}{\partial q_2} \\
 &= p_1 p_2 - p_2 p_1 + q_1 \frac{\partial U}{\partial q_2} - q_2 \frac{\partial U}{\partial q_1} \\
 &= 0.
 \end{aligned}$$

The last equation follows from the fact that  $U$  is a function of  $|q| = \sqrt{q_1^2 + q_2^2}$  only.

**Hooke problem** The two-dimensional central force problem  $(\mathbb{R}^2, g_{flat}, f r^2)$ , where  $r$  is the distance of the particle from the center  $O \in \mathbb{R}^2$  and  $f \in \mathbb{R}$  is a mass-factor, is called the Hooke problem. If the sign of  $f$  is positive, then the force is repulsive, and all orbits form branches of hyperbolae with their centers at  $O$ . On the other hand, if the sign of  $f$  is negative, the force is attractive, and all orbits form ellipses with their centers at  $O$ . In such

attractive cases, the potential  $-fr^2$  is referred to as harmonic potential, and the corresponding system is called harmonic oscillator. We allow both attractive and repulsive cases and call the corresponding both systems Hooke problems. The Hamiltonian of the Hooke problem is given by

$$H = \frac{p_x^2 + p_y^2}{2} + f(x^2 + y^2)$$

and is clearly separable into  $x$ -component  $H_x = p_x^2/2 + fx^2$  and  $y$ -component  $H_y = p_y^2/2 + fy^2$ . The integrability immediately follows from  $\dot{H}_x = \{H_x, H\} = 0$  and  $\dot{H}_y = \{H_y, H\} = 0$ . In any dimensional Euclidean space, the Hooke problem  $H = \sum \frac{p_i^2}{2} + f_i q_i^2$  is integrable since the functions  $F_i = \frac{p_i^2}{2} + f_i q_i^2$  are independent first integrals and satisfy  $\{F_i, F_j\} = 0$ .

The Hooke problem is important in applications because many physical situations in which a particle moves near an equilibrium point can be approximated by Hooke problems.

**Kepler problem** Our second example of two-dimensional central force problems is the Kepler-Coulomb problem given by  $(\mathbb{R}^2, g_{flat}, m/r)$ , where  $r$  is the distance of the particle from the center  $O \in \mathbb{R}^2$  and  $m \in \mathbb{R}$  is a mass-factor. If the sign of  $m$  is positive, then the force is attractive, and the orbits are either ellipses, parabolae, or branches of hyperbolae with the focus at the center  $O$ . On the other hand, if the sign of  $m$  is negative, the force is repulsive, and all orbits are branches of hyperbolae with the other focus at the center. As for the Hooke case, we allow both signs. Usually, the Kepler problem refers to the attracting case, and the Coulomb problem refers to the repulsive case. For simplicity, we call both cases Kepler problems in this thesis.

Besides the angular momentum and the total energy, the Kepler problem also preserves the *Laplace-Runge-Lenz vector*

$$A = \mathbf{p} \times \mathbf{L} - m \frac{\mathbf{r}}{r},$$

where  $\mathbf{r}$  and  $\mathbf{p}$  are the position vector and the momentum vector, respectively, and  $\mathbf{L}$  is the angular momentum vector  $\mathbf{r} \times \mathbf{p}$ .

The Kepler problem is a very important problem in celestial mechanics because the two-body problem under their mutual gravitational attraction can be reduced to the Kepler problem. This means that using the solutions of the Kepler problem, the two-body problem is also solved. The Kepler problem also represents the motion of two electrically charged particles since Coulomb's law also obeys an inverse-square law. We compute and illustrate possible orbits of the Kepler problem in the next subsection.

**Euler's two-center problem** We consider a particle moving around the two fixed Kepler centers in a plane. This system represents the motion of a planet in a solar system containing two suns at fixed centers. Suppose that two fixed centers are placed at  $Z_1$  and  $Z_2$  in the plane, then the corresponding two-center problem is defined as

$$\left( \mathbb{R}^2, g_{flat}, \frac{m_1}{|q - Z_1|} + \frac{m_2}{|q - Z_2|} \right),$$

with mass-factors  $m_1, m_2 \in \mathbb{R}$ . This system was first studied by Euler and has been shown to be integrable in [16]. Later Jacobi showed the separation of its Hamilton-Jacobi equation with elliptic coordinates [28]. This method of separation is customarily used to show the integrability of this system [57]. In 2008, Mathúna gave closed-form solutions for Euler's two-center problem in [39].

**Stark problem** We consider a system in the plane given in the form of

$$\left( \mathbb{R}^2, g_{flat}, \frac{s}{|q|} + gq_1 \right),$$

where  $s, g \in \mathbb{R}$ , so that the Kepler problem is further modified by the additional influence from  $gq_1$ . Such a system is called the *Stark problem* and physically describes the motion of an electron in the field of a proton and a constant electric field in the  $q_1$ -direction.

This system is integrable since it is separable in parabolic coordinates as explained in [35, Section 48]. This separability is represented in Section 2.4 by using the complex squared mapping for the more general class of systems which is called *Stark-type problems* given in the form of

$$\left( \mathbb{R}^2, g_{flat}, \frac{s}{|q|} + V(q) \right), \quad V \in C^\infty(\mathbb{R}^2, \mathbb{R}).$$

See also [10] for examples of the Stark-type problems and their integrability results.

**Lagrange problem** A natural mechanical system defined as the superposition of two Kepler problems and one Hooke problem with the Hooke center placed in the middle of Kepler centers was first considered by Lagrange [34]. We call such a system

$$\left( \mathbb{R}^2, g_{flat}, \frac{m_1}{|q - Z_1|} + \frac{m_2}{|q - Z_2|} + f \left| q - \frac{Z_1 + Z_2}{2} \right|^2 \right),$$

where  $Z_1, Z_2 \in \mathbb{R}^2$ , the *Lagrange problem*. The integrability for this system has been established by Albouy in [1] using projective dynamics. The projective dynamical approach with its extension to billiard systems is explained in Chapter 3. See also Theorem 8 and its proof.

### 1.1.5 Solution Curves for Kepler Problem in the Plane

We here compute solution curves for the Kepler problem in the plane. We start with the central force problem with a force function  $U(r)$  in polar coordinates  $(r, \phi)$  in the plane. The angular momentum which is given by

$$C = r^2 \dot{\phi} \quad (1.1)$$

is the conserved quantity when the force is central. The Newton's equations can be written in terms of polar coordinates as

$$\ddot{r} - r\dot{\phi}^2 = F_r \quad (1.2)$$

$$r\ddot{\phi} + 2\dot{r}\dot{\phi} = F_\phi, \quad (1.3)$$

where  $F_r$  and  $F_\phi$  are the  $r$ - and  $\theta$ -component of the force, respectively. When the force is central,  $F_\phi$  is identical to zero and the second equation implies the conservation of the angular momentum. Indeed, in such cases one can see that

$$\dot{C} = r(r\ddot{\phi} + 2\dot{r}\dot{\phi}) = 0.$$

Using this, we can eliminate  $\dot{\phi}$  from the equation (1.2) and get

$$\ddot{r} = F_r + \frac{C^2}{r^3}.$$

Again, from the conservation of  $C$ , we have

$$\frac{d}{dt} = \frac{d\phi}{dt} \frac{d}{d\phi} = \frac{C}{r^2} \frac{d}{d\phi}.$$

Thus we get the first time derivative of  $r$  in the following form:

$$\dot{r} = \frac{C}{r^2} \frac{dr}{d\phi}.$$

Also, we get the second time derivative of  $r$  represented as

$$\ddot{r} = \frac{C^2}{r^2} \frac{d}{d\phi} \left( \frac{1}{r^2} \frac{dr}{d\phi} \right) \quad (1.4)$$

Set the new variable  $\rho = \frac{1}{r}$ , then we have

$$\frac{dr}{d\phi} = \frac{dr}{d\rho} \frac{d\rho}{d\phi} = -\frac{1}{\rho^2} \frac{d\rho}{d\phi}.$$

Using this, the equation (1.4) can be rewritten into

$$\ddot{r} = -C^2 \rho^2 \frac{d^2 \rho}{d\phi^2}.$$

By combining with the equation (1.2), we get

$$-C^2 \rho^2 \frac{d^2 \rho}{d\phi^2} - C^2 \rho^3 = F_r.$$

We now restrict the system to be the Kepler problem,  $F_r = -m/r^2 = -m\rho^2$ . In such cases, after dividing the above equation by  $-C^2 \rho^2$  we obtain

$$\frac{d^2 \rho}{d\phi^2} + \rho = \frac{m}{C^2}.$$

We can solve this differential equation and get the general solution given by

$$\rho(\phi) = A \cos(\phi - g) + \frac{m}{C^2}.$$

We can take  $g \in [0, 2\pi)$  so that  $A$  is positive. We now go back to the variable  $r = 1/\rho$ . If  $m > 0$ , then the force is attractive and we can rewrite the above equation into

$$r(\phi) = \frac{p}{e \cos(\phi - g) + 1},$$

where  $p = \frac{C^2}{m}$  and  $e = Ap$  are positive constants. For the repulsive case  $m < 0$ , we have

$$r(\phi) = \frac{p}{e \cos(\phi - g) - 1},$$

where  $p = \frac{C^2}{|m|}$  and  $e = Ap$  are again positive constants. The constant  $e$  is called *eccentricity* and the value of  $e$  determines the shape of solution curves. Namely, they determine circles when  $e = 0$ , ellipses when  $0 < e < 1$ , parabolae when  $e = 1$ , and branches of hyperbolae when  $1 < e$ .

In Chapter 4, we illustrate the computation of solution curves for the more general class of central force problems obtained by direct integration. These Kepler orbits can be seen as their special case.

### 1.1.6 Levi-Civita Regularization

The Kepler force function has its singularity at the center of attraction. This relates to the singularity of the collisional motions of the two-body problem in which two masses approach and collide with each other. To remove the singularity of the Kepler problem, we transform the system into the new coordinates using the complex square mapping. This procedure is called the *Levi-Civita regularization*.

We start with the shifted Hamiltonian of the Kepler problem

$$\frac{|p|^2}{2} + \frac{m}{|q|} - f = 0$$

on the zero-energy hypersurface. We now identify the plane  $\mathbb{R}^2$  as the complex plane  $\mathbb{C}$  and consider the complex square mapping  $z \mapsto z^2 : \mathbb{C} \rightarrow \mathbb{C}$ . Its cotangent lift given by

$$(z, w) \mapsto \left( q = z^2, p = \frac{w}{2\bar{z}} \right)$$

pulls back the system to

$$\frac{|w|^2}{8|z|^2} + \frac{m}{|z|^2} - f = 0.$$

On the zero-energy level, we may multiply this transformed Hamiltonian by  $|z|^2$  (see also Lemma 1) and obtain

$$\frac{|w|^2}{8} + m - f|z|^2 = 0$$

which is nothing else than the Hamiltonian of the Hooke problem on  $-m$ -energy hypersurface. One can see that the transformed system is regular at  $z = 0$ , so the singularity of the Kepler problem is now regularized.

We will use the Levi-Civita regularization in the framework of mechanical billiard systems in Chapter 2 as an application of conformal transformation on integrable billiards.

## 1.2 A bit of Billiards

We now consider the presence of the piecewise smooth elastic reflection wall  $\mathcal{B}$  in a mechanical system  $(M, g, U)$ . At the elastic reflection wall, the particle follows the law of reflection such that the incoming velocity and the outgoing velocity have the same norm and their angles with the normal vector agree

up to orientation. The total energy  $E$  is preserved under such reflections. We denote the corresponding mechanical billiard systems by  $(M, g, U, \mathcal{B})$ .

In the following subsections, we introduce important classes of regular and chaotic mechanical billiard systems and show their dynamical features. Most of the existing results presented here are for free billiard systems, and much of their content is based on the book [32] by Kozlov and Treshchëv.

### 1.2.1 Law of Reflections

We consider a natural mechanical system  $(M, g, U)$  which determines the motion of a particle in  $M$ , and the presence of a piecewise smooth reflection wall  $\mathcal{B}$  in  $M$  at which the particle gets reflected back elastically. More precisely, at the smooth part of  $\mathcal{B}$ , the velocity of the particle changes as follows: let  $v^-$  and  $v^+$  be the velocities before and after the reflection at  $q \in \mathcal{B}$  such that

$$v^- = v_t^- + v_n^-, \quad v^+ = v_t^+ + v_n^+$$

where  $v_t^-$  and  $v_t^+$  are the tangent vectors and  $v_n^-$  and  $v_n^+$  are the normal vectors to  $\mathcal{B}$ , respectively. The law of reflection says the tangent component stays unchanged while the normal component changes its direction *i.e.*

$$v_t^- = v_t^+, \quad v_n^- = -v_n^+.$$

Realize that the kinetic energy does not change under such reflections. Therefore, the total energy is preserved under reflections as well as along the flow.

At the breakpoints of the piecewise smooth wall  $\mathcal{B}$ , reflections are in general not well-defined, which typically does not happen for most trajectories. Therefore we may also allow this case as well.

### 1.2.2 Integrable Billiards

For mechanical billiard systems, the condition to be integrable is much stricter than for natural mechanical systems since we additionally require the conservation under reflections. A function is called the first integral of  $(M, g, U, \mathcal{B})$  if and only if it is constant along the flow of the underlying system  $(M, g, U)$  and also at reflections against the wall  $\mathcal{B}$ .

**Definition 2.** *A  $N$ -dimensional mechanical billiard  $(M, g, U, \mathcal{B})$  is integrable if there exists  $N$  independent first integrals for the billiard system  $(M, g, U, \mathcal{B})$  which are in involution.*

We here list examples of integrable mechanical billiards in the plane  $\mathbb{R}^2$ .

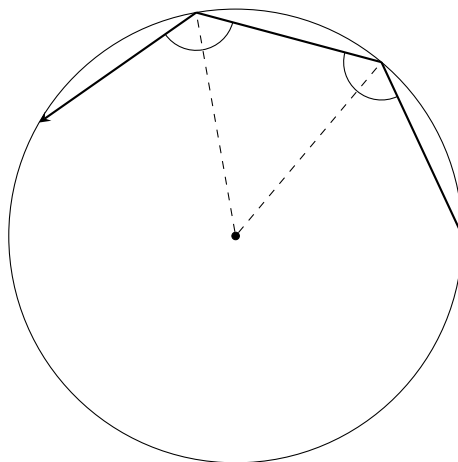


Figure 1.1: Circular billiards trajectory

**Integrable free billiards** For the free motion case, the corresponding billiard system is called free billiards. If we restrict to smooth closed convex reflection walls, there are only two known examples of integrable free billiards. The simplest one is the free billiard with a circular reflection wall. Figure 1.1 illustrates a possible billiard trajectory of the circular free billiards. In such a case, the integrability is very easy to check since one can see that the angle of reflection is preserved. The second example is the one with an elliptic reflection wall. The integrability of such a system has been shown by Birkhoff [6]. One can find the direct verification on the conservation of the Joachimsthal first integral in Appendix 2.A under reflections at conic section reflection walls.

**Birkhoff-Poritsky Conjecture** The following famous conjecture integrable free billiards attributed to Birkhoff and Poritsky [43].

**Conjecture** (Birkhoff-Poritsky Conjecture). *Any closed convex, smooth reflection wall of an integrable free billiards in the plane is either a circle or an ellipse.*

This conjecture has not been proven yet; however, there has been remarkable progress recently made by Kaloshin and Sorrentino [29]. In this paper, they showed the local version of the conjecture: if free billiards with a perturbation of an ellipse as a reflection wall is integrable, then its reflection wall must be an ellipse. Additionally, an algebraic version of this conjecture in the plane and on constant curvature surfaces has recently been

shown by Glutsyuk [24],[25]. Bialy and Mironov showed this conjecture for centrally-symmetric  $C^2$ -smooth convex billiards based on the rigidity of total integrability [4].

**Integrable mechanical billiards with central force** We now consider non-constant force functions and their corresponding mechanical billiard systems. If a billiard system  $(M, g, U, \mathcal{B})$  is integrable, we call  $\mathcal{B}$  as an integrable reflection wall for  $(M, g, U)$ . For central force problems in the plane, any lines passing through the origin and any circles with the center at the origin are integrable reflection walls since (the square of) the angular momentum is preserved under reflections at such a wall.

**Integrable Hooke billiards** In addition to the above two types of integrable reflection walls, for the Hooke problem  $(\mathbb{R}^2, g_{flat}, fr^2)$ , any lines are integrable. This fact can be easily deduced from the separability of the Hooke problem. Also, for the Hooke problem, any ellipse or hyperbola with the center at the origin  $O$  is an integrable reflection wall. The integrability for an elliptic case can be deduced from the classical Jacobi work on geodesics on ellipsoids [28]. Indeed, by letting one minor axis in three-dimensional ellipsoids be zero, one gets free billiards in an ellipse, and the presence of the Hooke potential with the center of attraction at the center of an ellipse can be added without breaking integrability [17]. Additionally, the integrability of two centered confocal elliptic reflection walls is shown by Pustovoitov in [45]. Later, by the same author, the integrability of any combinations of confocal ellipses and confocal hyperbolae has also been confirmed [46].

**Integrable Kepler billiards** The Kepler problem  $(\mathbb{R}^2, g_{flat}, m/r)$  with a line reflection wall not containing the origin attracted particular attention as the special case of *Boltzmann's billiard systems*, and its integrability has been shown by Gallavotti and Jauslin [23] in 2019. More general cases of Boltzmann's billiard systems and their dynamical features will be discussed in Section 1.3.

**Integrable Stark billiards** The Stark problem  $(\mathbb{R}^2, g_{flat}, \frac{s}{|q|} + gq_1)$  admits any parabola with the focus at  $O$  and the  $q_1$ -axis as the main axis as an integrable reflection wall. The integrability of such billiards has been firstly shown by Korsch and Lang in [31]. In Chapter 2, we provide an alternative proof using conformal transformations.

### 1.2.3 Free Elliptic Billiards

In this subsection, we explain important dynamical features of elliptic free billiards following the book [32, Chapter IV]. Consider the free billiard system in the plane  $\mathbb{R}^2$  with the reflection wall given by the equation

$$\frac{x^2}{A^2} + \frac{y^2}{B^2} = 1, \quad A \geq B.$$

This billiard system has the Joachimsthal first integral given by

$$\frac{x\dot{x}}{A^2} + \frac{y\dot{y}}{B^2},$$

which is preserved under the billiard mapping sending the point of reflection and the direction of the velocity at the point to the next reflection point and the direction of the velocity at this point. See also Appendix 2.A for the direct verification for the conservation. We now investigate its dynamics by using the method of separation. Consider a family of confocal conic sections given by

$$\frac{x^2}{A^2 + \lambda} + \frac{y^2}{B^2 + \lambda} - 1 = 0. \quad (1.5)$$

Note that for each non zero value  $(x, y)$ , the above equation has two distinct roots  $\lambda_1, \lambda_2$  such that  $\lambda_1 > \lambda_2$ . Moreover,  $\lambda_1$  and  $\lambda_2$  are contained in the intervals  $(-B^2, \infty)$  and  $(-A^2, -B^2)$ , respectively: The variable  $\lambda_1$  determines an ellipse and the other variable  $\lambda_2$  determines a hyperbola. We regard such a pair  $(\lambda_1, \lambda_2)$  as new coordinates in  $\mathbb{R}^2$  and call it elliptic coordinates. By solving the equation (1.5) for  $x^2$  and  $y^2$ , we obtain

$$x^2 = \frac{(A^2 + \lambda_1)(A^2 + \lambda_2)}{A^2 - B^2}, \quad y^2 = -\frac{(B^2 + \lambda_1)(B^2 + \lambda_2)}{A^2 - B^2}$$

By taking their time derivative, we get

$$\begin{aligned} 2x\dot{x} &= \frac{(A^2 + \lambda_2)\dot{\lambda}_1 + (A^2 + \lambda_1)\dot{\lambda}_2}{A^2 - B^2}, & 2y\dot{y} &= \frac{(B^2 + \lambda_2)\dot{\lambda}_1 + (B^2 + \lambda_1)\dot{\lambda}_2}{B^2 - A^2} \\ \Rightarrow \dot{x}^2 &= \frac{((A^2 + \lambda_2)\dot{\lambda}_1 + (A^2 + \lambda_1)\dot{\lambda}_2)^2}{4(A^2 + \lambda_1)(A^2 + \lambda_2)(A^2 - B^2)}, & \dot{y}^2 &= \frac{((B^2 + \lambda_2)\dot{\lambda}_1 + (B^2 + \lambda_1)\dot{\lambda}_2)^2}{4(B^2 + \lambda_1)(B^2 + \lambda_2)(B^2 - A^2)}. \end{aligned}$$

Using these, we obtain the kinetic energy in elliptic coordinates represented as

$$K = \frac{1}{8} \left( \frac{(\lambda_1 - \lambda_2)\dot{\lambda}_1^2}{(A^2 + \lambda_1)(B^2 + \lambda_1)} + \frac{(\lambda_2 - \lambda_1)\dot{\lambda}_2^2}{(A^2 + \lambda_2)(B^2 + \lambda_2)} \right).$$

With conjugate momenta defined as

$$\mu_1 := \frac{\partial K}{\partial \dot{\lambda}_1} = \frac{(\lambda_1 - \lambda_2)\dot{\lambda}_1}{4(A^2 + \lambda_1)(B^2 + \lambda_1)}, \quad \mu_2 := \frac{\partial K}{\partial \dot{\lambda}_2} = \frac{(\lambda_2 - \lambda_1)\dot{\lambda}_2}{4(A^2 + \lambda_2)(B^2 + \lambda_2)},$$

we can write the Hamiltonian  $H$  into

$$H = 2 \left( \frac{(A^2 + \lambda_1)(B^2 + \lambda_1)\mu_1^2}{\lambda_1 - \lambda_2} + \frac{(A^2 + \lambda_2)(B^2 + \lambda_2)\mu_2^2}{\lambda_2 - \lambda_1} \right).$$

We can modify this into the separated form as

$$(A^2 + \lambda_1)(B^2 + \lambda_1)\mu_1^2 - H\lambda_1/2 = (A^2 + \lambda_2)(B^2 + \lambda_2)\mu_2^2 - H\lambda_2/2 = \kappa = \text{const.}$$

From above, we get the equations of motions for  $\lambda_1$  and  $\lambda_2$  such as

$$\dot{\lambda}_1 = \pm \frac{4\sqrt{\Psi(\lambda_1)}}{\lambda_1 - \lambda_2}, \quad \dot{\lambda}_2 = \pm \frac{4\sqrt{\Psi(\lambda_2)}}{\lambda_1 - \lambda_2},$$

where  $\Psi(\lambda_k) := (A^2 + \lambda_k)(B^2 + \lambda_k)(H\lambda_k/2 + \kappa)$  for  $k = 1, 2$ . The variables  $\lambda_1$  and  $\lambda_2$  move within the range where  $\Psi(\lambda_k) \geq 0$  holds. More precisely, there are the following two possible cases; (i) when  $-A^2 < -\frac{2\kappa}{H} < -B^2$ ,  $\lambda_1$  and  $\lambda_2$  move within the intervals

$$-A^2 \leq \lambda_2 \leq -\frac{2\kappa}{H}, \quad -B^2 \leq \lambda_1 \leq 0,$$

respectively, (ii) when  $-B^2 < -\frac{2\kappa}{H} < 0$ ,  $\lambda_1$  and  $\lambda_2$  move within the intervals

$$-A^2 \leq \lambda_2 \leq -B^2, \quad -\frac{2\kappa}{H} \leq \lambda_1 \leq 0,$$

respectively. For each case, the variables  $\lambda_1$  and  $\lambda_2$  increase/decrease monotonically until they reach one of the boundary points of the intervals; after reaching such points, they start decreasing/increasing their values and repeat the same behavior. From this observation, we find that for the first case,  $\lambda_2$ , and for the second case  $\lambda_1$ , attains the value  $-2\kappa/H$  as an endpoint of the intervals. This behavior leads to the following famous theorem on elliptic billiards:

**Theorem** (Poncelet theorem for elliptic billiards). *A free billiard trajectory inside an elliptic reflection wall remains tangent to a fixed conic section which is confocal to the elliptic wall.*

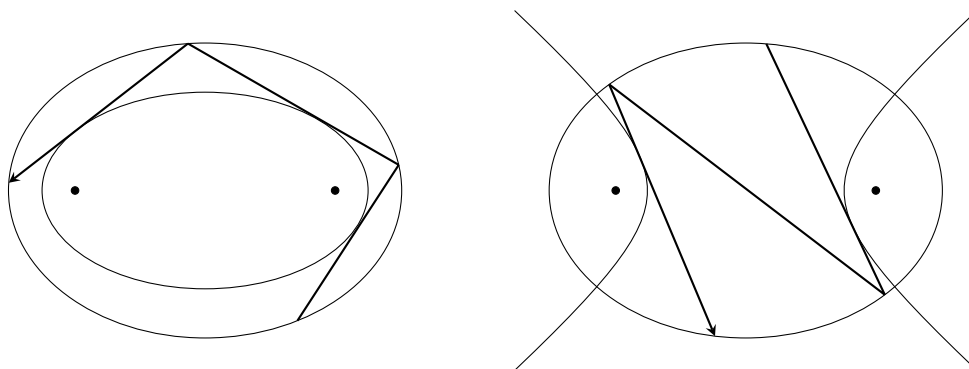


Figure 1.2: Confocal elliptic and hyperbolic caustics for elliptic billiards

Such confocal conics, which are tangent to billiard trajectories inside the wall, are called *caustics*. Figure 1.2 illustrates some possible billiard trajectories inside of an ellipse with an elliptic and a hyperbolic caustic.

**Remark 4.** *The method of separation with elliptic coordinates as above also works for the free billiard systems inside of an ellipsoid in  $N$ -dimensional space, and one can derive the analogous results on conic caustics.*

### 1.2.4 Chaotic Billiards

The existence of additional first integrals or caustics is, in general, not guaranteed. Whereas we expect regular motion or caustics for integrable systems, non-integrable systems may possess complicated motion. Indeed, certain non-integrable billiards are known to be chaotic. In the following, we will define one of the important statistical features, ergodicity, and introduce ergodic billiard systems.

**Definition 3.** *Let  $(M, \Sigma, \mu)$  be a probabilistic measure space and let  $T$  be a measure preserving mapping on  $(M, \Sigma, \mu)$  i.e.  $\mu(A) = \mu(T^{-1}(A))$  for all  $A \in \Sigma$ .  $T$  is called ergodic if and only if  $T$  has no proper positive measure invariant subset i.e. if  $T^{-1}(A) = A$  for some  $A \in \Sigma$  then  $\mu(A) = 0$  or  $\mu(A) = 1$ .*

This condition is equivalent to say that for almost all points  $x \in M$  the trajectory of  $T$  (*i.e.* the sequence  $\{T^n(x)\}_{n=1}^\infty$ ) is dense in  $M$ . If there exists at least one trajectory which is dense, then the system is said to be transitive. Trivially, ergodic systems are transitive, but the inverse is not true.

In order to describe ergodic billiard systems, we introduce billiard mappings. We now consider a free billiard system in the plane with a bounded closed piecewise smooth reflection wall  $\mathcal{B}$ . Let  $L$  be the total length of  $\mathcal{B}$  and parameterize points of  $\mathcal{B}$  by the arc length  $s \in [0, L)$ . We now suppose the particle hits the wall at  $s \in \mathcal{B}$  with the velocity vector  $v$ . We set  $\varphi \in [0, 2\pi)$  be an angle that the vector makes with the wall  $\mathcal{B}$  at  $s$ .

Consider a single trajectory of the billiard system and suppose  $(s_1, \varphi_1)$  and  $(s_2, \varphi_2)$  be consecutive reflection points. We now define the corresponding billiard mapping as

$$T : (s_1, \varphi_1) \mapsto (s_2, \varphi_2) : [0, L) \times [0, 2\pi) \rightarrow [0, L) \times [0, 2\pi).$$

Note that the correspondence given by this mapping allows us to perfectly reproduce a trajectory of the billiard system. Additionally, the billiard mapping preserves the measure on  $[0, L) \times [0, 2\pi)$  given by

$$\sin \varphi \, ds \, d\varphi.$$

See for example [53, Chapter 3] for the verification of the measure preservation. When the billiard mapping  $T$  satisfies the ergodic property, the corresponding billiard system is called ergodic. If there exists an additional first integral, its level sets are necessarily invariant subsets; therefore, integrable systems cannot be ergodic.

If the reflection wall consists of only smooth convex inward components (see Figure 1.3 for example), billiard systems inside of such reflection walls are called scattering billiard systems. Due to the inward convexity, two very close parallel vectors move further apart after the reflection. As a result of this defocusing property, scattering systems exhibit chaotic behavior.

The following result was established by Sinai.

**Theorem** (Sinai [48]). *Scattering billiard systems are ergodic.*

As an example of scattering billiards with a smooth reflection wall, we can consider the free billiard in the two-dimensional torus  $\mathbb{T}^2$  outside of the circular reflection wall (Figure 1.4).

Some ergodic billiard systems which are not scattering have been discovered by Bunimovich. A smooth component of a curve that is convex outward/inward is called focusing/scattering. Bunimovich established the

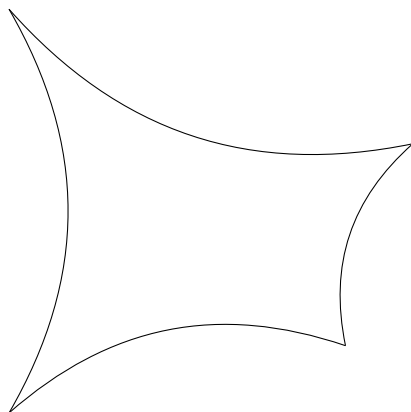


Figure 1.3: Scattering billiards

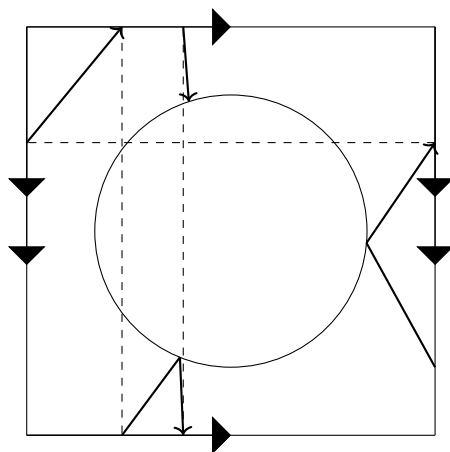


Figure 1.4: Scattering billiards on the torus

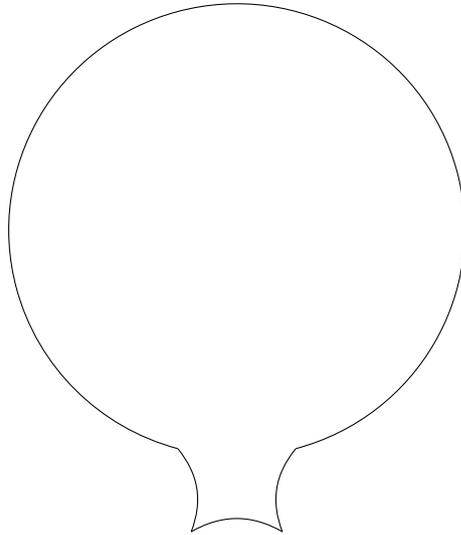


Figure 1.5: Example of Bunimovich's ergodic billiards

condition of focusing and scattering components of reflection walls to be ergodic [8]. As an example, the billiard system inside of a reflection wall depicted in Figure 1.5, which consists of a large focusing component and small scattering components, is ergodic.

In [9], Bunimovich presented examples of ergodic billiards with no scattering components. The most famous example of such ergodic billiards is the billiard system inside of a stadium-like smooth reflection wall which consists of symmetric two half circles and two line segments tangent to them (see Figure 1.6).

In the presence of non-constant force function, less ergodic billiard sys-

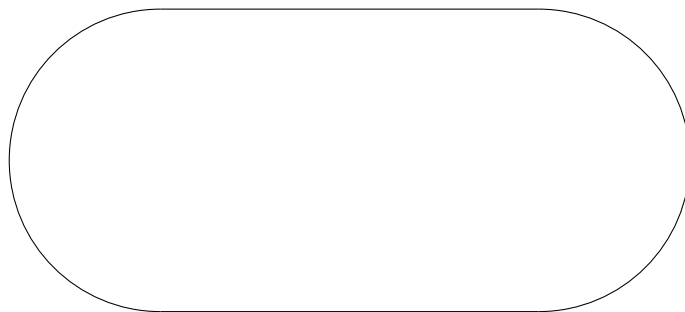


Figure 1.6: Stadium-shaped ergodic billiards

tems have been shown. In [33], Kubo has shown the ergodicity of the system of a particle in the two-dimensional torus with a compound central field by regarding the system as perturbed Sinai's ergodic billiards. In a different context, Boltzmann asserted that the billiard system in the force field given by the Kepler potential with centrifugal correction with a line reflection wall not passing the center is ergodic [7]. A detailed explanation of Boltzmann's billiard system is provided in the next section.

### 1.3 Boltzmann's Billiards

In [7], Boltzmann considered the following mechanical billiard model: the model is defined via the central force problem in  $\mathbb{R}^2$  with a force function

$$U_{\alpha,\beta} := \frac{\alpha}{2r} - \frac{\beta}{2r^2},$$

in which  $r$  is the distance of the moving particle to the origin and  $\alpha, \beta \in \mathbb{R}$  are parameters, with a line in  $\mathbb{R}^2$  with distance  $\gamma > 0$  to the center as a wall of reflection. Realize that the force function  $U_{\alpha,\beta} = \frac{\alpha}{2r} - \frac{\beta}{2r^2}$  consists of the gravitational force  $\frac{\alpha}{2r}$  and the additional centrifugal force  $\frac{\beta}{2r^2}$ . In the special case of  $\alpha > 0, \beta = 0$ , the force function  $U_{\alpha,\beta}$  determines the attractive Kepler problem. In such a case, the billiard systems in  $y \leq \gamma$  and  $y \geq \gamma$  are equivalent by mirroring each reflected arc against the wall at  $y = \gamma$ .

Boltzmann considered this as a toy model which illustrates his ergodic hypothesis. His assertions obtained in this paper are, once fixing the energy,

1. the billiard mapping of the system preserves a measure, and
2. the dynamics is ergodic with respect to this measure for certain values of parameters.

The first assertion was addressed in his paper with the computation of the corresponding billiard mapping and its Jacobian; however, his proof has been largely incomplete. In this thesis, we have completed the measure-preservation proof and also the computation of the billiard mapping (see Chapter 4).

The second assertion is now known to be incorrect when  $\beta = 0$ , as the system is shown to be integrable via different approaches in [23],[19],[61]. In [22], Gallavotti made his assertion that the system is integrable in this case, based on the numerical indications. Later in [23], Gallavotti and Jauslin confirmed this assertion on non-ergodicity by constructing an additional first

integral for the system. Its integrable behavior is analyzed by Felder in [19], and the Poncelet property of the systems is shown. An alternative proof for the integrability of the system is given by Zhao in [61] from the viewpoint of projective dynamics. The concept of projective dynamics and his projective proof are explained in Chapter 3 with extensions to the more general class of billiard systems. Moreover, the explicit analysis in [19] shows that KAM stability holds for system with  $(\alpha, \beta)$  such that  $|\beta/\alpha|$  is sufficiently small. Thus, in order for Boltzmann's ergodic assertion to hold, it is necessary for the parameter  $\beta$  to have large norm as compared to  $\alpha$ .

For the case of large  $\beta$ , theoretically, we do not know yet if the system is ergodic or not. In Chapter 4, we present our numerical simulations for such cases. The numerical results show the largely varied dynamical behavior depending on the parameter setting of  $\alpha, \beta, \gamma$ , and also the energy value. Given the numerical indication, we expect that the system is non-ergodic for most parameter values and ergodic for some specific parameter settings. To address the ergodicity and non-ergodicity of this system rigorously is our future goal.

## 1.4 New Integrable Mechanical Billiards by Conformal Transformations

The examples of integrable mechanical billiards listed in Section 1.2 have been found independently under different contexts. In Chapter 2, we will show that many of these integrable mechanical systems in the plane are connected via conformal transformations as is described in Theorem 1.

We firstly remark that the free billiard in the plane is conformal equivalent to infinitely many billiard systems defined in central force problems on a particular fixed energy level. This result is obtained by transforming the free billiard system with the cotangent lift of any complex mapping on  $\mathbb{C}$  in the form  $z \mapsto z^k$ ,  $k \in \mathbb{N}$ . Particularly with the complex square mapping  $z \mapsto z^2$ , it is classically known that the Hooke problem and the Kepler problem are corresponded to each other (Levi-Civita regularization). From the conformality of this mapping, this correspondence extends to the Hooke billiards and Kepler billiards. With the same mapping, a special class of systems with modified Kepler problems are transformed into separable systems. We call such systems Stark-type systems and call corresponding billiard systems Stark billiards. A similar technique also applies to Euler's two-center problem, which is a superposition of two Kepler problems. For this case, a conformal mapping given by  $z \mapsto \frac{z + \bar{z}}{2}$  transforms the two-center problem

into some separable system.

As a result of these conformal correspondences, we obtained new types of integrable mechanical billiards, namely,

- conic sections focused at the center for the Kepler billiards;
- well-oriented parabola focused at the center for Stark-type billiards;
- confocal conic sections for Euler's two-center problem.
- Moreover, some of these integrable conic section reflection walls in the Kepler and in the two-center problem are allowed to be combined when they are confocal.

## 1.5 Projective Integrable Mechanical Billiards

As well as mechanical systems in the plane, we now consider billiard systems defined on surfaces with constant curvatures and study their integrability. In Chapter 3, we explain correspondences between integrable billiards on such surfaces and integrable billiards in the plane via projection. In general, projections of natural mechanical systems are no longer natural mechanical systems. However, some special classes of systems have their corresponding natural mechanical systems as projections. This is actually the case of the Hooke and the Kepler problems.

The spherical Hooke problem is defined as a natural mechanical system on the unit sphere in  $\mathbb{R}^3$  with the force function  $f \tan^2 \theta_Z$ , where  $f$  is a mass-factor and  $\theta_Z$  is a central angle made with the moving particle and the Hooke center  $Z$  at the South pole  $(0, 0, -1)$  on the sphere. This spherical system is projected to the planer Hooke problem in the plane  $V := \{z = -1\}$  by the central projection. Analogously, the hyperbolic Hooke problem is defined as a natural mechanical system in a sheet of the two-sheeted hyperbolic plane

$$x^2 + y^2 - z^2 = -1$$

in the Minkowski space  $\mathbb{R}^{2,1}$  with the force function  $f \tanh^2 \theta_Z$ , where  $f$  is a mass-factor and  $\theta_Z$  is a central hyperbolic angle made with the moving particle and the Hooke center  $Z$  at the "South pole"  $(0, 0, -1)$  in the hyperbolic plane. By the central projection, this hyperbolic system is also projected to the planer Hooke problem in the plane  $V := \{z = -1\}$ .

Similar results are obtained for the Kepler problems. The spherical Kepler problem is defined as a natural mechanical system on the unit sphere with the force function  $m \cot \theta_Z$ , where  $m$  is a mass-factor, and  $\theta_Z$  is a central

angle made with the moving particle and the Kepler center  $Z$  on the sphere. It is projected to the planer Kepler problem in the plane  $V$  with an affine change in the metric. Analogously, the hyperbolic Kepler problem is defined as a natural mechanical system in a sheet of the two-sheeted hyperbolic plane in  $\mathbb{R}^{2,1}$  with the force function  $m \coth \theta_Z$ , where  $m$  is a mass-factor and  $\theta_Z$  is a central hyperbolic angle made with the moving particle and the Kepler center  $Z$  in the hyperbolic plane. As well as the spherical case, this hyperbolic system is also projected to the planer Kepler problem in  $V$  with an affine change in metric. Unlike the Hooke problem, we can freely set the position of the Kepler center on the sphere and the hyperbolic plane, but the metric in  $V$  has to be chosen compatibly.

The Lagrange problem is defined as the superposition of two Kepler problems and one Hooke problem with the Hooke center placed in the middle of Kepler centers. From the projective properties of the Kepler and the Hooke problems, we can show that the Lagrange problem also possesses its analogous systems on the sphere and in the hyperbolic plane as its projections. The detailed proofs for these facts are described in Chapter 3.

For billiard systems, we need projective correspondences on the laws of reflection against reflection walls in addition to the correspondence on the underlying systems. This additional requirement is not satisfied in general but for some special types of reflection walls. As a fact, the central projection projects spherical/hyperbolic conic sections to conic sections in the plane. Additionally, it relates incoming and outgoing vectors at each reflections walls when the reflection walls consist of confocal conic sections.

Combining these facts, we get the following result on the integrability of billiards with the Lagrange problem.

**Theorem 7** (From Chapter 3). *The mechanical billiard problems defined in the plane, on a sphere and in a hyperbolic plane with the Lagrange problem and with any combination of confocal conic sections with foci at the two Kepler centers as reflection wall, are integrable.*

By confocal conic sections, we shall mean those with the centers of the two singular Kepler centers as foci. By setting some of the mass-factors to zero, we get several systems as particular cases, including the two-center problem, the Kepler problem, and the Hooke problem. For the planer case, this theorem covers many integrable Kepler and Hooke billiard systems in the plane listed in the previous section, which are originally treated with conformal transformation. Thus, the theorem above provides an alternative proof of their integrability as well as extensions to the sphere and the hyperbolic plane.

We also show that, as in the planer case, the conformal transformation relates the integrable Kepler billiards in the hyperbolic plane and the integrable Hooke billiards defined on the sphere and in the hyperbolic plane.

## 1.6 Comparison of Projective and Conformal Approaches

In this thesis, we use two different approaches, based respectively on projective dynamics and conformal transformations, to establish the integrability of certain two-dimensional mechanical billiard systems.

Conformal transformations provide conformal correspondences between two different mechanical billiard systems. The method applies well to fixed energy levels, and does not require the systems to be integrable and may potentially also be used to study the dynamics of non-integrable mechanical billiards. For the two-dimensional planer case, there exist many conformal mappings. Indeed, any analytic mapping on the complex plane is conformal. On the other hand, for higher dimensional case, the variety of conformal mappings is severely limited by Liouville's theorem. Therefore, possible conformal correspondences between integrable mechanical billiards in higher dimensional space are also limited<sup>1</sup>

The projective method applies to very specific mechanical systems and very specific reflection walls, and does not seem to be suitable for non-integrable billiards. On the other hand, the method can also be applied in higher dimensions which in the ideal case would provide an additional first integral for the underlying mechanical system. This, together with some requirement of symmetry, might provide a way to generalize some of the integrability results obtained in this thesis to higher dimensions.

## 1.7 Further Questions

**Projective integrable billiards for higher-dimensional case** So far, our results are restricted to billiard systems in two-dimensional space. In the next step, it is natural to consider the higher-dimensional cases.

In contrast to the conformal transformation explained in Chapter 2, the projective method used in Chapter 3 can be directly applied to the case of higher-dimensional problems and will always provide two first integrals for corresponded two systems. However, in higher-dimensional cases, this is

---

<sup>1</sup>In special cases there are alternatives, such as the Kustaanheimo-Stiefel transformation which relates 3-dimensional Kepler problem with 4-dimensional Hooke problem.

not sufficient, and we need to identify additional first integrals towards the understanding of the following question.

**Question 1.** *What are the integrable mechanical billiard in high dimensional space that can be established by the method of projective dynamics?*

**Analysis on periodic and quasi-periodic orbits of integrable billiards** For continuous Hamiltonian systems, their integrability implies the existence of action-angle variables. This is equivalent to saying that the motion on an energy hypersurface is either periodic or quasi-periodic. For billiard systems, due to the existence of reflections, systems are no longer continuous Hamiltonian; instead, we can describe such systems as discrete systems by computing their corresponding billiard mappings. For integrable Boltzmann's systems with a zero centrifugal term ( $\beta = 0$ ), Felder constructed action-angle variables and showed that the motion is quasi-periodic for generic values of the first integrals in [19]. As a consequence, this result also implies the applicability of the KAM theory, which means that even in the presence of small centrifugal term, the system possesses deformed invariant tori, which denies ergodicity.

**Question 2.** *Can we explicitly analyze the integrable dynamics of the other integrable Kepler, Hooke, and two-center billiard systems with conic section reflection walls we studied in Chapter 2?*

**Ergodicity/non-integrability of Boltzmann's billiard system** From the KAM theory, we already know that Boltzmann's billiard system with a small centrifugal term does not hold ergodicity. However, we can still hope for ergodicity for systems with a sufficiently large centrifugal term. Indeed, our numerical simulations in Chapter 4 show chaotic behavior for some parameters. See e.g. Fig 4.7.

**Question 3.** *Can we analytically show the ergodicity (or alternatively non-integrability) of Boltzmann's billiard system with a large centrifugal term?*

**Periodic orbits of Boltzmann's billiard system** For general attracting Boltzmann's billiard system, there is always a periodic trajectory that gives a fixed point of the corresponding billiard mapping. Indeed, when the angular momentum is zero, the particle falls straight down toward the center of attraction. If the particle hits the wall perpendicularly, it gets reflected back in the same direction as it comes and comes back to the same point on the wall. Studying such a periodic orbit is important in examining whether

the system is ergodic. This is because systems cannot be ergodic as long as they possess stable (in Lyapunov sense) periodic orbits. Besides this type of periodic orbit, our numerical simulation also indicates the existence of other periodic orbits, which seems to be stable for a large centrifugal term.

**Question 4.** *Are there any other periodic orbits for such systems? Can we establish the stability results for these periodic orbits?*

### **Birkhoff-Poritsky conjecture for integrable mechanical billiards**

Via conformal transformation and projection, we have established the integrability of the Kepler, Hooke, two-center, and Lagrangian billiard systems with conic section reflection wall in the plane, on the sphere, and in the hyperbolic plane.

**Question 5.** *Can we prove that they are the only smooth closed integrable reflection wall for these billiard systems?*

## 1.8 Structure of this Thesis

Later chapters are constructed as follows:

**Chapter 2** In Section 2.1, we recall the general setting of mechanical billiard systems and summarize known examples of integrable mechanical billiards systems. In Section 2.2, we introduce conformal transformations between mechanical billiard systems. In particular, we explain that conformal transformations preserve the integrability of mechanical billiards. As a first application, we show that with conformal transformations, we get infinitely many families of planar mechanical billiards which are integrable at one particular energy level. In Section 2.3, we explain the duality between the Hooke billiard and the Kepler billiard and establish our results concerning them. In Section 2.4, we study the integrability of Stark-type mechanical billiards. In particular, we provide a short alternative proof to the theorem of Korsch-Lang [31]. In Section 2.5, we apply Birkhoff's conformal transformation to the classical Euler's two-center problem and establish our integrability results concerning this system.

**Chapter 3** In Section 3.1, we explain the general setting of mechanical systems on a two-dimensional manifold and summarize previous studies on integrable mechanical systems on surfaces with constant curvatures. We also explain their projective correspondence and introduce prior work on

projective dynamics. In Section 3.2, we explain the settings and the principle properties of projective dynamics and define projective correspondences of billiard systems. In Section 3.3, we recall the projective properties of the Hooke and the Kepler problems and their spherical/hyperbolic analogous systems. We also show the projective property of Lagrange problems as has been discovered in [2]. In Section 3.4, we prove Theorem 7 for the planar and the spherical cases, and we discuss some subcases. In Section 3.5, we briefly discuss the hyperbolic case and establish Theorem 7 for this case. The conformal correspondences among the Hooke and the Kepler billiards in the hyperbolic space and the Hooke billiard on the hemisphere are discussed in Section 3.6.

**Chapter 4** In Section 4.1, we construct new canonical coordinates for Boltzmann's billiard system, which is used in Section 4.2, where we provide the proof of measure preservation (symplectic property) of the billiard mapping of Boltzmann's billiard system based on symplectic reduction procedure. In Section 4.3, we compute the orbits for the Kepler problem with an additional centrifugal term and provide explicit representation for the billiard mapping of general Boltzmann's billiard system. In Section 4.4, we present our numerical simulation results of the billiard trajectories based on the computation in the previous section. In Section 4.5 we introduce the Koopman operator corresponding to the billiard mapping and characterize the ergodicity of the system by its eigenvalue problem. Towards the end, we numerically approximate the eigenvalue problem of the Koopman operator and present our numerical results.

# Chapter 2

## Conformal Transformation on Integrable Mechanical Billiards (joint with L. Zhao)

This chapter is based on the paper [54] co-authored with Lei Zhao.

In this chapter we explain that several integrable mechanical billiards in the plane are connected via conformal transformations. We first remark that the free billiards in the plane are conformal equivalent to infinitely many billiard systems defined in central force problems on a particular fixed energy level. We then explain that the classical Hooke-Kepler correspondence can be carried over to a correspondence between integrable Hooke-Kepler billiards. As part of the conclusion we show that any focused conic section gives rise to integrable Kepler billiards, which brings generalizations to a previous work of Gallavotti-Jauslin [23]. We discuss several generalizations of integrable Stark billiards. We also show that any confocal conic sections give rise to integrable billiard systems of Euler's two-center problems.

### 2.1 Preliminaries

#### 2.1.1 General Setting of Mechanical Billiard Systems

The dynamics of billiards in the plane in which a particle moves freely along straight lines in a "billiard table" and reflects elastically at a reflection wall is a widely-studied subject. In this chapter we study a type of variants of such systems, namely planar mechanical billiards, in which the particle is assumed to move under the additional influence of a conservative force field derived from a potential.

Our general setting is the following: We consider a mechanical system on two-dimensional Riemannian manifold  $(M, g)$  with a force function  $U : M \rightarrow \mathbb{R}$ . The potential is  $V = -U$ . The dynamics is given by the corresponding second-order Newton's equation

$$\nabla_{\dot{q}}\dot{q} = \nabla_g U(q), \quad q \in M,$$

in which  $\nabla$  is the Levi-Civita connection of  $g$ . Moreover, we assume that the motion is elastically reflected against a  $C^1$ -smooth curve  $\mathcal{B} \subset M$ . This then defines a billiard system when we specify (when necessary) a component of  $M \setminus \mathcal{B}$  as a billiard table where the motions of interest take place. We shall not need this specification for the purpose of this chapter. We thus define the corresponding mechanical billiard system as the quadruplet  $(M, g, U, \mathcal{B})$ .

Note that as compared to the case of free billiards, it is not always necessary to assume that the billiard table is bounded in order for the billiard mapping to be well-defined, for example when the force forces the trajectories to meet the reflection wall  $\mathcal{B}$  again. Moreover, in such cases we may as well remove part of  $\mathcal{B}$  which may possibly lead to a still well-defined, albeit discontinuous billiard mapping.

A first integral of the system  $(M, g, U, \mathcal{B})$  is a first integral of  $(M, g, U)$  which is invariant under the reflections at  $\mathcal{B}$ . The energy  $E = T - U$  is always a first integral of the system. As we are in dimension 2, such a system is called integrable if there exists another first-integral of this system independent of  $E$ .

Due to the conservation of energy  $E$ , we can moreover restrict the mechanical billiard system to an energy hypersurface  $\{E = e\}$ . We denote the corresponding billiard system by  $(M, g, U, \mathcal{B}, e)$ . Accordingly, this restricted system is called integrable if there exists an additional non-trivial first integral of the system defined on  $\{E = e\}$ . In this chapter, we primarily use this definition of integrability since it is natural to fix its energy when we consider a billiard system.

The free motion case ( $U = 0$ ) corresponds to the classical free billiards. In this case, any of its positive energy hypersurfaces carry the same dynamics. In contrast to this, a general mechanical system can have essentially different behavior on different energy surfaces and analogously also the mechanical billiard systems. Therefore it is often necessary to specify the energy values  $e$  or the subset of possible energy values  $\mathcal{E}$  under consideration. We write  $(M, g, U, \mathcal{B}, \mathcal{E})$  to emphasize also the region of energy under consideration. Such a system is integrable if the system is integrable for all  $e \in \mathcal{E}$ . On the other hand, a "reflection wall"  $\mathcal{B}$  such that  $(M, g, U, \mathcal{B}, \mathcal{E})$  is integrable, is called an integrable reflection wall for the mechanical system  $(M, g, U, \mathcal{B}, \mathcal{E})$ .

Note that for the discussion of integrability, we do not require that the billiard mapping to be always well-defined.

Already in the free billiard case with no additional force, billiard systems may carry rich dynamics and offers class of examples illustrating many dynamical phenomena [53]. The book [32] also discusses several aspects of mechanical billiards.

### 2.1.2 Known Examples of Integrable Mechanical Billiard Systems

For free motion in 2-dimensional plane  $\mathbb{R}^2$ , there are two types of integrable billiard systems. The simplest one is the one with a circular reflection wall. In this case, one can easily see that the angle of reflection is preserved, hence it is an additional first integral. The second example is provided with an elliptic reflection wall. The integrability of such a system has been shown by Birkhoff [6]. This integrability can be generalized in the case of free motions in 2-dimensional sphere  $\mathbb{S}^2$  and the hyperbolic space  $\mathbb{H}^2$ , in which circular and elliptic reflection walls are also integrable [58][50]. Additionally, a conjecture attributed to Birkhoff and Poritsky states that any closed convex reflection wall of an integrable billiard system is either a circle or an ellipse [43]. This conjecture has not been fully proven yet, but there are important progresses recently made [29]. Also, an algebraic version of the conjecture for billiards on the plane and constant curvature surfaces has recently been proved by Glutsyuk [24][25].

Many examples of integrable mechanical billiard systems with the presence of a non-constant potential function have been identified as well. We start our list with a class of relatively easy examples: In a central force problem in  $\mathbb{R}^2$ , in which  $V$  is a function of  $|q|$  only, then circles with center at  $O$  and lines passing through the center  $O$  are integrable reflection walls: In both cases, it is direct to check that the norm of the angular momentum is preserved under reflections at these reflection walls. The very same argument works also on the sphere  $\mathbb{S}^2$ , and on the hyperbolic plane  $\mathbb{H}^2$ .

A number of integrable mechanical billiards are defined for the Kepler problem and the Hooke problem, with respectively force functions of the forms  $U = \frac{s}{r}$  and  $U = fr^2$ , where  $r$  is the distance of the particle from a fixed center  $O \in \mathbb{R}^2$  and the factors  $f, s \in \mathbb{R}$  can take both signs, allowing both attractive and repulsive forces.

In the Hooke problem, it is direct to see that any line is integrable. Centered conic sections are also integrable, for which the case of a centered ellipse follows from the classical work of Jacobi on the integrability of a

quadratic radial potential of the form  $r^2$  restricted to a triaxis ellipsoid in  $\mathbb{R}^3$ , by letting one of the axis of the ellipsoid tends to zero [28][17]. Additionally, the integrability of two centered confocal elliptic reflection walls is shown by Pustovoitov in [45]. Later, by the same author, the integrability of reflection walls consist of centered confocal ellipses and centered confocal hyperbola is also established [46]. In addition, the centered elliptic reflection walls are integrable for certain potentials given by certain polynomials of even degrees in  $\mathbb{R}^2$  [32][60].

The Kepler problem in  $\mathbb{R}^2$  with a line not passing through the attractive center is contained in a class of mechanical billiard systems proposed by Boltzmann in [7], who expected that such systems to be ergodic and in particular non-integrable. Based on a close examination of Boltzmann's argument and some numerical investigations, Gallavotti has conjectured that the contrary is actually true, namely this mechanical billiard system should actually be integrable. This has been confirmed by Gallavotti and Jauslin in [23], with alternative proofs in [19] and [61]. Moreover, such systems can be generalized to  $\mathbb{S}^2$  and  $\mathbb{H}^2$  [61].

It has been also known that a parabolic reflection wall whose focus is at the origin is integrable for the Stark problem in which the potential is a linear combination of a Kepler and a uniform gravitational potential  $U = gy$  with constant  $g \in \mathbb{R}$  [31]. This result has its significance in optics, and such a parabolic mirror has been constructed in experiments [20]. In Section 2.3, we shall give a short alternative proof of the theorem of [31] as well as bring certain extensions.

More recently, for the planar system with potential  $U := \frac{k}{2}(x^2 + y^2) + \frac{\alpha^2}{2x^2} + \frac{\beta^2}{2y^2}$ , Kobtsev showed that any centered ellipse with semi-axis  $a, b$  forms an integrable reflection wall [30].

The integrable dynamics of some of these integrable mechanical billiards have been extensively investigated as well. For this we refer to [21] and the references therein.

### 2.1.3 Purpose of this Chapter

These examples of integrable mechanical billiards have been found independently under different contexts. In this chapter, our main goal is to illustrate how conformal transformations transform integrable mechanical billiard systems.

As application, we shall start by showing that via conformal transformations one gets from integrable free billiards in the plane some classes of

planar immersed curves which are integrable reflection walls for certain central force problem in the plane on its zero-energy level. The complexity of these curves makes us wonder whether this simple corollary admit different but as simple solutions, if we first fix the potential and ask to identify these integrable reflection walls.

We shall then apply the well-known complex square mapping, [38][26][36][37] which induces a duality between the Hooke and the Kepler problems, to obtain a duality between integrable Hooke and Kepler billiards. The same transformation also leads to many new classes of integrable mechanical billiards in systems similar to the Stark problem. We shall also apply a closely-related conformal mapping due to Birkhoff to Euler's two-center problem and identify its integrable reflection walls.

In this way many known examples of integrable mechanical billiards are related. Besides, we have also identified some classes of integrable billiards which we think are new, namely

- conic sections focused at the center for the Kepler billiards;
- well-oriented parabola focused at the center for Stark-type billiards;
- confocal conic sections for Euler's two-center problem.
- Moreover, some of these integrable conic section reflection walls in the Kepler and in the two-center problem are allowed to be combined when they are confocal.

## 2.2 Conformal Transformations and Mechanical Billiards

### 2.2.1 Duality between Integrable Mechanical Billiards

We start our discussion by the following definition of integrable mechanical system.

**Definition 4.** *Let  $(M, g)$  be a 2-dimensional Riemannian manifold,  $U$  a smooth function on  $M$ ,  $\mathcal{B} \subset M$  a  $C^1$ -curve, and  $\mathcal{E} \subset \mathbb{R}$  such that  $(M, g, U, \mathcal{B}, \mathcal{E})$  is a 2-dimensional mechanical billiard, meaning that  $(M, g, U)$  is a natural mechanical system and the motions are assumed to carry energies from  $\mathcal{E}$  and are reflected elastically at  $\mathcal{B}$ . We call the system  $(M, g, U, \mathcal{B}, \mathcal{E})$  integrable when there exists an additional  $C^\infty$  function*

$$G : T^*M \rightarrow \mathbb{R}$$

independent of its energy  $E$ , which is preserved by the motions and by reflections at  $\mathcal{B}$ .

**Definition 5.** Let  $M$  and  $M'$  be two smooth manifolds and  $\phi : M \rightarrow M'$  be a  $k$ -to-1 regular mapping. Then its cotangent lift  $\Phi : T^*M \rightarrow T^*M'$  is defined as

$$\Phi(x, \xi) = (x', \xi'), \quad x \in M, \xi \in T_x^*M, x' \in M', \xi' \in T_{x'}^*M',$$

with

$$x' = \phi(x), \quad \xi' = (d\phi_x^*)^{-1}\xi,$$

where  $(d\phi_x^*)^{-1}$  is the inverse mapping of the isomorphism  $d\phi_x^* : T_{\phi(x)}^*M' \rightarrow T_x^*M$  that is an adjoint of the derivative  $d\phi_x : T_xM \rightarrow T_{\phi(x)}M$  at  $x$ .

Moreover,  $\Phi$  preserves the canonical symplectic forms on the cotangent bundles. More precisely we shall show that the cotangent lift  $\Phi$  pulls the tautological one-form  $\alpha$  on  $T^*M'$  back to the tautological one-form  $\alpha'$  on  $T^*M$ , i.e.  $\Phi^*\alpha' = \alpha$ . This means pointwise

$$(d\Phi)_p^*(\alpha')_{p'} = (\alpha)_p,$$

where  $(d\Phi)_p^*$  is the adjoint of the derivative  $d\Phi$  at  $p$  and  $p' = \phi(p)$ . Let  $\pi : T^*M \rightarrow M$  and  $\pi' : T^*M' \rightarrow M'$  be footprint projections such that

$$\pi(x, \xi) = x, \quad \pi'(x', \xi') = x', \quad x \in M, \xi \in T_x^*M, x' \in M', \xi' \in T_{x'}^*M'.$$

The tautological one-forms  $\alpha, \alpha'$  are defined pointwise as

$$(\alpha)_p = (d\pi)_p^*\xi, \quad (\alpha')_{p'} = (d\pi')_{p'}^*\xi',$$

where  $p = (x, \xi), p' = (x', \xi')$  and  $(d\pi)_p^*, (d\pi')_{p'}^*$  are adjoints of the derivatives of  $\pi$  and  $\pi'$  at  $p$  and  $p'$  respectively. We now have

$$\begin{aligned} (d\Phi)_p^*(\alpha')_{p'} &= (d\Phi)_p^*(d\pi')_{p'}^*\xi' = (d(\pi' \circ \Phi))_p^*\xi' = (d(\phi \circ \pi))_p^*\xi' \\ &= (d\pi)_p^*(d\phi)_p^*\xi' = (d\pi)_p^*\xi = (\alpha)_p. \end{aligned}$$

Now we are ready to state our first theorem.

**Theorem 1.** Let  $(M, g, U, \mathcal{B}, \mathcal{E})$  and  $(M', g', U', \mathcal{B}', \mathcal{E}')$  be two 2-dimensional natural mechanical systems, where  $\mathcal{E}$  and  $\mathcal{E}'$  consist of regular values of the energies. Let  $\phi : M \rightarrow M'$  be a conformal  $k$ -to-1 smooth regular mapping for some  $k \in \mathbb{N}_+$  and assume that  $\phi(\mathcal{B}) \subset \mathcal{B}'$ . Suppose also that its cotangent lift  $\Phi : T^*M \rightarrow T^*M'$  sends each energy hypersurface with energy  $e \in \mathcal{E}$  to an energy hypersurface with energy  $e' \in \mathcal{E}'$ .

*Under these assumptions, if  $(M', g', U', \mathcal{B}', \mathcal{E}')$  is integrable, then  $(M, g, U, \mathcal{B}, \mathcal{E})$  is also integrable. Additionally, if  $(M, g, U, \mathcal{B}, \mathcal{E})$  is integrable and  $\psi(\mathcal{B}') \subset \mathcal{B}$  for a smooth inverse branch  $\psi : M' \rightarrow M$  of  $\phi : M \rightarrow M'$ , and its cotangent lift  $\Psi : T^*M' \rightarrow T^*M$  sends each energy hypersurface with energy  $e' \in \mathcal{E}'$  to an energy hypersurface with energy  $e \in \mathcal{E}$ , then  $(M', g', U', \mathcal{B}', \mathcal{E}')$  is also integrable.*

*Proof.* We first suppose that  $(M', g', U', \mathcal{B}', \mathcal{E}')$  is integrable. Since the energies from  $\mathcal{E}'$  and  $\mathcal{E}$  are mapped to each other, the vector fields  $X_H$  and  $X_{\Phi^*H'}$  leave the common energy hypersurface

$$\{H = e\} = \{\Phi^*H' = e'\} \quad e \in \mathcal{E}, e' \in \mathcal{E}'$$

invariant, on which both vector fields are non-vanishing by the assumption that  $e$  is a regular value of  $H$ . Thus, there exists a smooth function  $\rho : T^*M \rightarrow \mathbb{R} \setminus \{0\}$  such that  $X_H = \rho X_{\Phi^*H'}$ . This means  $X_H$  and  $X_{\Phi^*H'}$  agree up to time parametrization.

From integrability of  $(M', g', U', \mathcal{B}', e')$ , there exists a first integral  $G'$  that is independent of energy  $H'$ . Thus

$$\mathcal{L}_{X_{H'}}G'|_{H'=e'} = \{H', G'\}|_{H'=e'} = 0,$$

where  $\mathcal{L}_{X_{H'}}$  is the Lie derivative along the vector field  $X_{H'}$ . By setting  $G := \Phi^*G'$ , we obtain

$$\mathcal{L}_{X_H}G|_{H=e} = \rho \mathcal{L}_{X_{\Phi^*H'}}G|_{H=e} = \rho \{\Phi^*H', G\}|_{H=e} = 0.$$

So,  $G$  is conserved along the flow of  $X_H$  on  $\{H = e\}$ .

Now, we check the conservation of  $G$  before and after the reflection at  $\mathcal{B}$ . Take a point  $b \in \mathcal{B}$ , then  $b' = \phi(b)$  lies in  $\mathcal{B}'$  from the assumption  $\phi(\mathcal{B}) \subset \mathcal{B}'$ . Let  $(v'_-, v'_+)$  be a pair of incoming and outgoing vector at  $b' \in \mathcal{B}'$  so that  $v'_-$  and  $v'_+$  have the same  $g'$ -metric and angles they made with the normal agree up to sign. There exists  $(v_-, v_+)$  such that  $(d\phi_b(v_-), d\phi_b(v_+)) = (v'_-, v'_+)$ . From the conformality of  $\phi$ , the vectors  $v_-$  and  $v_+$  have the same  $g$ -metric and the angle with the normal agree at  $b \in \mathcal{B}$  up to sign. Therefore  $(v_-, v_+)$  are vectors before and after an elastic reflection at  $b$ . Since  $G'$  is invariant under the reflection at  $\mathcal{B}'$ ,  $G := \Phi^*G'$  is then invariant under the reflection at  $\mathcal{B}$ .

We now suppose that  $(M, g, U, \mathcal{B}, \mathcal{E})$  is integrable. Since  $\phi : M \rightarrow M'$  is a regular  $k$ -to-1 covering map, there exists  $k$  smooth regular inverse branches of  $\phi$ . Let  $\psi : M' \rightarrow M$  be such an inverse branch. The above argument now works the same for  $\psi$  in place of  $\phi$ . □

**Remark 5.** *When the billiard mappings are well-defined, then the above theorem actually shows that they are (semi-)conjugate which implies their equivalence (up to covering) in the sense of dynamical systems.*

**Remark 6.** *The theorem can be directly generalized to certain multi-dimensional case as well. Nevertheless, in view of Liouville's theorem, conformal mappings on a domain of  $\mathbb{R}^d$ ,  $d \geq 3$  are rather limited. Thus we may in general expect more non-trivial applications in the two-dimensional case.*

Pulling back a mechanical billiard system by the cotangent lift of a conformal mapping without restricting its energy gives another mechanical billiard system without the necessity to change time, where the kinetic energy is transformed into a quadratic form of velocity depending on the base point in the configuration space. In our applications, we shall rather fix its energy and make proper time change in order to have an iso-energetic correspondence between mechanical billiards in the plane with standard kinetic energies.

Before applying this theorem to concrete problems, we first state a lemma concerning the time-reparametrization of a Hamiltonian system on a fixed energy hypersurface.

**Lemma 1.** *Let  $H(p, q)$  be a Hamiltonian function defined on  $T^*\mathbb{R}^2$  equipped with its canonical symplectic form. Set  $\hat{H} := g(q) \cdot H$  where  $g(q) > 0$  is a  $C^\infty$ -smooth function of  $q$ . Then the two systems defined by  $H$  and  $\hat{H}$  are equivalent up to a time-reparametrization given by  $d\hat{t} = dt/g(q)$  on their zero energy-hypersurfaces.*

*Proof.* The statement immediately follows from the equation of motion:

$$\begin{aligned}\dot{q} &= \frac{\partial \hat{H}}{\partial p} = g(q) \cdot \frac{\partial H}{\partial p}, \\ \dot{p} &= \frac{\partial \hat{H}}{\partial p} = g'(q) \cdot H + g(q) \cdot \frac{\partial H}{\partial q} = g(q) \cdot \frac{\partial H}{\partial q},\end{aligned}$$

when being restricted to their common zero energy-hypersurfaces. □

We now apply Theorem 1 to some central force problems.

**Theorem 2.** *Let  $f, s \in \mathbb{R}$  be two real parameters. For any  $k \in \mathbb{N}$ ,  $k \geq 2$  the cotangent lift of the conformal mapping*

$$\mathbb{C} \setminus O \mapsto \mathbb{C} \setminus O, z \mapsto q = z^k$$

*gives the transformation between two hamiltonians*

$$\frac{|w|^2}{2} + f|z|^{2k-2} + s$$

and

$$\frac{|p|^2}{2} + \frac{s}{|q|^{2-2/k}} + f$$

on their zero-energy surface, up to time parametrization.

In particular, it gives

- for  $(f > 0, s < 0)$ ,  $(f < 0, s > 0)$ , or  $(f < 0, s < 0)$ , an iso-energetic transformation between two central force systems. In particular, when  $k = 2$  and  $f > 0, s < 0$ , between the Hooke system of isotropic harmonic oscillators and the Kepler system in the plane.
- for  $(f = 0, s < 0)$  or  $(s = 0, f < 0)$ , an iso-energetic transformation between the free motion in the plane with positive energy and some homogeneous central force systems at their energy zero.
- for  $f = s = 0$ , a trivial iso-energetic transformation between zero-energy free motions in the plane.

*Proof.* The cotangent lift for  $\phi : z \mapsto z^k$  is given by

$$\Phi : (z, w) \mapsto \left( q = z^k, p = \frac{w}{k\bar{z}^{k-1}} \right).$$

and is a symplectic map. This follows from our discussions above but it is also direct to have a verification with complex notations. Indeed, the canonical symplectic form  $\omega_0 = \sum dq_i \wedge dp_i$  is given by  $\omega_0 = d\alpha_0$ , where  $\alpha_0 = \sum p_i dq_i$  is the tautological one-form. When we identify  $\mathbb{R}^2$  and  $\mathbb{C}$  and describe  $p = p_1 + ip_2$  and  $q = q_1 + iq_2$ , we can rewrite the tautological one-form into  $\alpha_0 = \text{Re}(\bar{p}dq)$ . By substituting  $q = z^k$  and  $p = \frac{w}{k\bar{z}^{k-1}}$ , we obtain  $\text{Re}(\bar{p}dq) = \text{Re}(\bar{w}dz)$ , thus  $\omega_0(p, q) = \omega_0(z, w)$ .

For normalization purpose, we would prefer the conformal symplectic transformation

$$\Phi : (z, w) \mapsto \left( q = z^k, p = \frac{w}{\bar{z}^{k-1}} \right).$$

which is equivalent to making an additional inessential constant change of time which then pulls the system

$$\frac{|p|^2}{2} + \frac{s}{|q|^{2-2/k}} + f = 0$$

back to

$$\frac{|w|^2}{2|z|^{2k-2}} + \frac{s}{|z|^{2k-2}} + f = 0.$$

On this energy level we may now apply Lemma 1 and multiply the Hamiltonian by the factor  $|z|^{2k-2}$  which just reparametrizes the flow on this energy hypersurface. With this we get

$$\frac{|w|^2}{2} + f|z|^{2k-2} + s = 0.$$

which is the system with Hamiltonian  $\frac{|w|^2}{2} + f|z|^{2k-2} + s$  on its zero-energy level.  $\square$

We remark that this has been used by McGehee for regularization purpose [40].

## 2.2.2 Mechanical Billiards from Free Billiards

We now draw our first consequences in the case  $f = 0$ . In this case one of the two systems is the system of free motions in the plane. It is classically known that a free billiard with a conic section as a reflection wall is integrable [6][53][32]. Namely, it allows elliptic, hyperbolic, parabolic, and line boundaries as integrable reflection walls. We shall deduce this from our discussions on integrable Hooke/Kepler billiards in Section 2.3, and include a direct proof for this fact in an Appendix 2.A.

A conic section in the plane is described with six parameters as

$$Az_1^2 + Bz_1z_2 + Cz_2^2 + Dz_1 + Ez_2 + F = 0, \tag{2.1}$$

where all coefficients are real numbers and  $A, B$ , and  $C$  are not all zero. Since multiplication by a common factor to all the coefficients does not change the curve that it describes, only five out of the six parameters are free. In addition, when we identify conic sections which differ from each other just by scalings and rotations, then only three of the parameters are free.

From this fact and Theorem 1, we directly get the following proposition as an easy corollary.

**Proposition 1.** *For any  $k \in \mathbb{N}, k \geq 2$ , the system  $(\mathbb{C}, g_{flat}, 1/|q|^{2-2/k}, 0)$  on zero-energy surface admit 5-parameter family of smooth integrable reflection walls without ruling out the scalings and the rotations, and 3-parameter family of smooth integrable reflection walls while ruling out the scalings and the rotations.*

We may as well consider the case  $s = 0$  which also gives rise to free motion. With the same argument we get the following proposition:

**Proposition 2.** *For any  $k \in \mathbb{N}, k \geq 2$ , the system  $(\mathbb{C}, g_{flat}, |z|^{2k-2}, 0)$  on the zero-energy surface admit 5-parameter family of smooth integrable reflection walls without ruling out the scalings and the rotations, and 3-parameter family of smooth integrable reflection walls while ruling out the scalings and the rotations.*

We illustrate these propositions in the case  $k = 2$ . The complex square mapping  $z \mapsto z^2 = q$  gives its lift

$$\begin{aligned} q_1 &= z_1^2 - z_2^2 \\ q_2 &= 2z_1z_2 \\ p_1 &= \frac{z_1w_1 - z_2w_2}{z_1^2 + z_2^2} \\ p_2 &= \frac{z_1w_2 + z_2w_1}{z_1^2 + z_2^2}. \end{aligned}$$

after changing time-parametrization.

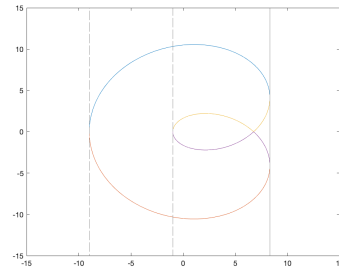
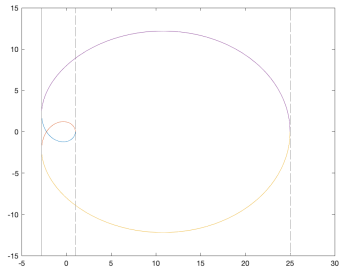
Figure 2.1 shows the reflection walls that are transformed from the ellipses/hyperbolae

$$\frac{(z_1 - c_1)^2}{a^2} \pm \frac{(z_2 - c_2)^2}{b^2} = 1$$

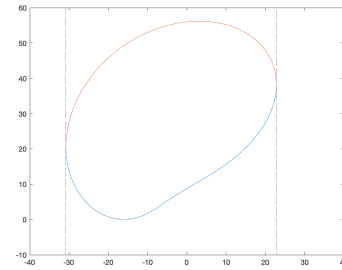
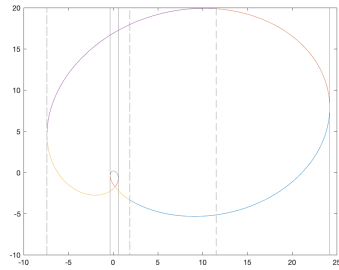
by the mapping above  $z \mapsto z^2$ , in the case of  $f = 0$ . Notice that for a non-centrally symmetric curve, its centrally symmetric reflection is another branch of the pre-image of its image under the complex square mapping. Since centrally symmetric points are mapped to the same point under the complex square mapping which is locally a diffeomorphism, the image may thus have self-intersection points. For a non-centered ellipse, its image contains self-intersection points when the center of the ellipse is not too far away from the origin. The situation is exactly the contrary for a non-centered hyperbola: its image contains self-intersections points when its center is sufficiently far from the origin.

We shall provide a direct verification of the integrability of transformed curves when  $s = 0$  in Appendix 2.B.

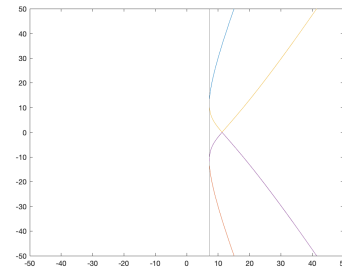
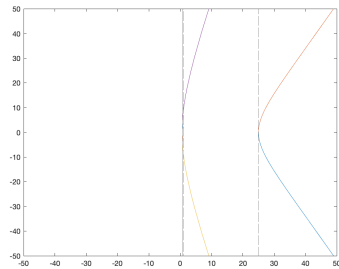
The law of reflections should also corresponds to each other through the conformal complex square mapping. This gives the following law of reflection at the target space of the mapping: A particle is supposed to be reflected against the curve in the target space when the corresponding motions in the source space does so. Otherwise the particle just crosses the curve. Figure 2.2 illustrates this rule, in which the left picture shows what happens the source space, and the right picture in the target space. The dashed curve in the left picture is the centrally symmetric image of the reflection wall. A pair



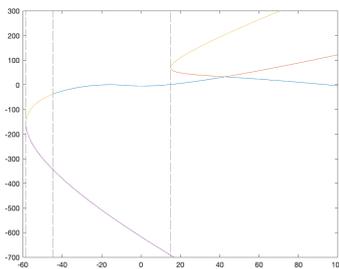
a. ellipse,  $a = 3, b = 2, c_1 = 2, c_2 = 0$     b. ellipse,  $a = 3, b = 2, c_1 = 0, c_2 = 1$



c. ellipse,  $a = 3, b = 2, c_1 = 2, c_2 = 1$     d. ellipse,  $a = 3, b = 2, c_1 = 3, c_2 = 4$



e. hyperbola,  $a = 3, b = 2, c_1 = 2, c_2 = 0$     f. ellipse,  $a = 3, b = 2, c_1 = 0, c_2 = 1$



g. hyperbola,  $a = 3, b = 2, c_1 = 3, c_2 = 4$

Figure 2.1: Transformed ellipses/hyperbolae by  $z \mapsto z^2$

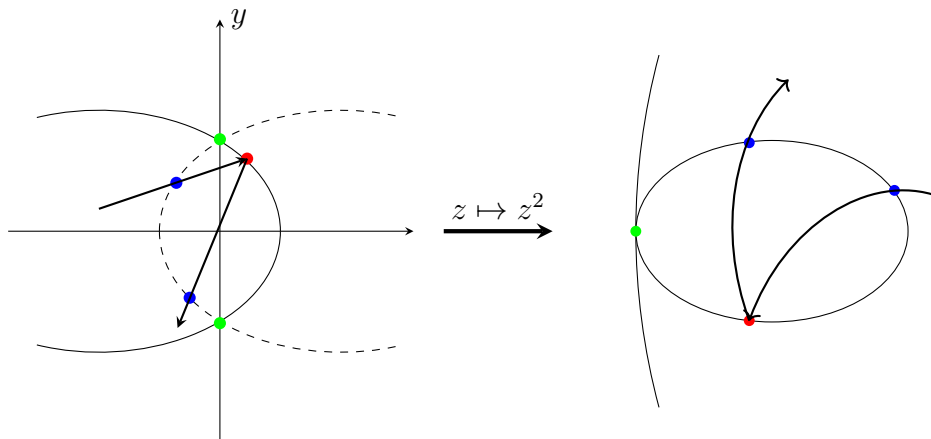


Figure 2.2: The laws of reflections before and after the transformation induced by the complex square mapping

of centrally symmetric points lying in the reflection wall colored in green in the source space are mapped to one point which is an self-intersection point in the target space. A reflection point colored in red in the source space is mapped again to a reflection point in the target space, and vice versa. The blue points indicate where the particle just crosses without reflections in the source and the target spaces.

As in the case of the complex square mapping  $z \mapsto z^2$ , the two inverse branches are given respectively as

$$z_1 = \frac{q_2}{\sqrt{-2q_1 + 2\sqrt{q_1^2 + q_2^2}}}, \quad z_2 = \frac{\sqrt{-2q_1 + 2\sqrt{q_1^2 + q_2^2}}}{2}$$

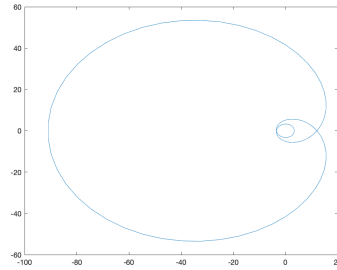
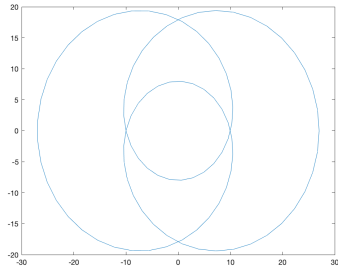
and

$$z_1 = -\frac{q_2}{\sqrt{-2q_1 + 2\sqrt{q_1^2 + q_2^2}}}, \quad z_2 = -\frac{\sqrt{-2q_1 + 2\sqrt{q_1^2 + q_2^2}}}{2}.$$

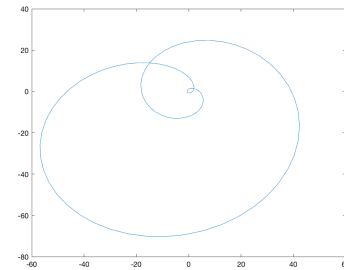
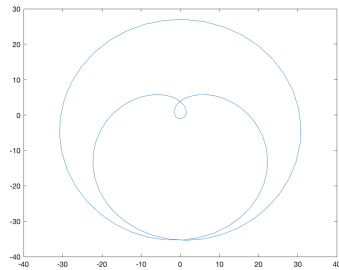
After eliminating the square roots in the equations, the quadratic curves given by the equation (2.1) are mapped into some fourth-order equations of  $q_1$  and  $q_2$ , so the transformed curve is more complicated and can be hard to identify via a more direct method.

Next we consider the case  $k = 3$ . Figure 2.3 shows the image of ellipses/hyperbolae

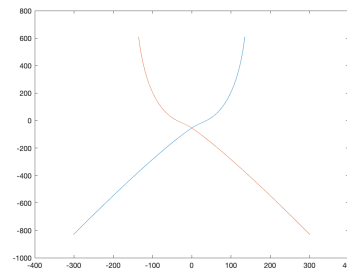
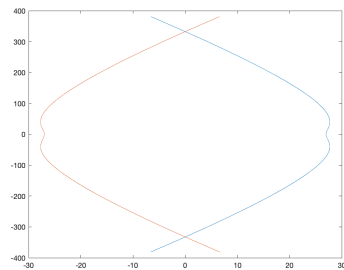
$$\frac{(z_1 - c_1)^2}{a^2} \pm \frac{(z_2 - c_2)^2}{b^2} = 1$$



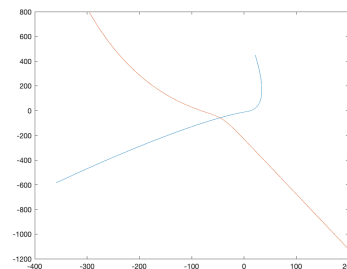
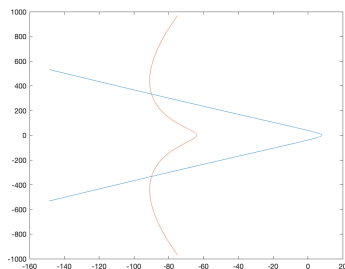
a. ellipse,  $a = 3, b = 2, c_1 = 0, c_2 = 0$     b. ellipse,  $a = 3, b = 2, c_1 = 1.5, c_2 = 0$



c. ellipse,  $a = 3, b = 2, c_1 = 0, c_2 = 1$     d. ellipse,  $a = 3, b = 2, c_1 = 1, c_2 = 1$



e. hyperbola,  $a = 3, b = 2, c_1 = 0, c_2 = 0$     f. ellipse,  $a = 3, b = 2, c_1 = 0, c_2 = 1$



g. hyperbola,  $a = 3, b = 2, c_1 = 1, c_2 = 0$     h. hyperbola,  $a = 3, b = 2, c_1 = 1, c_2 = 1$

Figure 2.3: Transformed ellipses/hyperbolae by  $z \mapsto z^3$

by the conformal mapping  $z \mapsto z^3 = q$ . One can see that the transformed curves from centered ellipses give four self-intersection points. As the center of an ellipse moves away from the origin, the number of self-intersection points is reduced to two, and further to zero when the center is sufficiently far from the origin. For hyperbolae, there always exist at least one self-intersection in the transformed curves.

In the case of  $fs \neq 0$ , much less integrable reflection walls are known. In the next section we shall analyze the situation in the Hooke and Kepler problems.

## 2.3 Hooke, Kepler Billiards and their Dualities

Recall that by Hooke problem we refer to the mechanical system defined in the plane with force function  $fr^2$ , in which  $r$  is the distance of the particle to the center and  $f \neq 0$  is a real parameter. The force field is attractive/repulsive when  $f$  is negative/positive. We accept both cases. Similarly by Kepler problem we refer to the mechanical system define in the plane with force function  $sr^{-1}$  in which  $s \neq 0$  is a real parameter. Again we accept both signs of  $s$ .

### 2.3.1 Integrable Hooke Billiards

Billiard systems defined with the Hooke problem is relatively well-studied and the following integrable reflection walls are known: Centered ellipses [28][17], lines, and combinations of confocal centered conic sections [45][46]. Note that we call a conic section centered, when its center is at the origin. In the following theorem we provide a direct verification for the integrability of centered conic section reflection walls in Hooke billiards.

**Theorem 3.** *The attractive/repulsive Hooke billiard*

$$(\mathbb{C}, g_{flat}, -f|z|^2, \mathcal{B})$$

*with  $\mathcal{B}$  being a centered conic section reflection wall is integrable.*

*Proof.* By using the rotational symmetry, we can write a centered conic ellipses as

$$F := \frac{z_1^2}{a^2} + \frac{z_2^2}{b^2} - 1 = 0.$$

Without loss of generality we can assume that  $a \geq b$ . Let  $w := (w_1, w_2)$  and  $w' = (w'_1, w'_2)$  denote the linear momenta, respectively, before and after the

reflection against this centered elliptic reflection wall. Set  $F_1 := \partial F / \partial z_1$  and  $F_2 := \partial F / \partial z_2$ .

The normal vector at a point on  $F = 0$  is given by

$$n := (F_1, F_2).$$

The normal component of  $w$  is thus

$$w_n := \frac{w \cdot n}{|n|^2} n = \left( \frac{(w_1 F_1 + w_2 F_2) F_1}{F_1^2 + F_2^2}, \frac{(w_1 F_1 + w_2 F_2) F_2}{F_1^2 + F_2^2} \right)$$

From the law of elastic reflection, the momenta after the reflection  $w'$  is

$$w' = w - 2w_n,$$

that is

$$\begin{aligned} w'_1 &= w_1 - \frac{2(w_1 F_1 + w_2 F_2) F_1}{F_1^2 + F_2^2} \\ &= \frac{a^4 w_1 z_2^2 - 2a^2 b^2 w_2 z_1 z_2 - b^4 w_1 z_1^2}{a^4 z_2^2 + b^4 z_1^2}, \\ w'_2 &= w_2 - \frac{2(w_1 F_1 + w_2 F_2) F_2}{F_1^2 + F_2^2} \\ &= \frac{-a^4 w_2 z_2^2 - 2a^2 b^2 w_1 z_1 z_2 + b^4 w_2 z_1^2}{a^4 z_2^2 + b^4 z_1^2}. \end{aligned}$$

We now search for possible first integrals of this Hooke billiard system. The Hamiltonian of the system is  $|w|^2/2 + f|z|^2$ , which admits three independent first integrals from its separability and rotational symmetry:

$$2fz_1^2 + w_1^2, \quad 2fz_2^2 + w_2^2, \quad z_1 w_2 - z_2 w_1.$$

So any combinations of (functions of) these first integrals are again an first integral. We set

$$\tilde{G}(z_1, z_2, w_1, w_2) := k_1(2fz_1^2 + w_1^2) + k_2(2fz_2^2 + w_2^2) + (z_1 w_2 - z_2 w_1)^2$$

in which we square the angular momentum in order to have a quadratic function on  $(w_1, w_2)$  and  $k_1, k_2 \in \mathbb{R}$  are coefficients to be determined. After the

reflection at the reflection wall,  $(z_1, z_2, w_1, w_2)$  is mapped to  $(z_1, z_2, w'_1, w'_2)$ . The difference between the values of  $\tilde{G}$  before and after the reflection becomes

$$\begin{aligned} & \tilde{G}(z_1, z_2, w_1, w_2) - \tilde{G}(z_1, z_2, w'_1, w'_2) = \\ & \frac{4z_1z_2(a^4w_1w_2z_2^2 + a^2b^2w_1^2z_1z_2 - a^2b^2w_2^2z_1z_2 - b^4w_1w_2z_1^2)}{a^4z_2^2 + b^4z_1^2} \times \\ & \frac{a^4z_2^2 + a^2b^2z_1^2 - a^2b^2z_2^2 - b^4z_1^2 - a^2b^2k_1 + a^2b^2k_2}{a^4z_2^2 + b^4z_1^2}. \end{aligned}$$

Set

$$Z(z_1, z_2) := a^4z_2^2 + a^2b^2z_1^2 - a^2b^2z_2^2 - b^4z_1^2 - a^2b^2k_1 + a^2b^2k_2.$$

This is a factor in the numerator which does not depend on the momenta, and therefore its nullity implies preservation of  $G$  under reflections.

We deduce from  $F = 0$  that

$$Z = a^2b^2(a^2 - b^2 - k_1 + k_2).$$

Thus,  $Z$  equals to 0 if and only if

$$k_1 - k_2 = a^2 - b^2 = a^2e^2 \quad (2.2)$$

in which  $e$  is the eccentricity. After normalizing the coefficients, we thus get the following expression of the additional first integral as

$$G(z_1, z_2, w_1, w_2) := \frac{a^2e^2}{1 + a^2e^2}(2fz_1^2 + w_1^2) + \frac{1}{1 + a^2e^2}(z_1w_2 - z_2w_1)^2. \quad (2.3)$$

The case of a centered hyperbola given by

$$\frac{z_1^2}{a^2} - \frac{z_2^2}{b^2} - 1 = 0$$

can be treated similarly and we get the condition on  $k_1$  and  $k_2$  as

$$k_1 - k_2 = a^2 + b^2 = a^2e^2. \quad (2.4)$$

Thus, the first integral has the same formula (2.3). □

From the conditions (2.2) and (2.4) on the coefficients  $k_1$  and  $k_2$ , we can immediately deduce the integrability of reflection walls consist of confocal ellipses and hyperbolae.

**Corollary 1.** *The attractive/repulsive Hooke billiard*

$$(\mathbb{C}, g_{flat}, -f|z|^2, \mathcal{B})$$

with  $\mathcal{B}$  being any combination of confocal centered ellipses and hyperbolae is integrable.

*Proof.* Consider confocal centered ellipses in the form of

$$\frac{z_1^2}{a^2} + \frac{z_2^2}{a^2 - c^2} = 1, \quad a > c,$$

and confocal centered hyperbolae in the form of

$$\frac{z_1^2}{b^2} - \frac{z_2^2}{c^2 - b^2} = 1, \quad 0 < b < c.$$

For both cases, we obtain the same condition on the coefficients  $k_1$  and  $k_2$  such as

$$k_1 - k_2 = c^2,$$

thus there exists a common first integral given by

$$G(z_1, z_2, w_1, w_2) := \frac{c^2}{1 + c^2}(2fz_1^2 + w_1^2) + \frac{1}{1 + c^2}(z_1w_2 - z_2w_1)^2.$$

□

We note that by a direct limiting procedure we also get the integrability of the Hooke billiard with a line or any combination of parallel/perpendicular lines as an integrable boundary.

**Corollary 2.** *The attractive/repulsive Hooke billiard*

$$(\mathbb{C}, g_{flat}, -f|z|^2, \mathcal{B})$$

with  $\mathcal{B}$  being any combination of parallel/perpendicular lines is integrable.

*Proof.* When we take a limit  $e \rightarrow \infty$  in the first integral (2.3), we obtain the form:

$$w_1^2 + 2fz_1^2$$

which is invariant under reflections against a line which is parallel to  $z_1$ - or  $z_2$ -axis, as well as for any combinations of lines which are parallel to the  $z_1$ - or  $z_2$ -axis. □

**Remark 7.** *The Hooke billiard also allows other integrable reflection walls. As a more or less trivial example, any combination of lines passing through the center are integrable with the first integral  $(z_1w_2 - z_2w_1)^2$ .*

### 2.3.2 Integrable Kepler Billiards

As opposed to the study of Hooke billiards, the study of Kepler billiard, on the other hand, seems to be rather recent. In [7], L. Boltzmann considered the billiard system of a central force problem in the plane, which includes the Kepler problem, with a line as wall of reflection. He asserted that any billiard system thus obtained is ergodic. Recently Gallavotti-Jauslin [23] disproved this assertion in the case that the central force problem is the Kepler problem, by actually showing the integrability of the corresponding billiard system. This integrability is revisited together with an in-detailed analysis on its integrable dynamics in Felder [19]. An alternative proof of this integrability based on projective invariance of the Kepler problem is provided in [61].

We now make a revisit of the first integral of Gallavotti-Jauslin  $G$  using the complex square mapping, thus provide yet another alternative proof for the integrability of Gallavotti-Jauslin [23] as well as some extensions.

**Lemma 2.** *The additional first integral*

$$G(z_1, z_2, w_1, w_2) := \frac{a^2 e^2}{1 + a^2 e^2} (2fz_1^2 + w_1^2) + \frac{1}{1 + a^2 e^2} (z_1 w_2 - z_2 w_1)^2$$

given in Theorem 3 of the Hooke billiard  $(\mathbb{C}, g_{flat}, -f|z|^2, \mathcal{B})$  is transformed, after multiplying by  $(1 + a^2 e^2)$ , under the complex square mapping  $\mathbb{C} \setminus O \rightarrow \mathbb{C} \setminus O, z \mapsto z^2$  into Gallavotti-Jauslin's first integral

$$A(p_1, p_2, q_1, q_2) := (p_1 q_2 - p_2 q_1)^2 - 2\tilde{a} \left( (-p_1 q_2 + p_2 q_1) p_2 - \frac{s q_1}{\sqrt{q_1^2 + q_2^2}} \right)$$

in which  $\tilde{a} = a^2 e^2 / 2$ , on the  $-f$ -energy hypersurface of the Kepler problem  $(\mathbb{C} \setminus O, g_{flat}, \frac{s}{|q|})$ .

*Proof.* We observe that  $(z_1 w_2 - z_2 w_1)^2$  is mapped into the squared angular momentum  $(q_1 p_2 - q_2 p_1)^2$ . Indeed, we see that

$$\begin{aligned} z_1 w_2 - z_2 w_1 &= \frac{(z_1^2 - z_2^2)(z_1 w_2 + z_2 w_1) - 2z_1 z_2 (z_1 w_1 - z_2 w_2)}{z_1^2 + z_2^2} \\ &= q_1 p_2 - q_2 p_1. \end{aligned}$$

We now consider the other term  $2fz_1^2 + w_1^2$ . With the relations

$$q_1 = z_1^2 - z_2^2, \quad q_2 = 2z_1 z_2,$$

we get

$$\begin{aligned} z_1^2 &= \frac{z_1^2 - z_2^2 + \sqrt{(z_1^2 - z_2^2)^2 + 4z_1^2 z_2^2}}{2} \\ &= \frac{q_1 + \sqrt{q_1^2 + q_2^2}}{2}, \end{aligned}$$

and

$$\begin{aligned} z_2^2 &= z_1^2 - q_1 \\ &= \frac{-q_1 + \sqrt{q_1^2 + q_2^2}}{2}. \end{aligned}$$

From these and  $w_1 = z_1 p_1 + z_2 p_2$ , we get

$$\begin{aligned} w_1^2 &= (z_1 p_1 + z_2 p_2)^2 \\ &= z_1^2 p_1^2 + 2z_1 z_2 p_1 p_2 + z_2^2 p_2^2 \\ &= \frac{1}{2} \left( p_1^2 q_1 - p_2^2 q_1 + 2p_1 p_2 q_2 + p_1^2 \sqrt{q_1^2 + q_2^2} + p_2^2 \sqrt{q_1^2 + q_2^2} \right). \end{aligned}$$

From these we see that  $2fz_1^2 + w_1^2$  is mapped into

$$f \left( q_1 + \sqrt{q_1^2 + q_2^2} \right) + \frac{1}{2} \left( p_1^2 q_1 - p_2^2 q_1 + 2p_1 p_2 q_2 + p_1^2 \sqrt{q_1^2 + q_2^2} + p_2^2 \sqrt{q_1^2 + q_2^2} \right).$$

After fixing the energy of the Hooke problem to  $s$  and transforming the resulting system via the complex square mapping we get the energy constraint

$$(p_1^2 + p_2^2)/2 - s/(\sqrt{q_1^2 + q_2^2}) + f = 0.$$

From which we deduce that

$$\begin{aligned} &f \left( q_1 + \sqrt{q_1^2 + q_2^2} \right) + \frac{1}{2} \left( p_1^2 q_1 - p_2^2 q_1 + 2p_1 p_2 q_2 + p_1^2 \sqrt{q_1^2 + q_2^2} + p_2^2 \sqrt{q_1^2 + q_2^2} \right) \\ &= - \left( (-p_1 q_2 + p_2 q_1) p_2 - s \cdot \frac{q_1}{\sqrt{q_1^2 + q_2^2}} - s \right). \end{aligned}$$

Therefore, the additional first integral

$$G(z_1, z_2, w_1, w_2) = a^2 e^2 (2fz_1^2 + w_1^2) + (z_1 w_2 - z_2 w_1)^2$$

is transformed into the form

$$A(p_1, p_2, q_1, q_2) := (p_1 q_2 - p_2 q_1)^2 - 2\tilde{a} \left( (-p_1 q_2 + p_2 q_1) p_2 - \frac{s q_1}{\sqrt{q_1^2 + q_2^2}} \right),$$

where  $\tilde{a} = a^2 e^2 / 2$  (which is the distance from the center to one of the foci in case when the transformed curve is a focused ellipse or hyperbola), on the  $-f$ -energy hypersurface of the Kepler problem.  $\square$

We say a conic section is *focused*, when the origin is a focus of it. Using the duality between the Kepler billiard system and the Hooke billiard system given in the Theorem 2, we deduce various integrable Kepler billiards from Theorem 3, that we summarize in the following theorem:

**Theorem 4.** *The Kepler system  $(\mathbb{C}, g_{flat}, \frac{s}{|q|}, \mathbb{R})$  admits any focused conic sections, degenerate cases allowed, as integrable reflection walls. These include*

1. any focused parabola
2. any focused ellipse
3. any focused hyperbola
4. any line.

The additional first integral is given in Lemma 2.

*Proof.* We discuss case by case.

1. Any lines are integrable reflection wall for the Hooke potential. By rotation-invariance it is enough to consider the case of a line given by the expression  $z_1 = c, c \in \mathbb{R} \setminus \{0\}$ , which is transformed by  $z \mapsto z^2 = q$  into the parabola

$$q_1 = -\frac{q_2^2}{4c^2} + c^2,$$

focused at the origin.

2. Consider a centered ellipse given by

$$\frac{z_1^2}{a^2} + \frac{z_2^2}{b^2} = 1 \tag{2.5}$$

We parametrize this elliptic curve as

$$z_1 = a \cos u, \quad z_2 = b \sin u$$

with a parameter  $u \in [0, 2\pi)$ . Then the image of this curve by the conformal mapping  $z \mapsto z^2 = q$  is given by

$$q_1 = a^2 \cos^2 u - b^2 \sin^2 u, \quad q_2 = 2ab \sin u \cos u.$$

which describes the focused ellipse

$$\frac{(q_1 - (a^2 - b^2)/2)^2}{(a^2 + b^2)^2/4} + \frac{q_2^2}{a^2b^2} = 1. \quad (2.6)$$

3. Consider a centered hyperbola given by

$$\frac{z_1^2}{a^2} - \frac{z_2^2}{b^2} = 1, \quad a \neq b, \quad (2.7)$$

parametrized as

$$z_1 = a \cosh u, \quad z_2 = b \sinh u$$

with parameter  $u \in (-\pi, \pi)$  for one branch and  $u \in (-\pi, \pi)$  for the other branch. Then the image of this curve by the conformal mapping  $z \mapsto z^2 = q$  is given by

$$q_1 = a^2 \cosh^2 u - b^2 \sinh^2 u, \quad q_2 = 2ab \sinh u \cosh u.$$

We thus get that the transformed curve satisfies

$$\frac{(q_1 - (a^2 + b^2)/2)^2}{(a^2 - b^2)^2/4} - \frac{q_2^2}{a^2b^2} = 1. \quad (2.8)$$

which describes a focused hyperbola. Indeed this image is seem to be a branch of this hyperbola. The pre-image of the other branch of this hyperbola is the confocal centered hyperbola given by

$$\frac{z_1^2}{b^2} - \frac{z_2^2}{a^2} = 1, \quad (2.9)$$

To see this, it is enough to exchange the roles of  $a$  and  $b$  in the above reasoning.

Since the pre-image of the focused hyperbola consists of two confocal hyperbolae, we may thus conclude with Corollary 1.

4. Finally, a hyperbola given by

$$\frac{z_1^2}{a^2} - \frac{z_2^2}{a^2} = 1$$

is transformed by the conformal mapping  $z \mapsto z^2 = q$  into the line

$$q_1 = a^2.$$

□

In appendix 2.C, for the purpose of comparison, we directly verify the invariance of Gallavotti-Jauslin's first integral in the case that the reflection walls are focused ellipses or focused hyperbola.

**Corollary 3.** *The Kepler system  $(\mathbb{C}, g_{flat}, \frac{s}{|q|}, \mathbb{R})$  admits any combination of confocal focused ellipses and hyperbolae as an integral reflection wall.*

*Proof.* It suffices to see that confocal centered ellipses/hyperbolae are transformed into confocal focused ellipses/hyperbolae by the complex square mapping  $z \mapsto z^2$ . This can be easily checked from the forms of a transformed focused ellipse (2.6) and a transformed focused hyperbola (2.8) by setting  $b^2 = a^2 - c^2$  for ellipses and  $b^2 = c^2 - a^2$  for hyperbolae. □

Similarly, from Corollary 2 we obtain integrable Kepler billiards with any combination of focused parabolae with collinear major axis.

**Corollary 4.** *The Kepler system  $(\mathbb{C}, g_{flat}, \frac{s}{|q|}, \mathbb{R})$  admits any combination of focused parabolae with collinear major axes as an integrable reflection wall.*

*Proof.* The argument follows directly from Theorem 4, Case 1 and Corollary 2. □

### 2.3.3 From Hooke/Kepler Billiards to Free Billiards

We now discuss the classical case of free billiards based on our discussions on integrable Hooke/Kepler billiards, by setting  $f = 0$  in the Hooke billiards, or  $s = 0$  in the Kepler billiards. The following proposition now becomes a direct corollary.

**Corollary 5.** *Free billiards admit conic section reflection walls as integrable reflection wall.*

We now link the additional first integral given by (2.3) to the well-known Joachimsthal first integral, as follows: From Theorem 3, in the case of  $f = 0$ , we have the additional first integral

$$(a^2 - b^2)w_1^2 + (z_1w_2 - z_2w_1)^2$$

for the free billiard with a centered elliptic integrable reflection wall given by

$$\frac{z_1^2}{a^2} + \frac{z_2^2}{b^2} = 1. \tag{2.10}$$

By dividing this by  $a^2b^2$ , we get

$$\begin{aligned}
 & \left( \frac{1}{b^2} - \frac{1}{a^2} \right) w_1^2 + \frac{(z_1w_2 - z_2w_1)^2}{a^2b^2} \\
 &= \frac{w_1^2}{b^2} - \frac{w_1^2}{a^2} + \frac{z_1^2w_2^2 - 2z_1z_2w_1w_2 + z_2^2w_1^2}{a^2b^2} \\
 &= \frac{w_1^2}{b^2} - \frac{w_1^2}{a^2} + \frac{z_2^2}{b^2} \cdot \frac{w_1^2}{a^2} + \frac{z_1^2}{a^2} \cdot \frac{w_2^2}{b^2} - \frac{2z_1z_2w_1w_2}{a^2b^2} \\
 &= \frac{w_1^2 + w_2^2}{b^2} - \left( 1 - \frac{z_2^2}{b^2} \right) \frac{w_1^2}{a^2} - \left( 1 - \frac{z_1^2}{a^2} \right) \frac{w_2^2}{b^2} - \frac{2z_1z_2w_1w_2}{a^2b^2} \\
 &= \frac{1}{b^2} - \left( \frac{z_1^2w_1^2}{a^4} + \frac{z_2w_2}{b^4} + \frac{2z_1z_2w_1w_2}{a^2b^2} \right) \\
 &= \frac{1}{b^2} - \left( \frac{z_1w_1}{a^2} + \frac{z_2w_2}{b^2} \right)^2.
 \end{aligned}$$

In the fourth equation, we used the equation of centered ellipse (2.10). In which we recognize the classical Joachimsthal first integral

$$\frac{z_1w_1}{a^2} + \frac{z_2w_2}{b^2}$$

of the free billiard with an elliptic boundary.

### 2.3.4 Conjectures related to the Birkhoff Conjecture

From Theorem 3 and in view of the Birkhoff-Poritsky's conjecture, we make the following conjectures for Hooke and Kepler billiards.

**Conjecture 1.** *The only Hooke billiards with smooth connected reflection walls which are integrable on all regular energy hypersurfaces are those with a branch of a centered conic section or a line.*

**Conjecture 2.** *The only Kepler billiards with smooth connected reflection walls which are integrable on all regular energy hypersurfaces are those with a focused conic section or a line.*

## 2.4 Integrable Stark-type Billiards

### 2.4.1 Separability and Integrability of Stark-type Billiards

In this section, we investigate some two degrees of freedom mechanical systems which are separable after the complex square mapping and integrable

reflection walls for such systems. We consider some special class of systems with force function given in the form of

$$\frac{s}{|q|} + V(q), \quad V \in C^\infty(\mathbb{R}^2 \setminus O, \mathbb{R}).$$

so that the Kepler problem is further modified by the additional influence from  $V(q)$ . The Hamiltonian of such a system is

$$H = \frac{|p|^2}{2} - \frac{s}{|q|} - V(q_1, q_2). \quad (2.11)$$

On its fixed energy hypersurface  $\{H + f = 0\}$  we may again transform the system by the complex square mapping after a proper time change as described in Theorem 1 which then leads to the system

$$\hat{H} = \frac{|w|^2}{2} - s + f(z_1^2 + z_2^2) - (z_1^2 + z_2^2)V(z_1^2 - z_2^2, 2z_1z_2).$$

Now the transformed Hamiltonian  $\hat{H}$  is separable in  $(z_1, z_2)$  coordinates if and only if the term

$$(z_1^2 + z_2^2)V(z_1^2 - z_2^2, 2z_1z_2)$$

is separable in  $(z_1, z_2)$  coordinates. When the function  $V(q)$  satisfies this separability condition, we call such systems (2.11) *Stark-type systems*. By using the separability of Stark-type systems, we obtain infinitely many integrable Stark-type billiard systems as we state in the following Theorem

**Theorem 5.** *There exists infinitely many potential functions  $V$  such that the system*

$$H = \frac{|p|^2}{2} - \frac{s}{|q|} - V(q_1, q_2)$$

*allows any focused parabola with the  $q_1$ -axis as the main axis as an integrable reflection wall.*

*Proof.* Assume that the system  $H$  is of Stark-type, so that the transformed Hamiltonian is separable, *i.e.*

$$\hat{H} = \frac{|w|^2}{2} + s - f(z_1^2 + z_2^2) + (z_1^2 + z_2^2)V(z_1^2 - z_2^2, 2z_1z_2) = \hat{H}_1(z_1, w_1) + \hat{H}_2(z_2, w_2).$$

From its separability, this system has the additional first integral  $\hat{H}_1(z_1, w_1)$ , which is invariant under the reflections against a line which is parallel to the

$z_1$ - or  $z_2$ -axis. Now since any lines which is parallel to the  $z_1$ - or  $z_2$ -axis is transformed into a focused parabola in the form of

$$q_1 = -\frac{q_2^2}{4c^2} + c^2$$

or

$$q_1 = \frac{q_2^2}{4c^2} - c^2$$

by the mapping  $z \mapsto z^2$ , by Theorem 1, the original system allows any focused parabola with the  $q_1$ -axis as the main axis as an integrable reflection wall.

We are just left to show that there exists infinitely many Stark-type systems. We assume that the function  $V$  depending only on  $z_1^2 - z_2^2$  and  $2z_1z_2$  satisfies

$$(z_1^2 + z_2^2)V(z_1^2 - z_2^2, 2z_1z_2) = g_1(z_1) + g_2(z_2)$$

for some smooth even functions  $g_1, g_2 \in C^\infty(\mathbb{R}, \mathbb{R})$ , i.e.  $g_1(-z_1) = g_1(z_1)$  and  $g_2(-z_2) = g_2(z_2)$  for all  $z_1, z_2 \in \mathbb{R}$ . We then define  $V(z_1^2 - z_2^2, 2z_1z_2) := \frac{g_1(z_1) + g_2(z_2)}{z_1^2 + z_2^2}$ , and we may then solve  $V$  as a function of  $q_1 = z_1^2 - z_2^2$  and  $q_2 = 2z_1z_2$ , which is possible since  $\frac{g_1(z_1) + g_2(z_2)}{z_1^2 + z_2^2}$  is centrally symmetric.  $\square$

This theorem is an analogue of [10, Theorem 3.1] in the setting of mechanical billiards.

## 2.4.2 Examples of Stark-type Billiard Systems

In the following, we discuss some concrete examples of Stark-type systems.

**Stark problem** Firstly we consider the Stark problem by setting  $V(q) = gq_1$ . The Stark problem can be interpreted as a planer system consists of gravitational potential and an external constant force field. The Hamiltonian of this problem is given by

$$H = \frac{|p|^2}{2} - gq_1 - \frac{s}{|q|}.$$

which on its energy hypersurface  $\{H + f = 0\}$  is then transformed into the system

$$\hat{H} = \frac{|w|^2}{2} - g(z_1^4 - z_2^4) + f(z_1^2 + z_2^2) - s.$$

which is separable in  $(z_1, z_2)$  coordinates. From this we get

**Corollary 6.** *The Stark problem  $(\mathbb{R}^2 \setminus O, g_{flat}, \frac{s}{|q|} + gq_1)$  admit any focused parabola with the  $q_1$ -axis as the main axis as integrable reflection wall. In particular, by setting respectively  $s = 0$  we get that any focused parabola with the  $q_1$ -axis as the main axis is an integrable reflection wall in a uniform gravitational field along the  $q_1$ -direction.*

Note that this argument on the integrability of the Stark problem using conformal transformation provides an alternative proof of the theorem of Korsch-Lang [31].

**Frozen-Hill's Problem with Centrifugal Correction** Setting  $V = gq_1^2 + gq_2^2/4$  gives rise to the so-called frozen-Hill's problem with centrifugal corrections [10]. The Hamiltonian of this system is given by

$$H = \frac{|p|^2}{2} - \frac{s}{|q|} - gq_1^2 - \frac{g}{4}q_2^2.$$

Similarly as in the case of Stark problem, on its energy-hypersurface  $\{H + f = 0\}$  we transform the system into

$$\hat{H} = \frac{|p|^2}{2} - s - (z_1^2 + z_2^2)(g(z_1^2 - z_2^2)^2 + gz_1^2z_2^2 - f),$$

which can be written as

$$\hat{H} = \frac{|p|^2}{2} - s - g(z_1^6 + z_2^6) + f(z_1^2 + z_2^2)$$

which is separable in  $(z_1, z_2)$  coordinates. We thus get

**Corollary 7.** *The frozen Hill's problem with centrifugal corrections  $(\mathbb{R}^2 \setminus O, g_{flat}, \frac{s}{|q|} + gq_1^2 + \frac{g}{4}q_2^2)$  admits any focused parabola with the  $q_1$ -axis as the main axis as integrable reflection wall.*

## 2.5 Integrable Mechanical Billiards of Two-center Problem

We now consider the two center problem in the plane  $\mathbb{C}$  with the two centers at  $-1, 1 \in \mathbb{C}$ . The Hamiltonian of this system with mass factors  $m_1, m_2$  (which can take both signs), is given by

$$H = \frac{|p|^2}{2} - \frac{m_1}{|q-1|} - \frac{m_2}{|q+1|}.$$

A classical way to show the integrability of this system uses its separability in elliptic-hyperbolic coordinates [57]. Set  $r_1 = |q - 1|$ ,  $r_2 = |q + 1|$  and define the elliptic-hyperbolic coordinates as

$$\xi = \frac{r_1 + r_2}{2}, \quad \eta = \frac{r_1 - r_2}{2}.$$

In this coordinate system, the curves  $\xi = \text{const.}$  and  $\eta = \text{const.}$  describe, respectively, ellipses and branch of hyperbolae in the plane. Note that confocal ellipses in general intersect a branch of confocal hyperbola in 0 or 2 points and thus the change of coordinates  $q \mapsto (\xi, \eta)$  is in general a 2-to-1 transformation. The above Hamiltonian is then transformed into

$$H(p_\xi, p_\eta, \xi, \eta) = \frac{1}{\xi^2 - \eta^2} \left( \frac{1}{2}(\xi^2 - 1)^2 p_\xi^2 - (m_1 + m_2)\xi + \frac{1}{2}(\eta^2 - 1)^2 p_\eta^2 + (m_1 - m_2)\eta \right).$$

in which  $(p_\xi, p_\eta)$  are the conjugate coordinate to  $(\xi, \eta)$  respectively. By fixing  $H = -f$  and changing the time by multiplying the Hamiltonian  $H + f$  by  $(\xi^2 - \eta^2)$  on the zero energy surface, we obtain the new Hamiltonian

$$K(p_\xi, p_\eta, \xi, \eta) = \frac{1}{2}(\xi^2 - 1)^2 p_\xi^2 - (m_1 + m_2)\xi + \frac{1}{2}(\eta^2 - 1)^2 p_\eta^2 + (m_1 - m_2)\eta + f(\xi^2 - \eta^2)$$

which is separable, showing its integrability. The curves  $\xi = \text{const.}$  and  $\eta = \text{const.}$  actually give integrable reflection walls of the two-center problem, as we shall establish below. Note that the elliptic-hyperbolic coordinate system is not conformal, therefore we have to use the following approach.

The conformal mapping that we are going to use for our purpose is the following one by Birkhoff [5]:

$$z \mapsto q = \frac{z + z^{-1}}{2}, \quad \mathbb{C} \setminus \{0\} \rightarrow \mathbb{C},$$

in real coordinates we have

$$q_1 = z_1 + \frac{z_1}{z_1^2 + z_2^2}, \quad q_2 = z_2 - \frac{z_2}{z_1^2 + z_2^2}$$

which is conjugate to the complex square mapping by a Möbius Transformation [59], [11].

We use the cotangent lift of this mapping, given by the expression

$$q = \frac{z + z^{-1}}{2}, \quad p = \frac{2w}{1 - \bar{z}^{-2}}.$$

to pull the shifted Hamiltonian  $K = H - f$  back to the expression

$$\frac{2|z|^4|w|^2}{|z+1|^2|z-1|^2} - \frac{2m_1|z|}{|z-1|^2} - \frac{2m_2|z|}{|z+1|^2} + f.$$

By changing time on the zero-energy hypersurface, we obtain the new Hamiltonian

$$\hat{K} = \frac{|w|^2}{2} - \frac{m_1|z+1|^2}{2|z|^3} - \frac{m_2|z-1|^2}{2|z|^3} + f \frac{|z-1|^2|z+1|^2}{4|z|^4} = 0.$$

**Proposition 3.** *The mapping  $z \mapsto \frac{z+z^{-1}}{2}$  pulls confocal ellipses back to two centered circles, and pulls confocal hyperbolae to a pair of lines passing through the center.*

*Proof.* A confocal ellipse is given by the equation

$$\frac{q_1^2}{b^2+1} + \frac{q_2^2}{b^2} - 1 = 0. \quad (2.12)$$

with  $b > 0$  as a parameter.

With the conformal mapping we use, the LHS of the above equation is transformed into

$$\begin{aligned} & \frac{(b^2 z_1^2 + (b^2 + 1) z_2^2)((z_1^2 + z_2^2)^2 + 1) + (2b^2 z_1^2 - 2(b^2 + 1) z_2^2)(z_1^2 + z_2^2)}{4b^2(b^2 + 1)(z_1^2 + z_2^2)^2} - 1 \\ &= \frac{(b^2 z_1^2 + (b^2 + 1) z_2^2)((z_1^2 + z_2^2)^2 - 2(2b^2 + 1)(z_1^2 + z_2^2) + 1)}{4b^2(b^2 + 1)(z_1^2 + z_2^2)^2}. \end{aligned}$$

and thus the transformed equation is equivalent to

$$(z_1^2 + z_2^2)^2 - 2(2b^2 + 1)(z_1^2 + z_2^2) + 1 = 0$$

which, seen as a quadratic equation of  $z_1^2 + z_2^2$ , has two positive solutions, giving rise to two centered circles.

For confocal hyperbolae, we set  $b$  in (2.12) as a purely imaginary number such that  $b^2 + 1 > 0$ , then the equation

$$(z_1^2 + z_2^2)^2 - 2(2b^2 + 1)(z_1^2 + z_2^2) + 1 = 0$$

has no real-valued solutions and we get that the transformed equation of (2.12) is equivalent to

$$(b^2 z_1^2 + (b^2 + 1) z_2^2) = 0$$

which describes a pair of lines passing through the origin. Note that they are the two asymptotes of the confocal hyperbola

$$\frac{z_1^2}{b^2+1} + \frac{z_2^2}{b^2} - 1 = 0.$$

□

The separability of the (properly-transformed) two-center Hamiltonian in the elliptic-hyperbolic coordinates is thus equivalent to the separability of  $\hat{K}$  in polar coordinates. We now verify the latter.

We set  $z = re^{i\theta}$ , and denote the conjugate momenta by  $p_\theta, p_r$  respectively. Explicitly we have  $w = p_r \mathbf{e}_r + \frac{p_\theta}{r} \mathbf{e}_\theta$ . The transformed Hamiltonian  $\hat{K}$  into the polar coordinates  $(p_r, p_\theta, r, \theta)$  with zero energy zero becomes

$$\begin{aligned} \hat{K} &= \frac{1}{2} \left( p_r^2 + \frac{p_\theta^2}{r^2} - \frac{2(m_1 - m_2) \cos \theta}{r^2} - \frac{(m_1 + m_2)(r^2 + 1)}{r^3} + 2f \frac{r^4 + r^2 + 1 - 4r^2 \cos^2 \theta}{r^4} \right) \\ &= 0. \end{aligned}$$

By multiplying this by  $2r^2$ , we obtain

$$r^2 p_r^2 + p_\theta^2 - 2(m_1 - m_2) \cos \theta - \frac{(m_1 + m_2)(r^2 + 1)}{r} + 2f \frac{r^4 + r^2 + 1}{r^2} - 8f \cos^2 \theta = 0,$$

which is now seen to be separable. From this we have the following additional first integral

$$r^2 p_r^2 - \frac{(m_1 + m_2)(r^2 + 1)}{r} + 2f \frac{r^4 + r^2 + 1}{r^2},$$

showing the integrability of the system.

In the next lemma, we establish the integrability of centered circular reflection walls and centered line reflection walls in this system.

**Lemma 3.** *Any combination of centered circles and lines passing through the origin are integrable reflection walls for the system  $\hat{K}$  (at its zero-energy level).*

*Proof.* It is sufficient to check invariance of  $p_r^2$  before and after the reflection against the reflection walls. For centered circular reflection walls, the  $\theta$ -component  $r\dot{\theta}$  of the conjugate momenta  $w$  is preserved and the sign of the  $r$ -component  $\dot{r}$  is switched after the reflection. At a line passing through the origin, the  $r$ -component is preserved and the sign of the  $\theta$ -component is switched after the reflection. Hence, in both cases, the value  $p_r^2 = \dot{r}^2$  is unchanged before and after the reflection against these reflection walls.  $\square$

We now deduce the following theorem for billiards defined with the two-center problems:

**Theorem 6.** *The two center problem in the plane admits any combination of confocal ellipses and confocal hyperbolae as an integrable reflection wall.*

*Proof.* This follows directly from Proposition 3 and Lemma 3. □

We note that this results related to the argument in [31] on separability of the elliptic free billiards and first integrals of the two-center problem.

**Remark 8.** *By letting one mass parameter in the two center problem be zero, we obtain the the Kepler billiards with any combination of confocal focused ellipses/hyperbolae as an integrable reflection wall directly form the theorem above. This thus provides an alternative proof of Corollary 3.*

**Remark 9.** *By letting one mass parameter be zero and sending it to infinity, we obtain the integrable Kepler billiards with a focused parabola as the limiting cases from focused ellipses or hyperbolae. Additionally we may also deduce the same result for focused parabolae with collinear major axes as the limiting case from combinations of focused ellipses/hyperbolae. This argument provides an alternative proof of Corollary 4.*

## 2.A Integrability of Conic Section Boundaries of Free Planar billiards

Here we will give a proof for integrability of conic section boundaries in free motion case.

Consider the elliptic/hyperbolic reflection walls in the form

$$\frac{x_1^2}{a^2} \pm \frac{x_2^2}{b^2} = 1.$$

The classical Joachimsthal integral can be written in the form of the product of the velocity and normal vector as follows:

$$J(x, v) := -\frac{1}{2}\langle v, \nabla f(x) \rangle,$$

where  $f = x_1^2/a^2 \pm x_2^2/b^2$  and  $x$  lies in  $f = 1$ . Let  $(x, v)$  be the pair of reflection point and the reflected vector at  $x$ , and let  $(x', v')$  be the consecutive reflection point and the reflected vector at  $x'$ . Then we will check that

$$J(v, x) - J(v', x') = -\frac{1}{2}\langle v, \nabla f(x) \rangle + \frac{1}{2}\langle v', \nabla f(x') \rangle = 0.$$

Since the reflection is elastic, the vector  $v+v'$  is tangent to the ellipse/hyperbola at  $x'$  and  $\nabla f(x')$  is normal to the ellipse/hyperbola at  $x'$ , hence we have

$$\langle v + v', \nabla f(x') \rangle = 0.$$

Using this to substitute  $v'$ , we only need to show that

$$\langle v, \nabla f(x) + \nabla f(x') \rangle = 0.$$

Additionally, we know that  $v$  and  $x - x'$  agree up to some scaling, hence it suffices to show that

$$\langle x - x', \nabla f(x) + \nabla f(x') \rangle = 0.$$

Now we write

$$\langle x - x', \nabla f(x) + \nabla f(x') \rangle = \langle x, \nabla f(x) \rangle + \langle x, \nabla f(x') \rangle - \langle x', \nabla f(x) \rangle - \langle x', \nabla f(x') \rangle.$$

Notice that  $x$  and  $x'$  are points of the ellipse/hyperbola  $f = c$ , therefore we have  $\langle x, \nabla f(x) \rangle = \langle x', \nabla f(x') \rangle = 2$ . Also, we get  $\langle x, \nabla f(x') \rangle - \langle x', \nabla f(x) \rangle = 0$  from the direct computation. As the conclusion,  $J$  is preserved under the

reflection at the elliptic/hyperbolic reflection wall. Note that in Proposition 5 we give an alternative proof for the integrability of elliptic/hyperbolic reflection walls.

Next, we consider parabolic reflection walls. In this case, the additional first integral is given by

$$\gamma = C \cdot \sin \theta,$$

where  $C$  is the angular momentum with respect to the focus of the parabola, and  $\theta$  is the angle that the incoming vector makes in a counter-clockwise direction with the axis of symmetry of the parabola. We here employ the part of the proof for the integrability of confocal parabolae boundaries appears in [42]. There are three cases to consider; (1) the incoming vector cuts the segment between the apex and the focus of the parabola, (2) goes through the outside of the focus, (3) passes the focus, or goes parallel to the axis of symmetry. We here describe the proof for the second case. Figure 2.4 illustrates this case (2); the incoming line segment  $IB$  goes through the outside of the focus and gets reflected back at  $B$ . The outgoing direction is given by  $BR$ . Denote the focus of the parabola by  $F$  and set the perpendicular line from  $F$  to the line  $IB$  and denote the intersection point by  $K$ . Likewise, we denote the intersection point of the line  $BR$  and the perpendicular line from  $F$  to  $IB$ , by  $L$ . Construct the line  $BG$  which is parallel to the axis of symmetry. Additionally, let  $BN$  be normal to the parabola at  $B$ . Set  $C$  and  $C'$  be the angular momenta with respect to the focus of the incoming and outgoing vectors, respectively. Then the quantities before and after reflection  $\gamma, \gamma'$  are given by

$$\gamma = C \cdot \sin \theta, \quad \gamma' = C' \cdot \sin \theta',$$

where  $\theta, \theta'$  are the angles made by  $IB$  and  $BR$  from the axis of symmetry, respectively. We will show that  $\gamma = \gamma'$ . For this to hold, it is enough to show this while replacing the angular momenta  $C$  and  $C'$  respectively by  $|FK|$  and  $|FL|$  in the expression. Set  $\angle FBN = \angle NBG = \alpha$  and  $\angle IBF = \angle RBG = \beta$  in which the angles are non-oriented. Then we have

$$\sin \theta = \sin(2\alpha - \beta), \quad \sin \theta' = \sin \beta,$$

and

$$|FK| = |FB| \sin \beta, \quad |FL| = |FB| \sin(2\alpha - \beta).$$

Thus, we get

$$\gamma = |FB| \sin \beta \sin(2\alpha - \beta) = \gamma'.$$

The proof for the case (1) proceeds in a similar way and its details are given in [42]. The proof for the case (3) immediately follows from the fact that the parallel line to the axis is reflected directly to the focus and vice versa.

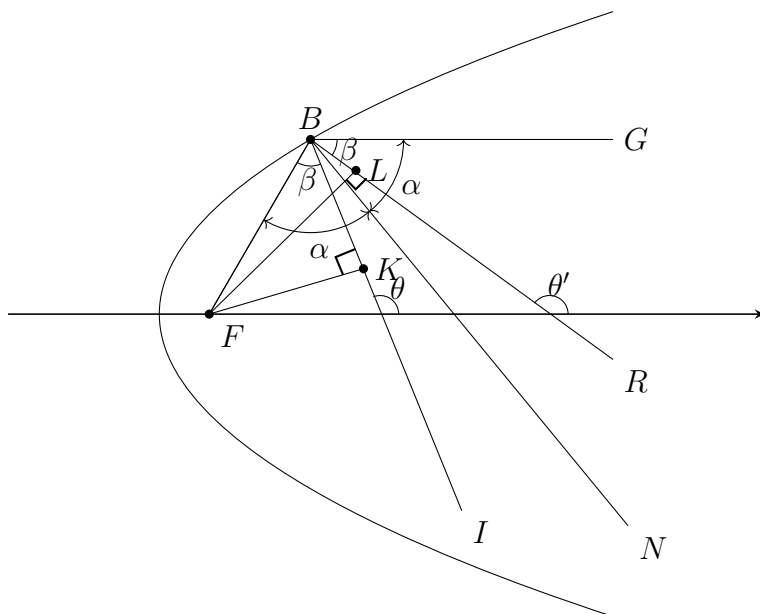


Figure 2.4: Illustration of parabolic boundary in case (2)

For parallel two lines reflection walls, it is trivial that the reflection angle is preserved.

As a conclusion, any conic section including degenerate ones are integrable reflection walls for free billiards.

## 2.B Invariance of Transformed Jauchimsthal First Integral

In this Appendix, we consider a special case of Theorem 2 with  $k = 2$  and  $s = 0$ , and we verify the integrability of the mechanical billiard system thus obtained on its zero-energy level with direct computation.

When  $k = 2$  and  $s = 0$ , the conformal mapping  $z \mapsto z^2$  gives a transformation between the free motion

$$H = \frac{|p|^2}{2} = f$$

on its  $f$ -energy level,  $f > 0$  and the repulsive Hooke system

$$\hat{H} = \frac{|w|^2}{2} - f|z|^2 = 0$$

on its zero-energy level.

We take a non-centered ellipse

$$\frac{(q_1 - c_1)^2}{a^2} + \frac{(q_2 - c_2)^2}{b^2} = 1$$

which is an integrable reflection wall for free billiard. As one can see in Appendix 2.A, the Joachimsthal first integral is given by

$$\frac{\tilde{q}_1 p_1}{a^2} + \frac{\tilde{q}_2 p_2}{b^2},$$

where  $(\tilde{q}_1, \tilde{q}_2)$  is the point of reflection. For our purpose, to simplify the computations, we consider the squared Joachimsthal first integral which we interpolate along the free flow as:

$$J := \frac{(b + c_2 - q_2)(b - c_2 + q_2)p_1^2 + 2p_2(-q_2 + c_2)(-q_1 + c_1)p_1 + p_2^2(a + c_1 - q_1)(a - c_1 + q_2)}{a^2 b^2}.$$

By the mapping  $z \mapsto z^2$ , the non-centered elliptic reflection wall is transformed into

$$\frac{(z_1^2 - z_2^2 - c_1)^2}{a^2} + \frac{(2z_1 z_2 - c_2)^2}{b^2} = 1.$$

We now transform the first integral  $J$  by the same mapping. With Maple, we obtained the following form:

$$\begin{aligned} \hat{J} = & \frac{1}{(z_1^2 + z_2^2)a^2 b^2} \cdot (-w_2^2 z_1^6 + 2w_1 w_2 z_1^5 z_2 + ((-w_1^2 - 2w_2^2)z_2^2 + 2c_1 w_2^2 - 2c_2 w_1 w_2)z_1^4 \\ & + 2(2w_2 w_1 z_2^2 + c_2(w_1^2 + w_2^2))z_2 z_1^3 + ((-2w_1^2 - w_2^2)z_2^4 + (-2c_1 w_1^2 + 2c_1 w_2^2 - 4c_2 w_1 w_2)z_2^2 \\ & + w_1^2(b^2 - c_2^2) + 2c_1 c_2 w_1 w_2 + w_2^2(a^2 - c_1^2))z_1^2 + 2(w_1 w_2 z_2^4 + c_2(w_1^2 + w_2^2)z_2^2 \\ & + c_1 c_2 w_1^2 + w_1(a^2 - b^2 - c_1^2 + c_2^2)w_2 - c_1 c_2 w_2^2)z_2 z_1 + (-w_1^2 z_2^4 + (-2c_1 w_1^2 - 2c_2 w_1 w_2)z_2^2 \\ & + (a^2 - c_1^2)w_1^2 - 2c_1 c_2 w_1 w_2 + w_2^2(b^2 - c_2^2))z_2^2). \end{aligned}$$

A direct (but unnecessary) computation with Maple shows that

$$\{\hat{H}, \hat{J}\} = \sum_{i=1,2} \frac{\partial \hat{H}}{\partial w_i} \frac{\partial \hat{J}}{\partial z_i} - \frac{\partial \hat{H}}{\partial z_i} \frac{\partial \hat{J}}{\partial w_i} = 0$$

on  $\{\hat{H} = 0\}$ . This means that  $\hat{J}$  is invariant along the transformed flow on  $\{\hat{H} = 0\}$ .

Now we verify the invariance of  $\hat{J}$  before and after the reflection against the transformed reflection wall. Set

$$F := \frac{(z_1^2 - z_2^2 - c_1)^2}{a^2} + \frac{(2z_1 z_2 - c_2)^2}{b^2} - 1$$

and define  $F_1 := \partial F / \partial z_1$  and  $F_2 := \partial F / \partial z_2$ . The normal vector to the curve  $\{F = 0\}$  is given by

$$n := (F_1, F_2)$$

and thus the normal component of  $w := (w_1, w_2)$  is obtained as

$$w_n := \frac{w \cdot n}{|n|^2} n = \left( \frac{(w_1 F_1 + w_2 F_2) F_1}{F_1^2 + F_2^2}, \frac{(w_1 F_1 + w_2 F_2) F_2}{F_1^2 + F_2^2} \right).$$

From the law of elastic reflection, the momenta after the reflection  $w' := (w'_1, w'_2)$  is described as

$$w' = w - 2w_n.$$

The difference before and after the reflection is computed as

$$\hat{J}(z_1, z_2, w'_1, w'_2) - \hat{J}(z_1, z_2, w_1, w_2) = D_1 \cdot D_2,$$

where

$$D_1 := (-z_1^2 + z_2^2 + z + c_1)(z_1^2 - z_2^2 + a - c_1)b^2 - (-2z_1 z_2 + c_2)^2 a^2,$$

and  $D_2$  is a polynomial of  $z_1, z_2, w_1$ , and  $w_2$ . Since  $F \cdot a^2 \cdot b^2 = -D_1$ , the factor  $D_1$  becomes 0 at the reflection wall  $\{F = 0\}$ . Therefore,  $\hat{J}$  is invariant under the reflection. This means the transformed first integral  $\hat{J}$  is the first integral for the billiard system  $\hat{H} = 0$  with the transformed reflection wall  $\{F = 0\}$  on the zero-energy surface.

## 2.C Invariance of Gallavotti-Jauslin's First Integral

Here, we directly verify the invariance of Gallavotti-Jauslin's first integral which appeared in Lemma 2 of the Kepler billiard with  $s = 1$  with a focused elliptic and a focused hyperbolic reflection wall. By ruling out the rotational symmetry, we can write a focused ellipse as

$$\frac{(q_1 - \sqrt{a^2 - b^2})^2}{a^2} + \frac{q_2^2}{b^2} = 1.$$

Set  $F := \frac{(q_1 - \sqrt{a^2 - b^2})^2}{a^2} + \frac{q_2^2}{b^2} - 1$  and define  $F_1 := \partial F / \partial q_1$  and  $F_2 := \partial F / \partial q_2$ . Let  $(p_1, p_2)$  and  $(p'_1, p'_2)$  denote momenta, respectively, before and after the reflection against this focused conic section reflection wall. From the law of elastic reflection, we obtain

$$p'_1 = p_1 - \frac{2(p_1 F_1 + p_2 F_2) F_1}{F_1^2 + F_2^2},$$

$$p'_2 = p_2 - \frac{2(p_1 F_1 + p_2 F_2) F_2}{F_1^2 + F_2^2}.$$

Now we test the invariance of a first integral of the form

$$A := (-p_1 q_2 + p_2 q_1)^2 + l_1 \left( (-p_1 q_2 + p_2 q_1) p_1 + \frac{q_2^2}{\sqrt{q_1^2 + q_2^2}} \right) \\ + l_2 \left( (-p_1 q_2 + p_2 q_1) p_2 - \frac{q_1^2}{\sqrt{q_1^2 + q_2^2}} \right)$$

under the reflection against the reflection wall. The difference between the value of  $A$  before and after the reflection is computed as

$$A(q_1, q_2, p_1, p_2) - A(q_1, q_2, p'_1, p'_2) = \frac{-(F_1 p_2 - F_2 p_1)(F_1 p_1 + F_2 p_2)}{(F_1^2 + F_2^2)^2} \times \\ (F_1^2((l_1 - 2q_2)q_1 - l_2 q_2) + 2F_1 F_2(q_1^2 + l_2 q_1 + q_2(l_1 - q_2)) - F_2^2((l_1 - 2q_2)q_1 - l_2 q_2)).$$

Set

$$G := F_1^2((l_1 - 2q_2)q_1 - l_2 q_2) + 2F_1 F_2(q_1^2 + l_2 q_1 + q_2(l_1 - q_2)) - F_2^2((l_1 - 2q_2)q_1 - l_2 q_2).$$

When  $l_1 = 0, l_2 = -2\sqrt{a^2 - b^2}$ ,  $G$  becomes

$$G = \frac{8q_2(q_1 - \sqrt{a^2 - b^2})(a - b)(a + b)(q_2^2 a^2 - b^4 + b^2 q_1^2 - 2\sqrt{a^2 - b^2} b^2 q_1)}{a^4 b^4}$$

which is 0 at the reflection wall  $\{F = 0\}$ . Note that  $l_2 = -2\tilde{a}$  as appeared in Lemma 2 which in this case represents the center-focus distance of the ellipse under concern.

Analogously, we also get the integrability of focused hyperbolae reflection wall by setting  $b$  as a purely imaginary number.



# Chapter 3

## Projective Integrable Mechanical Billiards (joint with L. Zhao)

This chapter is based on the paper [55] co-authored with Lei Zhao.

In this chapter, we use the projective dynamical approach to integrable mechanical billiards as in [61] to establish the integrability of natural mechanical billiards with the Lagrange problem, which is the superposition of two Kepler problems and a Hooke problem, with the Hooke center at the middle of the Kepler centers, as the underlying mechanical systems, and with any combinations of confocal conic sections with foci at the Kepler centers as the reflection wall, in the plane, on the sphere and in the hyperbolic plane. This covers many previously known integrable mechanical billiards, especially the integrable Hooke, Kepler and two-center billiards in the plane, as has been investigated in [54], as subcases. The approach of [54] based on conformal correspondence has been also applied to integrable Kepler billiards in the hyperbolic plane to illustrate their equivalence with the corresponding integrable Hooke billiards on the hemisphere and in the hyperbolic plane as well.

### 3.1 Preliminaries

A two-dimensional mechanical billiard system  $(M, g, U, \mathcal{B})$  is defined on a two-dimensional Riemannian manifold  $(M, g)$  with a piecewise smooth curve  $\mathcal{B} \subset M$  playing the role of a reflection wall and with  $U : M \rightarrow \mathbb{R}$  an openly and densely defined smooth force function on  $M$  determining a natural mechanical system whose equation of motion is

$$\nabla_{\dot{q}} \dot{q} = \nabla U(q). \tag{3.1}$$

A particle moves according to the underlying force field and gets reflected elastically at  $\mathcal{B}$ , *i.e.* at the point of reflection the tangential component of the velocity does not change while the normal component change its signs. The kinetic energy  $K(q, \dot{q}) = \frac{1}{2}g_q(\dot{q}, \dot{q})$  is invariant under elastic reflections, and thus the total energy  $E(q, \dot{q}) = K(q, \dot{q}) - U(q)$  as well.

A two-dimensional mechanical billiard is called integrable, if there exists an additional first integral, *i.e.* a first integral of the underlying mechanical system invariant under the reflections, independent of the total energy  $E$ . Note that to address the problem of integrability, we do not insist on that the billiard mappings is always well-defined.

Some examples of integrable mechanical billiards are known:

For the free motion in the plane  $\mathbb{R}^2$ , the billiards with a circular or an elliptic reflection wall have well-defined billiard mappings and are integrable. The integrability of the circular case is very easy to check since the angle of reflection is preserved. The integrability of the elliptic case has been shown by Birkhoff [6]. This integrability result can be extended also to the billiard system on the two-dimensional sphere and the two-dimensional hyperbolic plane [58][50].

There are also known integrable billiard examples in the presence of non-constant force functions, the most studied systems are those defined with the Hooke or the Kepler problems.

The Hooke problem and the Kepler problem in the plane  $\mathbb{R}^2$  refer to the case when  $U = fr^2$  and  $U = m/r$  respectively, where  $r$  is the distance of the particle from the fixed center  $O \in \mathbb{R}^2$  and  $f, m \in \mathbb{R}$  are parameters which we assume can take both signs: The force may be either attractive or repulsive.

For the Hooke problem in  $\mathbb{R}^2$ , it is rather direct to check that the systems with any line as a reflection wall are integrable. Also the one with a centered conic section as a reflection wall is integrable, in which the case of centered ellipse follows directly from the classical work of Jacobi [28]. Recent work by Pustovoitov [45][46] showed that any confocal combination of centered conic sections are also integrable.

For the Kepler problem in  $\mathbb{R}^2$ , the billiard systems with a line reflection wall which is not passing the center were proposed by Boltzmann [7]. The integrability of such systems has been established recently by Gallavotti and Jauslin [23] with an analysis on the geometry of ellipses, with alternative proofs by [19] and [61]. In [54], we establish that any conic sections focused at the center and any confocal combination of them are also integrable, by using the classical Hooke-Kepler correspondence.

As compared to the Hooke and the Kepler problems, Euler's two-center problem in  $\mathbb{R}^2$  are not super-integrable and the billiard problem defined by it

seems to be less studied. In [54], we showed the integrability of such billiards with combinations of confocal conic sections reflection walls.

In this chapter, we explain that certain integrable mechanical billiards in the two-dimensional plane and constant curvature surfaces are related by projective correspondences. This allows us to yet extend some of our previous results in [54] concerning integrable mechanical billiards in the plane with further extensions to surfaces of constant curvatures.

Our main methodology in this chapter is based on the projective correspondence between mechanical billiards. This means that in addition to the projective correspondence of the underlying natural mechanical systems, also the laws of reflection are in correspondence to each other, so that a billiard trajectory in one system is projected to a billiard trajectory in the other system. The energies of the systems then give rise to a pair of independent first integrals for both of the two billiard systems. With this method, the projective correspondence between integrable planar and spherical Kepler billiards with a line or centered circle reflection wall was presented in [61]. The method can be thought of as an adaptation of the projective method for geodesic flows and free billiards as in [56], [49], [50], [51], [52] to the case of mechanical billiards.

In this chapter we consider the billiard systems defined through the Lagrange problem in the plane with  $U = m_1/r_1 + m_2/r_2 + fr^2$ , on a sphere with  $U = m_1 \cot \theta_{Z_1} + m_2 \cot \theta_{Z_2} + f \tan^2 \theta_{Z_{mid}}$  and in a hyperbolic plane with  $U = m_1 \coth \theta_{Z_1} + m_2 \coth \theta_{Z_2} + f \tanh^2 \theta_{Z_{mid}}$ , which are the problems of adding an elastic force to the two-center problem defined on such a space centered at the middle of the two centers. The precise definitions of the notations are given in Section 3.3 and Section 3.5. This integrable system has been identified by Lagrange [34] in the planer case. Note that such a system is singular at the Kepler centers, as well as a singular set created by the elastic force on the sphere, and is regular elsewhere.

By setting some of the mass factors to zero we get several systems as particular cases including the two-center problem, the Kepler problem, and the Hooke problem in the plane, on a sphere, and in a hyperbolic plane. By confocal conic sections we shall mean those with the two Kepler centers as foci.

**Theorem 7.** *The mechanical billiard problems defined in the plane, on a sphere and in a hyperbolic plane with the Lagrange problem and with any combination of confocal conic sections with foci at the two Kepler centers as reflection wall, are integrable.*

In the plane, the billiard problems defined through the Hooke, the Kepler, and the two-center problems with combinations of confocal conic sections are

therefore subcases of Theorem 7 and thus their integrability directly follows. These have been previously discussed via a different method, based on conformal transformations, in [54]. Theorem 7 provides an alternative proof of their integrability as well as extensions to the sphere and the hyperbolic plane.

Note that somehow in contrast to the conformal transformation used in Chapter 2, this projective method can be directly applied to the case of higher dimensional problems, and will always provide two first integrals for the Lagrange problems. We shall not discuss these higher dimensional problems in this chapter and will leave it for future works. Restricting to dimension 2 raises the question of whether some of the integrable systems can be indeed also related by conformal transformations. Toward the end of this chapter we shall present such links of integrable Kepler billiards in the hyperbolic plane, and the integrable Hooke billiards defined on the sphere and in the hyperbolic plane. In Proposition 13, we also show that a family of confocal focused hyperbolic conic sections are transformed into a family of confocal centered spherical/hyperbolic conic sections by the complex square mapping in conformal charts, which might have an independent geometrical interest.

## 3.2 Principles of Projective Dynamics

Let  $(M, g, U)$  be a natural mechanical system. The system *possesses a corresponding system* if there exists another natural mechanical system  $(M, g', U')$  such that they have the same orbits in  $M$  up to time-parametrizations. In this case, any first integral of  $(M, g, U)$  is also a first integral of  $(M, g', U')$  and vice versa. In particular, the energy  $E'$  of the second system  $(M, g', U')$  is a first integral of  $(M, g, U)$ . When  $E'$  is functional independent from the energy  $E$  of  $(M, g, U)$  we have an additional first integral of the system  $(M, g, U)$ . The same can be said for the system  $(M, g', U')$  in a completely similar way. In practice the underlying smooth manifolds may not be identical. In this case we assume them to be diffeomorphic and identify them by a proper diffeomorphism.

The subject of projective dynamics is to study correspondences of natural mechanical systems induced by projections. To explain further we write the equations of motion of a particle on a Riemannian manifold  $(M, g)$  moving in a force field  $F$ , as

$$\nabla_q \dot{q} = F(q). \quad (3.2)$$

Note that when  $F(q) = \nabla U(q)$  is the gradient of a force function, then we say that the system is *derived from a potential*. By definition the potential

is the negative of the force function. The procedure of the projection from  $M$  to  $M'$  by a diffeomorphism  $\phi : M \mapsto M'$  with a time reparametrization factor  $\rho : M' \mapsto \mathbb{R}$  is that a force field  $F$  on  $M$  is projected into the force field  $F' := \rho \cdot \phi_* F$ .

In words:

*The projection of the force field of a system is the force field given by the push-forward of the projection multiplied with a time reparametrization factor.*

Now arguing with force fields defined on a manifold, we have the following principle of superposition:

*The projection of superposition of the force fields is the superposition of the projections of the force fields.*

When the force fields are derived from potentials, then so is their superposition. In general, the projections of these force fields are no longer derived from potentials. However this indeed holds for special systems that we are going to address in this chapter, which provide corresponding systems to the original systems.

We now comment on billiard correspondences. For this it seems convenient to identify the base manifold  $M$  by a diffeomorphism and consider the law of reflection in  $M$  with respect to the two metrics. The tangential direction is free from the choice of the metric but the normal direction depends on the metric, and therefore a priori the elastic laws of reflections with respect to different metrics are different. We say that there is a billiard correspondence when the elastic laws of reflection agree in addition to the correspondence of underlying natural mechanical systems. As we can see, this depends on the choice of metric and the shape of the reflection wall. When there is a billiard correspondence, then the billiard trajectories, ignoring time parametrizations, correspond to each other by projection and therefore their billiard mappings are equivalent. Conserved quantities of one system are thus transformed into conserved quantities of the other system, and therefore the integrability of the billiard system also carries over.

We refer to [1], [2], [61] for further, more detailed presentations of projective dynamics.

### 3.3 Projective Properties of the Hooke, Kepler and Lagrange Problems

In this section, we discuss some projective properties of the Hooke and the Kepler problems and their spherical/hyperbolic analogous systems that we need.

Then we shall show that the Lagrange problem also has spherical/hyperbolic analogous systems by the principle of superposition of projective dynamics, which then gives to each of these systems a pair of independent first integrals including their own energies.

### 3.3.1 The Hemisphere-Plane Projection

We set  $V = \mathbb{R}^2 \times \{-1\} \subset \mathbb{R}^3$  and  $\mathcal{S} \subset \mathbb{R}^3$  the unit sphere in  $\mathbb{R}^3$ . The central projection from the origin of  $\mathbb{R}^3$  projects the open south-hemisphere  $\mathcal{S}_{SH}$  onto the plane  $V$ . We equip  $\mathcal{S}$  and  $\mathcal{S}_{SH}$  with their induced round metrics from  $\mathbb{R}^3$ , while on  $V$  we allow an affine change of metric. A force field  $F_V$  on  $V$  is carried to a force field  $\hat{F}_S$  on  $\mathcal{S}_{SH}$  by the push-forward of the central projection, which is consequently reparametrized into another force field  $F_S$  with the factor of time change uniquely determined by the projection.

The Euclidean norm of  $\mathbb{R}^3$  as well as its restriction to  $V$  is denoted by  $\|\cdot\|$ .

Let  $q \in \mathcal{S}_{SH}$  be projected to  $\tilde{q} \in V$  by the central projection:

$$q = \|\tilde{q}\|^{-1}\tilde{q}.$$

We write  $\dot{\cdot} := \frac{d}{dt}$  the time derivative. We start by the force field  $F_V$  in  $V$  and deduce the corresponding force field  $F_S$  on  $\mathcal{S}_{SH}$  which is equivalent to the other way around but the computation simplifies. The equation of motion of the system in  $V$  is

$$\ddot{\tilde{q}} = F_V(\tilde{q}).$$

We compute

$$\dot{q} = \|\tilde{q}\|^{-2}(\dot{\tilde{q}}\|\tilde{q}\| - \langle \nabla\|\tilde{q}\|, \dot{\tilde{q}} \rangle \tilde{q}).$$

We now take a new time variable  $\tau$  for the system on  $\mathcal{S}_{SH}$ , and  $' := \frac{d}{d\tau}$  such that

$$\frac{d}{d\tau} = \|\tilde{q}\|^2 \frac{d}{dt}. \quad (3.3)$$

We thus have

$$q' = (\dot{\tilde{q}}\|\tilde{q}\| - \langle \nabla\|\tilde{q}\|, \dot{\tilde{q}} \rangle \tilde{q}).$$

and

$$q'' = \|\tilde{q}\|^2(\ddot{\tilde{q}}\|\tilde{q}\| - (\langle \nabla\|\tilde{q}\|, \ddot{\tilde{q}} \rangle + \langle (\nabla\|\tilde{q}\|), \dot{\tilde{q}} \rangle) \tilde{q}).$$

Consequently we have

$$q'' = \|\tilde{q}\|^2(F_V(\tilde{q})\|\tilde{q}\| - \lambda(\tilde{q}, \dot{\tilde{q}}, \ddot{\tilde{q}})\tilde{q}). \quad (3.4)$$

in which we have set  $\lambda(\tilde{q}, \dot{\tilde{q}}, \ddot{\tilde{q}}) = \langle \nabla \|\tilde{q}\|, \ddot{\tilde{q}} \rangle + \langle (\nabla \|\tilde{q}\|), \dot{\tilde{q}} \rangle$ .

We observe that the first term of the right hand side of this equation depends only on  $\tilde{q}$  and consequently depends only on  $q \in \mathcal{S}_{SH}$  by central projection, while the second term is radial. Projecting both sides of this equation to the tangent space  $T_q \mathcal{S}_{SH}$  we get the equation of motion on  $\mathcal{S}_{SH}$ , assuming the form

$$\nabla_{q'} q' = F_S(q).$$

For our purpose, we would like to have natural mechanical systems which are centrally projected to natural mechanical systems, *i.e.* the question is, when we start from a natural mechanical system on  $\mathcal{S}_{SH}$  resp.  $V$ , then whether the projected system on  $V$  resp.  $\mathcal{S}_{SH}$  is also derived from a potential and is thus also a natural mechanical system. As we would expect this does not hold in general. Nevertheless, it actually holds for some important systems.

### 3.3.2 Projective Properties of the Hooke and Kepler Problems

We consider a central force problem  $F_S$  on  $\mathcal{S}$  with a distinguished center  $Z \in \mathcal{S}_{SH}$ . By assumption the force field is invariant under the  $SO(2)$ -action by rotations around  $Z$  on  $\mathcal{S}$ . The projected force field  $F_V$  on  $V$  is in general not derived from a potential. In the same way, a central force problem  $F_V$  in  $V$  with a center  $\tilde{Z}$  might not project to a system derived from a potential on  $\mathcal{S}_{SH}$ .

There are special cases that this does hold. The first is relatively easy to see: when  $Z = (0, 0, -1)$ , the projected force field  $F_V$  is also invariant under the  $SO(2)$ -action by rotations in  $V$  as inherited from rotations around the vertical axis in  $\mathbb{R}^3$ , and therefore  $F_V$  is derived from a potential. The second case is maybe not as easy to see: The point  $Z \in \mathcal{S}_{SH}$  can be chosen arbitrary, and  $F_V$  will be derived from a potential when  $F_S$  is the force field of the Kepler-Serret Problem on the sphere [47], and in this case  $F_V$  itself is the force field of a Kepler problem in  $V$  for a proper choice of an affine metric. Also, among the problems belonging to the first case, the Hooke problems have the property that  $F_V$  is derived from a potential for *any* affine metrics in  $V$ .

#### The Kepler Problems

We first discuss the case of the Kepler problems. The Kepler-Serret problem, or the spherical Kepler problem, is the natural mechanical system

$(\mathcal{S}, g_{st}, \hat{m} \cot \theta_Z)$ , in which  $g_{st}$  is the round metric on the sphere,  $\hat{m} \in \mathbb{R}$  is the mass-factor and  $\theta_Z$  is the central angle the moving particle made with  $Z$ . The system naturally restricts to a natural mechanical system  $(\mathcal{S}_{SH}, g_{st}, \hat{m} \cot \theta_Z)$  by restriction. In the case that  $Z$  is *vertical*,  $Z = (0, 0, -1)$ , it is not hard to see by a direct computation that the spherical Kepler problem is projected to the planar Kepler problem  $(V, \|\cdot\|, \hat{m}/\|\tilde{q}\|)$ . Consequently the orbits of the spherical Kepler problem are all conic sections on the sphere by means of orbital correspondence and analytic extension. A special property of the Kepler problem is that this remains true when  $Z$  is not vertical, up to a change of metric and of the mass factor [27]. See also [1], [61].

To normalize the situation we set  $Z = \left(0, \frac{a}{\sqrt{1+a^2}}, -\frac{1}{\sqrt{1+a^2}}\right) \in \mathcal{S}_{SH}$  for  $a \in \mathbb{R}$ , and  $\tilde{Z} = (0, a, -1)$  the projection point of  $Z$  in  $V$ . For  $\tilde{q} = (\tilde{x}, \tilde{y}, -1) \in V$  we define

$$\|\tilde{q}\|_a = \sqrt{\tilde{x}^2 + \frac{\tilde{y}^2}{1+a^2}} \quad (3.5)$$

which is an affine change of norm from the induced norm on  $V$  with origin at  $(0, 0, -1)$  of the standard Euclidean norm  $\|\cdot\|$  in  $\mathbb{R}^3$ .

**Proposition 4.** *The spherical Kepler problem  $(\mathcal{S}_{SH}, g_{st}, \hat{m} \cot \theta_Z)$  projects to the Kepler problem  $(V, \|\cdot\|_a, m/\|\tilde{q} - \tilde{Z}\|_a)$  such that  $m = \frac{\hat{m}}{\sqrt{1+a^2}}$ .*

*Proof.* With the procedure explained in Subsection 3.3.1, we arrive from a planar force field  $F_V$  to a spherical force field  $F_S$ .

We now consider the Kepler problem on  $V$ :

$$(V, \|\cdot\|_a, m\|\tilde{q} - \tilde{Z}\|_a^{-1}) \quad (3.6)$$

which determines the force field

$$F_V(\tilde{q}) := -m\|\tilde{q} - \tilde{Z}\|_a^{-3}(\tilde{q} - \tilde{Z}) \quad (3.7)$$

on  $V$ .

We now plug (3.7) into the right hand side of (3.4) and compute its projection to the tangent space of  $T_q\mathcal{S}_{SH}$ . We may effectively forget the second term in the right hand side of (3.4) since it projects to zero in  $T_q\mathcal{S}_{SH}$ . As for the first term in the right hand side of (3.4), we see that it is again central on  $\mathcal{S}_{SH}$  by the central projection. Therefore it is enough to compute its norm to determine the corresponding  $F_S$  on  $\mathcal{S}_{SH}$ .

For this purpose, we restrict the system to (oriented) planes passing through the centers  $Z, \tilde{Z}$  as well as the center  $O = (0, 0, 0)$  of  $\mathcal{S}_{SH}$ . These

planes in  $\mathbb{R}^3$  form an  $S^1$ -family. We compute the restricted force field on any of these planes.

We fix such a plane  $W$ , which necessarily intersects  $V$  by construction. Let  $\ell$  be the intersection line. Let  $G$  be the point on  $\ell$  such that  $OG$  is perpendicular to  $\ell$ . Let  $\phi$  be the angle between  $\ell$  and the intersection line  $\{(0, y, -1)\}$  of the  $yz$ -plane and  $V$ . The restriction to  $\ell$  of the function  $\|\tilde{q} - \tilde{Z}\|_a$  can be written as

$$\|\tilde{q} - \tilde{Z}\|_a = \|\tilde{q} - \tilde{Z}\| \sqrt{\sin^2 \phi + \frac{\cos^2 \phi}{1 + a^2}} = \|\tilde{q} - \tilde{Z}\| \sqrt{\frac{1 + a^2 \sin^2 \phi}{1 + a^2}}.$$

Thus the force field  $F_V(\tilde{q})$  restricted to  $\ell$  is given by

$$F_V(\tilde{q}) = -m \left( \frac{1 + a^2}{1 + a^2 \sin^2 \phi} \right)^{3/2} \|\tilde{q} - \tilde{Z}\|^{-3} (\tilde{q} - \tilde{Z}).$$

The line  $\ell$  passes through the two points  $\tilde{q}$  and  $\tilde{Z}$  and the equation of  $\ell$  is given by

$$y = \cot \phi x + a.$$

Let  $Z_0 = (0, 0, -1)$ , then  $G$  can be obtained as the point on  $\ell$  such that  $Z_0G$  is perpendicular to  $\ell$  and computed as

$$G := (-a \sin \phi \cos \phi, -a \sin^2 \phi, -1).$$

By (3.4), the corresponding force field on  $\mathcal{S}_{SH}$  is determined by the projection of  $\|\tilde{q}\|^3 F_V(\tilde{q})$  to  $T_q \mathcal{S}_{SH}$ , which is computed as

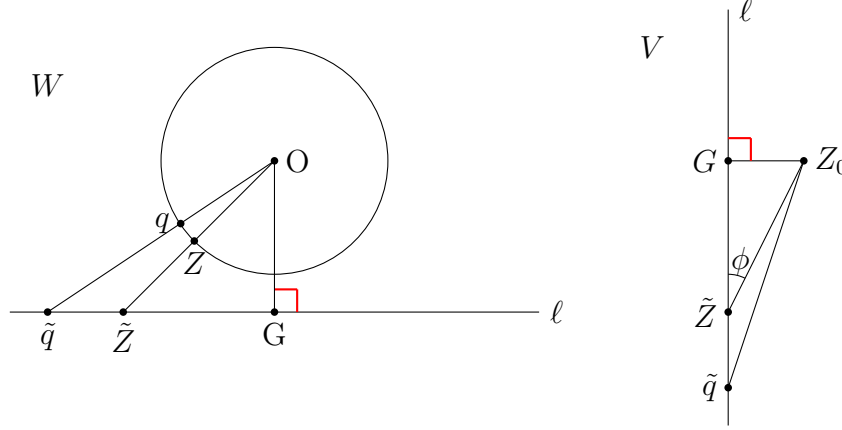
$$\|\tilde{q}\|^3 F_V(\tilde{q}) \cdot \cos \theta_G = \|\tilde{q}\|^3 F_V(\tilde{q}) \cdot \frac{\|G\|}{\|\tilde{q}\|} = \|\tilde{q}\|^3 F_V(\tilde{q}) \cdot \frac{\sqrt{1 + a^2 \sin^2 \phi}}{\|\tilde{q}\|} = \|\tilde{q}\|^2 \sqrt{1 + a^2 \sin^2 \phi} \cdot F_V(\tilde{q}),$$

where  $\theta_G = \angle \tilde{q}OG$ .

We now compute its norm as

$$\begin{aligned} & |m| \|\tilde{q}\|^2 \|\tilde{q} - \tilde{Z}\|^{-2} (1 + a^2)^{3/2} (1 + a^2 \sin^2 \phi)^{-1} \\ &= \sqrt{1 + a^2} |m| \|\tilde{q}\|^2 \|\tilde{Z}\|^2 \|\tilde{q} - \tilde{Z}\|^{-2} (1 + a^2 \sin^2 \phi)^{-1} \\ &= |\hat{m}| \|\tilde{q}\|^2 \|\tilde{Z}\|^2 \|\tilde{q} - \tilde{Z}\|^{-2} \|G\|^{-2} \\ &= |\hat{m}| \sin^{-2} \theta_Z. \end{aligned}$$

if we set  $m = \frac{\hat{m}}{\sqrt{1 + a^2}}$ . For the last equality we applied the law of sines for the triangle  $\tilde{q}O\tilde{Z}$ . The computation is illustrated in Figure 3.1.


 Figure 3.1: Sectional views on the planes  $W$  and  $V$ .

So after this computation we conclude that  $F_S$  is the central force field on  $\mathcal{S}_{SH}$  with strength  $|\hat{m}|\sin^{-2}\theta_Z$  in which  $\theta_Z$  is the central angle of  $q$  to  $Z$ , pointing toward  $Z$  or its antipodal point according to the sign of  $\hat{m}$ . This force field can be extended to the whole  $\mathcal{S}$  which is singular only at  $Z$  and its antipodal point, and is invariant under rotations along the line  $OZ$ . Restricting to a great circle passing through the point  $Z$  we conclude that this system is derived from the force function  $\hat{m}\cot\theta_Z$ .  $\square$

Note that among all homogeneous central force problems, this property of being projective invariant is unique for the Kepler problem [1].

### The Hooke Problems

The spherical Hooke problem is the system  $(\mathcal{S}, g_{st}, f \tan^2 \theta_Z)$  with  $f \in \mathbb{R}$ . This is seen to be the analytic extension of the projection  $(\mathcal{S}_{SH}, g_{st}, f \tan^2 \theta_Z)$  of the Hooke problem in the plane  $(V, \|\cdot\|, f\|\tilde{q}\|^2)$ . A special projective property of the Hooke problem is summarized in the following proposition. In contrast to the Kepler case, here we assume that the center for the Hooke problem is vertical *i.e.*  $Z = (0, 0, -1)$ .

**Proposition 5.** *The spherical Hooke problem  $(\mathcal{S}_{SH}, g_{st}, f \tan^2 \theta_Z)$  with  $Z = (0, 0, -1)$  projects to any of the Hooke problems in  $V$  of the form  $(V, \|\cdot\|_a, f\|\tilde{q}\|_a^2)$  for any  $a \in \mathbb{R}$ .*

*Proof.* The Hooke problem in  $V$  with respect to a norm  $\|\cdot\|_a$  is the system

$$(V, \|\cdot\|_a, f\|\tilde{q}\|_a^2).$$

The corresponding force field is given by

$$F_V(\tilde{q}) := 2f(\tilde{q} - Z).$$

A simple property which nevertheless worths to be mentioned, is that this force field is independent of  $a$ , *i.e.* this force field corresponds to *any* Hooke system of the above form.

The corresponding force field  $F_S$  on  $\mathcal{S}_{SH}$  is again determined by the central projection, and we obtain a central force field on  $\mathcal{S}_{SH}$  centered at  $Z$ , with the sign of  $f$  determines whether  $Z$  is attractive or repulsive just as in the planar case. Again, we just have to determine the norm of  $F_S$ . For this purpose, we restrict the system to any planes passing trough the center  $Z$  and the center  $O$  of  $\mathcal{S}_{SH}$ . With the same argument as in the proof of Proposition 4, we just have to compute the projection of  $\|\tilde{q}\|^3 F_V(\tilde{q})$  to the tangent space  $T_q \mathcal{S}_{SH}$ , given by

$$2f\|\tilde{q}\|^3 \cos \theta_Z(\tilde{q} - Z).$$

Its norm is computed as

$$2|f|\|\tilde{q}\|^3 \cos \theta_Z \|\tilde{q} - Z\| = 2|f| \frac{\cos \theta_Z \tan \theta_Z}{\cos^3 \theta_Z} = 2|f| \frac{\sin \theta_Z}{\cos^3 \theta_Z}.$$

By again restricting to a great circle passing trough the center  $Z$ , we get that this system has the force function  $f \tan^2 \theta_Z$ .  $\square$

### 3.3.3 The Lagrange Problems in the Plane and on the Sphere

The Lagrange problem in the plane  $\mathbb{R}^2$  is the system

$$(\mathbb{R}^2, \|\cdot\|, m_1/\|q - Z_1\| + m_2/\|q - Z_2\| + f\|q - (Z_1 + Z_2)/2\|^2), \quad (3.8)$$

with  $m_1, m_2, f \in \mathbb{R}$ , which is the superposition of two Kepler problems and a Hooke problem, with the Kepler centers placed symmetrically with respect to the Hooke center.

Similarly, we define the Lagrange problem on the sphere as the system

$$(\mathcal{S}, g_{st}, \hat{m}_1 \cot \theta_{Z_1} + \hat{m}_2 \cot \theta_{Z_2} + f \tan^2 \theta_{Z_{mid}}), \quad (3.9)$$

for which we assume that  $Z_2 \notin \{Z_1, -Z_1\}$ .  $\theta_P$  central angle of the moving particle to a point  $P \in \mathcal{S}$ ,  $Z_{mid}$  middle point of  $Z_1$  and  $Z_2$ .

Based on the previous Propositions 4 and 5, we see that the following remarkable theorem holds

**Theorem 8.** (Albouy [2]) *In the case  $Z_{mid}$  is vertical, then the spherical Lagrange problem on  $\mathcal{S}_{SH}$  with masses  $\hat{m}_1, \hat{m}_2, f$  is projected to a planar Lagrange problem in  $V$ , with the projections of the Kepler and Hooke centers as its own Kepler and Hooke centers, with the affine norm  $\|\cdot\|_a$  and parameters  $m_1, m_2, f$  as determined by Proposition 4.*

*Proof.* We assume that the  $Z_{mid}$  is vertical i.e.  $Z_{mid} = (0, 0, -1)$ . Additionally, for the normalization purpose, we set  $Z_1 = (0, a, -1)$  and  $Z_2 = (0, -a, -1)$ . We then define the norm in  $V$  as

$$\|q\|_a = \sqrt{x^2 + \frac{y^2}{1+a^2}}$$

for  $q = (x, y, -1)$ . The affine norm  $\|\cdot\|_a$  in  $V$  was chosen as common for all the three central force problems, two Kepler problems and a Hooke problem. By the principle of superposition, we may thus superpose them and the conclusion follows from the previous Propositions 4 and 5.  $\square$

As a consequence to Theorem 8, we have

**Proposition 6.** *The energy of the spherical Lagrange problem induces an additional first integral for the planar Lagrange problem independent of its energy. Vice versa, the energy of the planar Lagrange problem induces an additional first integral for the spherical Lagrange problem independent of its energy.*

*Proof.* The conservation of the energy of the planar problem in the spherical problem as well as the conservation of the energy of the spherical problem in the planar problem both follow from the fact that these systems are in correspondence, so their orbits in the configuration spaces are equivalent up to a time reparametrization.

To show their independence, we give their explicit expressions in a common chart as in [61]. To normalize our situation, we here again assume that  $Z_{mid} = (0, 0, -1)$ ,  $\tilde{Z}_1 = (0, a, -1)$ , and  $\tilde{Z}_2 = (0, -a, -1)$ . Then the planer energy for the Lagrange problem in  $V$  is described as

$$\begin{aligned} E_{pl} &= \frac{\|\dot{\tilde{q}}\|_a^2}{2} - f\|\tilde{q}\|_a^2 - \frac{m_1}{\|\tilde{q} - \tilde{Z}_1\|_a} - \frac{m_2}{\|\tilde{q} - \tilde{Z}_2\|_a} \\ &= \frac{1}{2} \left( \dot{\tilde{x}}^2 + \frac{\dot{\tilde{y}}^2}{1+a^2} \right) - f \left( \tilde{x}^2 + \frac{\tilde{y}^2}{1+a^2} \right) - \frac{m_1}{\sqrt{\tilde{x}^2 + \frac{(\tilde{y}-a)^2}{1+a^2}}} - \frac{m_2}{\sqrt{\tilde{x}^2 + \frac{(\tilde{y}+a)^2}{1+a^2}}}, \end{aligned}$$

where  $\tilde{q} = (\tilde{x}, \tilde{y}) \in V$  and  $(\dot{\tilde{x}}, \dot{\tilde{y}}) \in T_{\tilde{q}}V$

We now write the energy of the spherical problem in the gnomonic chart  $V$ . In  $\mathbb{R}^3$  the spherical kinetic energy is given by

$$\frac{x'^2 + y'^2 + z'^2}{2}, \quad (3.10)$$

where  $q = (x, y, z) \in \mathcal{S}_{SH}$  and  $(x', y', z') \in T_q\mathcal{S}_{SH}$ . Let  $q = (x, y, z) \in \mathcal{S}_{SH}$  and  $\tilde{q} = (\tilde{x}, \tilde{y} - 1) \in V$  be corresponded via the central projection as

$$x = \frac{\tilde{x}}{\sqrt{\tilde{x}^2 + \tilde{y}^2 + 1}}, \quad y = \frac{\tilde{y}}{\sqrt{\tilde{x}^2 + \tilde{y}^2 + 1}}, \quad z = -\frac{1}{\sqrt{\tilde{x}^2 + \tilde{y}^2 + 1}}.$$

Then the corresponding push-forward transformation from  $T_{\tilde{q}}V$  to  $T_q\mathcal{S}_{SH}$  is given by

$$\begin{pmatrix} x' \\ y' \\ z' \end{pmatrix} = \begin{pmatrix} \frac{\tilde{y}^2 + 1}{(\tilde{x}^2 + \tilde{y}^2 + 1)^{3/2}} & -\frac{\tilde{x}\tilde{y}}{(\tilde{x}^2 + \tilde{y}^2 + 1)^{3/2}} \\ -\frac{\tilde{x}\tilde{y}}{(\tilde{x}^2 + \tilde{y}^2 + 1)^{3/2}} & \frac{\tilde{x}^2 + 1}{(\tilde{x}^2 + \tilde{y}^2 + 1)^{3/2}} \\ \frac{\tilde{x}}{(\tilde{x}^2 + \tilde{y}^2 + 1)^{3/2}} & \frac{\tilde{y}}{(\tilde{x}^2 + \tilde{y}^2 + 1)^{3/2}} \end{pmatrix} \begin{pmatrix} \tilde{x}' \\ \tilde{y}' \end{pmatrix}$$

Using this, the projection of the spherical kinetic energy is represented as

$$\frac{(1 + \tilde{y}^2)\tilde{x}'^2 - 2\tilde{x}\tilde{y}\tilde{x}'\tilde{y}' + (1 + \tilde{x}^2)\tilde{y}'^2}{2(\tilde{x}^2 + \tilde{y}^2 + 1)^2}$$

at  $\tilde{q} = (\tilde{x}, \tilde{y}, -1) \in V$ . Remember that  $(\cdot)'$  is the time derivative with respect to the time parameter  $\tau$  defined as (3.3). From this, the spherical kinetic energy in the gnomonic chart has an expression [61]

$$K_{sp} := \frac{(1 + \tilde{y}^2)\dot{\tilde{x}}^2 - 2\tilde{x}\tilde{y}\dot{\tilde{x}}\dot{\tilde{y}} + (1 + \tilde{x}^2)\dot{\tilde{y}}^2}{2} = \frac{\dot{\tilde{x}}^2 + \dot{\tilde{y}}^2 + (\dot{\tilde{x}}\tilde{y} - \tilde{x}\dot{\tilde{y}})^2}{2}$$

at  $(\tilde{x}, \tilde{y}, -1) = (-x/z, -y/z, -1)$  in  $V$ , which can be seen as the combination of the planer kinetic energy and the squared angular momentum.

The spherical potential consists of the terms  $-f \tan^2 \theta_{Z_{mid}}$ ,  $-\hat{m}_1 \cot \theta_{Z_1}$ , and  $-\hat{m}_2 \cot \theta_{Z_2}$ . They are expressed in the gnomonic chart  $V$  as

$$-f(\tilde{x}^2 + \tilde{y}^2),$$

$$-\hat{m}_1 \frac{a\tilde{y} + 1}{\sqrt{(\tilde{y} - a)^2 + (1 + a^2)\tilde{x}^2}},$$

and

$$-\hat{m}_2 \frac{-a\tilde{y} + 1}{\sqrt{(\tilde{y} + a)^2 + (1 + a^2)\tilde{x}^2}},$$

respectively.

Combining these, we get the following expression of the spherical energy of the Lagrange problem in the gnomonic chart:

$$E_{sp} = \frac{(1 + \tilde{y}^2)\dot{\tilde{x}}^2 - 2\tilde{x}\tilde{y}\dot{\tilde{x}}\dot{\tilde{y}} + (1 + \tilde{x}^2)\dot{\tilde{y}}^2}{2} - \hat{m}_1 \frac{a\tilde{y} + 1}{\sqrt{(\tilde{y} - a)^2 + (1 + a^2)\tilde{x}^2}} - \hat{m}_2 \frac{-a\tilde{y} + 1}{\sqrt{(\tilde{y} + a)^2 + (1 + a^2)\tilde{x}^2}} - f(\tilde{x}^2 + \tilde{y}^2).$$

The functional independence of  $E_{pl}$  and  $E_{sp}$  now follows from these expressions. Indeed one can check that the Jacobi matrix

$$J := \begin{pmatrix} \frac{dE_{pl}}{d\tilde{x}} & \frac{dE_{pl}}{d\tilde{y}} & \frac{dE_{pl}}{d\dot{\tilde{x}}} & \frac{dE_{pl}}{d\dot{\tilde{y}}} \\ \frac{dE_{sp}}{d\tilde{x}} & \frac{dE_{sp}}{d\tilde{y}} & \frac{dE_{sp}}{d\dot{\tilde{x}}} & \frac{dE_{sp}}{d\dot{\tilde{y}}} \end{pmatrix}$$

has rank 2. To see this, it suffices to observe that the  $2 \times 2$  submatrix

$$\begin{pmatrix} \frac{dE_{pl}}{d\dot{\tilde{x}}} & \frac{dE_{pl}}{d\dot{\tilde{y}}} \\ \frac{dE_{sp}}{d\dot{\tilde{x}}} & \frac{dE_{sp}}{d\dot{\tilde{y}}} \end{pmatrix} = \begin{pmatrix} \dot{\tilde{x}} & \frac{\dot{\tilde{y}}}{1+a^2} \\ (\tilde{y}^2 + 1)\dot{\tilde{x}} - \tilde{x}\tilde{y}\dot{\tilde{y}} & -\tilde{x}\tilde{y}\dot{\tilde{x}} + (\tilde{x}^2 + 1)\dot{\tilde{y}} \end{pmatrix}$$

has rank 2.

Therefore we get an additional first integral for the planar problem from its corresponding spherical problem.

Similarly, the same argument equips the spherical problem in  $\mathcal{S}_{SH}$  with an additional first integral.

We now show that the projected planar energy to  $\mathcal{S}_{SH}$  extends to  $\mathcal{S}$  in an analytical way, outside of its singularities, thus the integrability extends to the problem on  $\mathcal{S}$ .

We first consider the kinetic energy and we provide a differently, more direct argument as in [61]. The planar kinetic energy at  $\tilde{q} = (\tilde{x}, \tilde{y}, -1)$  on  $V$  is given by

$$\frac{1}{2} \left( \dot{\tilde{x}}^2 + \frac{\dot{\tilde{y}}^2}{1 + a^2} \right) \quad (3.11)$$

for which we have taken the affine change of norm given by (3.5) into account. We now change the time parameter according to (3.3), then the above quantity can be rewritten into

$$\frac{1}{2} \left( \tilde{x}'^2 + \frac{\tilde{y}'^2}{1 + a^2} \right) (\tilde{x}^2 + \tilde{y}^2 + 1)^{-2}$$

Let  $q = (x, y, z) \in \mathcal{S}_{SH}$  be the centrally projected point of  $\tilde{q} = (\tilde{x}, \tilde{y}, -1) \in V$  on  $\mathcal{S}_{SH}$ . We have

$$\tilde{x} = -\frac{x}{z}, \quad \tilde{y} = -\frac{y}{z}.$$

Then the push-forward transformation from  $T_q\mathcal{S}_{SH}$  to  $T_{\tilde{q}}V$  is given by

$$\begin{pmatrix} \tilde{x}' \\ \tilde{y}' \end{pmatrix} = \begin{pmatrix} -\frac{1}{z} & 0 & \frac{x}{z^2} \\ 0 & -\frac{1}{z} & \frac{y}{z^2} \end{pmatrix} \begin{pmatrix} x' \\ y' \\ z' \end{pmatrix}.$$

Using this, we obtain the transformed expression of the planer kinetic energy (3.11) defined on  $\mathcal{S}_{SH}$  given by

$$\frac{((a^2 + 1)x'^2 + y'^2)z^2 - 2z'((a^2 + 1)xx' + yy')z + z'^2((a^2 + 1)x^2 + y^2)}{2(a^2 + 1)}. \quad (3.12)$$

at  $q = (x, y, z) \in \mathcal{S}_{SH}$ . Realize that this expression (3.12) of the planer kinetic energy can be analytically extended to the whole sphere  $\mathcal{S}$ .

For the potential

$$-\frac{m_1}{\sqrt{\tilde{x}^2 + \frac{(\tilde{y}-a)^2}{1+a^2}}} - \frac{m_2}{\sqrt{\tilde{x}^2 + \frac{(\tilde{y}+a)^2}{1+a^2}}} - f\left(\tilde{x}^2 + \frac{\tilde{y}^2}{1+a^2}\right)$$

of the planer Lagrange problem in  $V$ , just as in [61] we apply the change of coordinates

$$\tilde{x} = -\frac{x}{z}, \quad \tilde{y} = -\frac{y}{z}$$

which is derived from the central projection:  $V \ni (\tilde{x}, \tilde{y}, -1) \mapsto (x, y, z) \in \mathcal{S}_{SH}$ , and obtain the projected representation

$$-\frac{m_1 z}{\sqrt{\frac{a^2 x^2 - a^2 z^2 - 2a y z + x^2 - y^2}{(a^2 + 1)}}} - \frac{m_2 z}{\sqrt{\frac{a^2 x^2 - a^2 z^2 + 2a y z + x^2 - y^2}{(a^2 + 1)}}} - f\left(\frac{(a^2 + 1)x^2 + y^2}{(a^2 + 1)z^2}\right) \quad (3.13)$$

defined on  $\mathcal{S}_{SH}$ . This quantity can be analytically extended to the whole unit sphere  $\mathcal{S}$ , outside its singularities, which are the Kepler centers and their antipodal points and the horizontal equator  $\{(x, y, z) \in \mathcal{S} \mid z = 0\}$ , when the corresponding mass parameter is not zero.  $\square$

## 3.4 Integrable Lagrange Billiards

### 3.4.1 Billiard Correspondence at Confocal Conic Sections

In this subsection, we consider the problem of projective correspondence of a reflection wall  $\tilde{B}$  in  $V$  and its corresponding reflection wall  $B$  in  $\mathcal{S}_{SH}$ . Recall

that in this case a projective correspondence refers to the property that the laws of reflection in  $V$  and on  $\mathcal{S}_{SH}$  correspond to each other via the central projection. When this holds, then the billiard trajectories correspond to each other. This property does not hold for general reflection wall  $\tilde{B} \subset V$ . In this section we show that this nevertheless holds for any conic sections in  $V$  centered at  $(0, 0, -1)$ , with respect to a *compatible*  $\|\cdot\|_*$  in  $V$ , meaning that the  $\|\cdot\|$ -distance of the foci of the conic section, defined with respect to  $\|\cdot\|_*$ , equals  $2a$ .

**Proposition 7.** *Any centered confocal conic section  $\tilde{B} \subset V$  is projected to a centered confocal conic section  $B \subset \mathcal{S}_{SH}$ . The foci of  $B$  are the projection of the foci of  $\tilde{B}$  by the central projection. The law of reflection at  $\tilde{B}$  with respect to a compatible  $\|\cdot\|_*$  and the law of reflection at  $B \subset \mathcal{S}_{SH}$  correspond to each other.*

*Proof.* Since spherical Kepler problems in  $\mathcal{S}_{SH}$  and planer Kepler problems are in correspondence as described in Proposition 4, their orbits are projected to each other up to some time parametrization. Any connected component of confocal conic sections in a plane/on a sphere is an orbit of the planer/spherical Kepler problem with the center at one of the foci. Indeed any confocal ellipse and branch of any confocal hyperbola are orbits of Kepler problems with positive mass-factor, and for hyperbolas, the other branch is obtained as an orbit of Kepler problem with negative mass-factor. Each connected component of a confocal conic sections is projected to a connected component of a conic section with a focus at the projected center which is an orbit of the spherical/planer Kepler problem with the corresponding projected center. We now look at the other focus and its correspondence. For this purpose, we regard the same conic section as an orbit of the planer/spherical Kepler but with the center at the other focus. Then from the same projective argument, one can see that the other focus is also projected from the corresponding focus.

We will now check the projective correspondence between the laws of reflection at confocal conic sections in  $V$  and on  $\mathcal{S}_{SH}$ . We first construct such reflection walls in  $V$  and on  $\mathcal{S}_{SH}$ .

For the normalization purpose, we set two foci  $\tilde{Z}_1 = (0, a, -1)$ , and  $\tilde{Z}_2 = (0, -a, -1)$  in  $V$ , then the norm  $\|\cdot\|_a$  in  $V$  should be chosen as (3.5).

We consider a centered elliptic cone given by

$$\frac{x^2}{\tan^2 \alpha} + \frac{y^2}{\tan^2 \beta} - z^2 = 0, \quad (3.14)$$

with  $\alpha, \beta \in [0, \pi/2]$  such that

$$1 + a^2 = \frac{\tan^2 \beta + 1}{\tan^2 \alpha + 1}. \quad (3.15)$$

The intersection of  $V$  and the cone (3.14) gives a centered ellipse

$$\tilde{F} := \frac{\tilde{x}^2}{\tan^2 \alpha} + \frac{\tilde{y}^2}{\tan^2 \beta} - 1 = 0$$

defined in  $V$ . The foci  $(0, c), (0, -c)$  of the ellipse  $\tilde{F} = 0$  depends on the involved norm, and is computed as

$$\frac{c^2}{1 + a^2} = \frac{\tan^2 \beta}{1 + a^2} - \tan^2 \alpha \Leftrightarrow c^2 = a^2$$

This means the foci are at two centers  $\tilde{Z}_1$  and  $\tilde{Z}_2$ , thus the ellipse  $\tilde{F} = 0$  is confocal.

From the first and the second statement of this proposition, the intersection of this elliptic cone (3.14) and  $\mathcal{S}_{SH}$  is again a confocal ellipse on  $\mathcal{S}_{SH}$  and is given by the equation

$$F := \frac{x^2}{\sin^2 \alpha} + \frac{y^2}{\sin^2 \beta} - 1 = 0. \quad (3.16)$$

To see the projective correspondence of elastic reflections, we show that velocities before and after the reflection at  $F = 0$  on  $\mathcal{S}_{SH}$  is projected to velocities before and after the reflection at  $\tilde{F} = 0$  in  $V$ . Unfortunately we have not found a geometrical way to see this. Here we provide a proof with a direct computation.

Set

$$q := (x, y, z) = \left( \sin \alpha \cos \theta, \sin \beta \sin \theta, -\sqrt{1 - \sin^2 \alpha \cos^2 \theta - \sin^2 \beta \sin^2 \theta} \right)$$

which lies in a confocal ellipse  $F = 0$  on  $\mathcal{S}_{SH}$ . The tangent vector to the ellipse at the point  $q$  is given by

$$s := \left( -\sin \alpha \sin \theta, \sin \beta \cos \theta, -\frac{(\sin^2 \alpha - \sin^2 \beta) \sin \theta \cos \theta}{\sqrt{1 - \sin^2 \alpha \cos^2 \theta - \sin^2 \beta \sin^2 \theta}} \right),$$

and the normal vector is given by

$$n := \left( \frac{\sin \alpha \cos \theta}{\tan^2 \alpha}, \frac{\sin \beta \sin \theta}{\tan^2 \beta}, \sqrt{1 - \sin^2 \alpha \cos^2 \theta - \sin^2 \beta \sin^2 \theta} \right).$$

When the velocity vectors before the reflection at  $q$  is given as

$$v = k_1 \cdot s + k_2 \cdot n,$$

where  $k_1, k_2 \in \mathbb{R}$  are coefficients, then the reflected vector becomes as

$$w = k_1 \cdot s - k_2 \cdot n,$$

Clearly, tangent vectors are projected to tangent vectors along the reflection walls. To see that  $v$  and  $w$  are projected to velocities before and after the elastic reflection at the corresponding point  $\tilde{q}$  in  $\tilde{F} = 0$ , we observe that it suffices to check that the normal vector  $n$  is projected to the corresponding normal vector at  $\tilde{q} \in V$  with respect to the corresponding metric on  $V$ , since then  $v$  and  $w$  are projected to vectors in  $V$  having the same tangential component and opposite normal components.

The point  $q$  lying in  $F = 0$  is projected to the point

$$\begin{aligned} \tilde{q} &:= \left( -\frac{x}{z}, -\frac{y}{z}, -1 \right) \\ &= \left( \frac{\sin \alpha \cos \theta}{\sqrt{1 - \sin^2 \alpha \cos^2 \theta - \sin^2 \beta \sin^2 \theta}}, \frac{\sin \beta \sin \theta}{\sqrt{1 - \sin^2 \alpha \cos^2 \theta - \sin^2 \beta \sin^2 \theta}}, -1 \right) \end{aligned}$$

lying in  $\tilde{F} = 0$ .

The corresponding push-forward transformation from  $T_q \mathcal{S}_{SH}$  to  $T_{\tilde{q}} V$  is given by

$$\begin{pmatrix} \tilde{x}' \\ \tilde{y}' \end{pmatrix} = \begin{pmatrix} \frac{1}{\sqrt{(\cos^2 \alpha - \cos^2 \beta) \cos^2 \theta + \cos^2 \beta}} & 0 & \frac{\sin \alpha \cos \theta}{(\cos^2 \alpha - \cos^2 \beta) \cos^2 \theta + \cos^2 \beta} \\ 0 & \frac{1}{\sqrt{(\cos^2 \alpha - \cos^2 \beta) \cos^2 \theta + \cos^2 \beta}} & \frac{\sin \beta \cos \theta}{(\cos^2 \alpha - \cos^2 \beta) \cos^2 \theta + \cos^2 \beta} \end{pmatrix} \begin{pmatrix} x' \\ y' \\ z' \end{pmatrix}$$

Using this, the tangent vector  $s$  is projected to the (tangent) vector

$$\tilde{s} = \frac{1}{(\cos^2 \alpha - \cos^2 \beta) \cos^2 \theta + \cos^2 \beta} (-\sin \alpha \cos^2 \beta \sin \theta, \sin \beta \cos^2 \alpha \cos \theta)$$

and the normal vector  $n$  is projected to the vector

$$\tilde{n} = \frac{1}{\sin \alpha \sin \beta (\cos^2 \alpha - \cos^2 \beta) \cos^2 \theta + \cos^2 \beta} (\sin \beta \cos \theta, \sin \alpha \sin \theta).$$

We ignore the factors and take

$$\begin{aligned} \hat{s} &= (-\sin \alpha \cos^2 \beta \sin \theta, \sin \beta \cos^2 \alpha \cos \theta), \\ \hat{n} &= (\sin \beta \cos \theta, \sin \alpha \sin \theta). \end{aligned}$$

Their inner product with respect to  $\|\cdot\|_a$  is

$$\langle \hat{s}, \hat{n} \rangle_a = -\sin \alpha \sin \beta \cos^2 \beta \sin \theta \cos \theta + \frac{\tan^2 \alpha + 1}{\tan^2 \beta + 1} \sin \alpha \sin \beta \cos^2 \alpha \sin \theta \cos \theta = 0.$$

They are thus orthogonal. Hence, the projection  $\tilde{n}$  of  $n$  is indeed a normal vector at  $\tilde{q} \in \{\tilde{F} = 0\}$  in  $V$ .

Thus, the law of reflection at centered confocal ellipses in  $V$  and the law of reflection at centered confocal ellipses on  $\mathcal{S}_{SH}$  correspond to each other. The case of reflections at centered confocal hyperbolae is completely analogous.  $\square$

### 3.4.2 Integrability of Lagrange Billiards with Confocal Conic Section Reflection Walls

We now prove Theorem 7 for the planar and spherical problems.

*Proof.* From Proposition 7, we know the spherical and planer law of reflection at centered confocal conic sections are in correspondence, meaning that the incoming and the outgoing velocity vectors of an elastic reflection against such reflection walls in the plane are projected again to the incoming and outgoing velocity vectors of an elastic reflection against the corresponding reflection walls on the sphere, up to a time change which depends only on the point of reflection. Therefore the billiard trajectories on the sphere are projected to billiard trajectories in the plane in our situation, in which the underlying mechanical systems are in correspondence. As a consequence, the energy of the spherical system, written in the gnomonic chart  $V$ , is invariant under the reflections at a corresponding confocal conic section in  $V$ . Also, the energy of the planar system, while being expressed on  $\mathcal{S}_{SH}$  and further extended to  $\mathcal{S}$ , is invariant under the reflections on  $\mathcal{S}$  at a corresponding confocal conic section on the sphere. We get additional first integrals for both billiard systems independent of their energies. The proof is completed.  $\square$

### 3.4.3 Subcases of Integrable Lagrange Billiards

#### The integrable free billiards

The case  $m_1 = m_2 = f = 0$  of the system (3.8), and the case  $\hat{m}_1 = \hat{m}_2 = f = 0$  of the system (3.9) correspond respectively to the cases of free motions in the plane and on the sphere. We recover the classical theorem of Birkhoff in the planar and spherical case.

**Corollary 8.** *The free billiards in the plane and on the sphere with any combination of confocal conic section reflection walls are integrable.*

### The integrable Hooke billiards

The case  $m_1 = m_2 = 0, f \neq 0$  of the system (3.8), and the case  $\hat{m}_1 = \hat{m}_2 = 0, f \neq 0$  of the system (3.9) correspond respectively to the Hooke problems in the plane and on the sphere. In this case we recover the following theorem:

**Corollary 9.** *The Hooke billiards in the plane and on the sphere with any combination of confocal conic section reflection walls centered at the Hooke center are integrable.*

### The integrable Kepler billiards

The case  $m_1 = f = 0, m_2 \neq 0$  of the system (3.8), and the case  $\hat{m}_1 = f = 0, \hat{m}_2 \neq 0$  of the system (3.9) correspond respectively to the Kepler problems in the plane and on the sphere. In this case we recover the following theorem:

**Corollary 10.** *The Kepler billiards in the plane and on the sphere with any combination of confocal conic section reflection walls focused at the Kepler center are integrable.*

### The integrable Two-Center billiards

The case  $m_1, m_2 \neq 0, f = 0$  of the system (3.8), and the case  $\hat{m}_1, \hat{m}_2 \neq 0, f = 0$  of the system (3.9) correspond respectively to the two-center problems in the plane and on the sphere. In this case we recover the following theorem:

**Theorem 9.** *The billiards defined with the two-center problems in the plane and on the sphere with any combination of confocal conic section reflection walls focused at the two centers are integrable.*

### The integrable billiards with superposition of Hooke and Kepler Problems

The case  $m_1, f \neq 0, m = 0$  of the system (3.8), and the case  $\hat{m}_1, f \neq 0, \hat{m}_2 = 0$  of the system (3.9) correspond respectively to the superposition of a Hooke and a Kepler problems in the plane and on the sphere. In this case we recover the following theorem:

**Corollary 11.** *The billiards defined with the superposition of a Hooke and a Kepler problems in the plane and on the sphere with any combination of confocal conic section reflection walls focused the Kepler center and centered at the Hooke center are integrable.*

## 3.5 The Plane-Hyperboloid Projection and integrable Lagrange Billiards in the Hyperbolic Plane

We now discuss the projection between the plane and the hyperbolic space, with the hyperboloid model for the latter.

### 3.5.1 The Hyperboloid-Plane Projection

We consider the Minkowski space  $\mathbb{R}^{2,1}$ , equipped with the pseudo-Riemannian metric

$$dx^2 + dy^2 - dz^2. \quad (3.17)$$

Consider the embedded two-sheeted hyperboloid given by the equation

$$\mathcal{H} := \{(x, y, z) \in \mathbb{R}^{2,1} \mid x^2 + y^2 - z^2 = -1\}$$

and its lower sheet

$$\mathcal{H}_S := \{(x, y, z) \in \mathcal{H} \mid z < 0\}.$$

The restriction of the pseudo-Riemannian metric  $dx^2 + dy^2 - dz^2$  to  $\mathcal{H}$  is Riemannian, and equipped both sheets of  $\mathcal{H}$  with a *hyperbolic metric*. The space  $\mathcal{H}_S$  equipped with this hyperbolic metric is called the hyperboloid model of the hyperbolic plane.

We consider the plane  $V_H = \{z = -1\} \subset \mathbb{R}^{2,1}$  which is tangent to  $\mathcal{H}_S$  at its pole  $(0, 0, -1)$ . The central projection from the origin of  $\mathbb{R}^{2,1}$  projects the lower sheet of hyperboloid  $\mathcal{H}_S$  onto the unit disc  $D := \{(x, y) \in V_H \mid x^2 + y^2 < 1\}$  in  $V$ , and equips  $D$  with an induced hyperbolic metric, making it the Klein disc model for the hyperbolic plane.

We denote by  $\|\cdot\|_H$  the Minkowski norm in  $\mathbb{R}^{2,1}$ . Just as in the case of spherical-plane correspondence in Section 3.3.1, a force field  $F_H$  on  $\mathcal{H}_S$  is carried to a force field  $F_V$  on  $V$  by the central projection.

Indeed, in this setting, a point  $q \in \mathcal{H}_S$  is centrally projected to the point  $\tilde{q} \in V_H$ :

$$q = \|\tilde{q}\|_H^{-1} \tilde{q}.$$

Suppose we have a natural mechanical system in  $V_H$  with the equations of motion

$$\ddot{\tilde{q}} = F_V(\tilde{q}).$$

Thus we have

$$\dot{q} = \|\tilde{q}\|_H^{-2} (\dot{\tilde{q}} \|\tilde{q}\|_H - \langle \nabla \|\tilde{q}\|_H, \dot{\tilde{q}} \rangle \tilde{q}).$$

Again, we take a new time variable  $\tau$  for the system on  $\mathcal{H}_S$ , and write  $' := \frac{d}{d\tau}$  so that

$$\frac{d}{d\tau} = \|\tilde{q}\|_H^2 \frac{d}{dt}, \quad (3.18)$$

and consequently

$$q' = (\dot{\tilde{q}}\|\tilde{q}\|_H - \langle \nabla\|\tilde{q}\|_H, \dot{\tilde{q}} \rangle_H \tilde{q}),$$

$$q'' = \|\tilde{q}\|_H^2 (\ddot{\tilde{q}}\|\tilde{q}\|_H - (\langle \nabla\|\tilde{q}\|_H, \ddot{\tilde{q}} \rangle + \langle (\nabla\|\tilde{q}\|_H), \dot{\tilde{q}} \rangle) \tilde{q}).$$

We thus have

$$q'' = \|\tilde{q}\|_H^2 (F_V(\tilde{q})\|\tilde{q}\|_H - \lambda(\tilde{q}, \dot{\tilde{q}}, \ddot{\tilde{q}})\tilde{q}) \quad (3.19)$$

in which we have set  $\lambda(\tilde{q}, \dot{\tilde{q}}, \ddot{\tilde{q}}) = \langle \nabla\|\tilde{q}\|_H, \ddot{\tilde{q}} \rangle + \langle (\nabla\|\tilde{q}\|_H), \dot{\tilde{q}} \rangle$ . The gradient and the inner product are defined with respect to the pseudo-Riemannian metric (3.17).

The Levi-Civita connection of a pseudo-Riemannian manifold projects to the Levi-Civita connection of its embedded submanifold. In our case,  $\mathcal{H}_S$  is Riemannian with the induced metric from  $\mathbb{R}^{2,1}$ . So again by projecting both sides of this equation to the tangent space  $T_q\mathcal{H}_S$ , we get the equations of motion of the form

$$\nabla_{q'} q' = F_H(q).$$

We see that to switch from the plane-sphere correspondence as in Section 3.3.1 to the plane-hyperboloid correspondence with our setting, it is enough to properly change some signs in proper places while the others are completely similar. We shall make use of this similarity in the sequel to omit certain details.

### 3.5.2 Projective Properties of the Hooke and Kepler Problems in the Hyperbolic Plane

#### The Kepler Problems and the Hooke Problems

We first discuss the case of the Kepler problems. The hyperbolic Kepler problem is the natural mechanical system  $(\mathcal{H}_S, g_H, \hat{m} \coth \theta_Z)$ , in which  $g_H$  is the induced hyperbolic metric on  $\mathcal{H}_S$ ,  $\hat{m} \in \mathbb{R}$  is the mass-factor and the angle  $\theta_Z$  is the central hyperbolic angle the moving particle made with the center  $Z \in \mathcal{H}_S$ .

Without loss of generality, we set  $Z = \left(0, \frac{a}{\sqrt{1-a^2}}, -\frac{1}{\sqrt{1-a^2}}\right) \in \mathcal{H}_S$  for  $a \in (-1, 1)$ , and  $\tilde{Z} = (0, a, -1)$  the projection point of  $Z$  in  $D \subset V_H$ . For

$\tilde{q} = (\tilde{x}, \tilde{y}, -1) \in V_H$  we define

$$\|\tilde{q}\|_a = \sqrt{\tilde{x}^2 + \frac{\tilde{y}^2}{1-a^2}}. \quad (3.20)$$

Similar to the case of plane-spherical correspondence, we have

**Proposition 8.** *The hyperbolic Kepler problem  $(\mathcal{H}_S, g_H, \hat{m} \coth \theta_Z)$  projects to the planar Kepler problem  $(V_H, \|\cdot\|_a, m/\|\tilde{q} - \tilde{Z}\|_a)$  such that  $m = \frac{\hat{m}}{\sqrt{1-a^2}}$ .*

By analyticity, a proof of this proposition follows from Proposition 4 by formally substituting  $(x, y, a, z)$  by  $(ix, iy, ia, z)$  and argue with the equations of motion. The geometric proof of Proposition 4 also carries over to this hyperbolic case, but now using hyperbolic geometry.

Our second case is the Hooke problems. The hyperbolic Hooke problem is the natural mechanical systems given by  $(\mathcal{H}_S, g_H, f \tanh^2 \theta_Z)$  with the mass-factor  $f \in \mathbb{R}$ .

Analogously as in the Kepler case, we get the following correspondences between Hooke systems.

**Proposition 9.** *The hyperbolic Hooke problem  $(\mathcal{H}_S, g_H, f \tanh^2 \theta_Z)$  with  $Z = (0, 0, -1)$  projects to any of the Hooke problems in  $V$  of the form  $(V_H, \|\cdot\|_a, f\|\tilde{q}\|_a^2)$  for any  $a \in \mathbb{R}$ .*

In contrast to the Kepler case, we can freely choose the parameter  $a$  in the affine changed norm  $\|\cdot\|_a$  for the Hooke problems.

### 3.5.3 The Lagrange Problems in the Plane and in the Hyperbolic Plane

By superposing two hyperbolic Kepler problems and a hyperbolic Hooke problem, we obtain the hyperbolic Lagrange problem

$$(\mathcal{H}, g_H, \hat{m}_1 \coth \theta_{Z_1} + \hat{m}_2 \coth \theta_{Z_2} + f \tanh^2 \theta_{Z_{mid}}),$$

for which we assume that  $Z_1$  and  $Z_2$  are in the same sheet of two-sheeted hyperboloid  $\mathcal{H}$ . Here,  $\theta_P$  is a hyperbolic central angle of the moving particle to a point  $P \in \mathcal{H}$

By combining the previous Propositions 8 and 9, we get the following correspondence on the Lagrange problems in the plane and in the hyperbolic plane as an analogy of the spherical case.

**Theorem 10.** *In the case  $Z_{mid}$  is vertical, then the hyperbolic Lagrange problem on  $\mathcal{S}_H$  with masses  $\hat{m}_1, \hat{m}_2, f \in \mathbb{R}$  is projected to the planer Lagrange problem in  $V_H$ , with the projections of the Kepler and the Hooke centers as its own Kepler and Hooke centers, with the affine norm  $\|\cdot\|_a$  and parameters  $m_1, m_2, f$  as determined by Proposition 8.*

From this theorem, we get the following proposition as a consequence.

**Proposition 10.** *The energy of the hyperbolic Lagrange problem induces an additional first integral for the planer Lagrange problem independent of its energy. Vice versa, the energy of the planer Lagrange problem induces an additional first integral for the hyperbolic Lagrange problem independent of its energy.*

### 3.5.4 Integrable Lagrange Billiards in the Hyperbolic Plane

We here consider the presence of a confocal conic section reflection wall  $\tilde{B}$  in  $V_H$  and its corresponding reflection wall  $B$  in  $\mathcal{H}_S$ . The proof goes analogously as in the case of plane-spherical correspondence.

**Proposition 11.** *Any confocal conic section  $\tilde{B} \subset V_H$  is projected to a confocal conic section  $B \subset \mathcal{H}_S$ . The foci of  $B$  are the projection of the foci of  $\tilde{B}$  by the central projection. The law of reflection at  $\tilde{B}$  with respect to a compatible  $\|\cdot\|_*$  and the law of reflection at  $B \subset \mathcal{H}_S$  correspond each other.*

### 3.5.5 Proof of Theorem 7 in the Hyperbolic Case and the Subcases

With all these ingredients, the proof of Theorem 7 for the spherical and planar case from Section 3.4.2 carries directly to the hyperbolic case as well, which completes the proof of Theorem 7 in all cases.

Also, the subcases as listed in Section 3.4.3 carries to integrable systems defined on the hyperbolic plane as well.

## 3.6 The Complex Square Mapping and Hooke-Kepler Correspondence in the Hyperbolic Space and on the Sphere

The classical conformal correspondence between the planar Hooke and Kepler problems via the complex square mapping has been generalized to conformal

correspondences among the Hooke problems defined on the sphere, in the hyperbolic plane, and the Kepler problem defined in the hyperbolic plane by Nersessian and Pogosyan [41]. We explain that these conformal correspondences extend to integrable billiards defined with these natural mechanical systems.

We take the plane  $\{z = 0\}$  as a stereographic chart from the North pole  $(0, 0, 1)$  of the unit sphere  $\mathcal{S}$ . For the hyperbolic plane we take the Poincaré disc model in the unit disc in the plane  $\{z = 0\}$ , seen as projection of the hyperboloid model from the "North pole"  $(0, 0, 1)$ . We identify the plane  $\{z = 0\}$  with  $\mathbb{C}$  in which the Poincaré disc is  $\mathcal{D} := \{w \in \mathbb{C} \mid |w| < 1\}$ .

The round metric on  $\mathcal{S}$  is represented in the stereographic chart as

$$\frac{4}{(1 + |q|^2)^2} dq d\bar{q}. \quad (3.21)$$

Analogously the Poincaré disk  $\mathcal{D}$  is equipped with the hyperbolic metric

$$\frac{4}{(1 - |q|^2)^2} dq d\bar{q}. \quad (3.22)$$

The spherical kinetic energy in the stereographic chart is thus

$$\frac{(1 + |q|^2)^2 |p|^2}{8}$$

by using the cometric of (3.21). In this stereographic chart, the force functions of the spherical Hooke and spherical Kepler problems are given respectively as

$$-\frac{4f|q|^2}{(1 - |q|^2)^2}$$

and

$$\hat{m} \frac{1 - |q|^2}{2|q|},$$

respectively, with  $f, \hat{m} \in \mathbb{R}$ . Analogously, the hyperbolic kinetic energy in the Poincaré disk  $\mathcal{D}$  is

$$\frac{(1 - |q|^2)^2 |p|^2}{8},$$

with the force functions of the hyperbolic Hooke and hyperbolic Kepler problems

$$-\frac{4f|q|^2}{(1 + |q|^2)^2}$$

and

$$\hat{m} \frac{1 + |q|^2}{2|q|},$$

respectively, with  $f, \hat{m} \in \mathbb{R}$ .

**Proposition 12.** (*Nersessian-Pogosyan [41]*) *The spherical Hooke problem, the hyperbolic Hooke problem, and the hyperbolic Kepler problem are mutually in conformal correspondence.*

*Proof.* We start with the Hamiltonian of the spherical/hyperbolic Hooke problem

$$\frac{(1 \pm |z|^2)^2 |w|^2}{8} + \frac{4f|z|^2}{(1 \mp |z|^2)^2} - \hat{m} = 0$$

restricted to its  $\hat{m}$ -energy hypersurface. The signs determine whether it is the spherical or the hyperbolic problem we are considering. By multiplying both sides by  $\frac{(1 \mp |z|^2)^2}{|z|^2}$ , we get

$$\frac{(1 - |z|^4)^2 |w|^2}{8|z|^2} + 4f - \hat{m} \frac{(1 \mp |z|^2)^2}{|z|^2} = 0$$

We now apply the conformal transformation  $(z, w) \mapsto (z^2, w/2\bar{z}) := (p, q)$  and the transformed Hamiltonian becomes

$$\frac{(1 - |q|^2)^2 |p|^2}{8} + 4f - \hat{m} \frac{(1 \mp |q|)^2}{|q|} = 0.$$

after a proper time change. As we can rewrite this system into

$$\frac{(1 - |q|^2)^2 |p|^2}{8} + 4f - \hat{m} \frac{1 + |q|^2}{|q|} \pm 2\hat{m} = 0,$$

this is the Hamiltonian of a hyperbolic Kepler problem restricted to the energy level with energy  $-(4f \pm 2\hat{m})$ .

The same trick, with a multiplicative factor of  $\frac{(1 \mp |q|^2)^2}{(1 \pm |q|^2)^2}$  gives a transformation between the spherical and hyperbolic Hooke problems restricted to energy levels. □

**Corollary 12.** *In the Poincaré disc in the plane  $\{z = 0\} \cong \mathbb{C}$ , the curve representing a branch of a conic section on the hyperboloid model focused at the “South pole”  $(0, 0, -1)$  is transformed via the complex square mapping  $:\mathbb{C} \rightarrow \mathbb{C} : z \mapsto z^2$  into a curve simultaneously representing a conic section centered at the “South pole” on the hyperboloid model, and part of a conic section defined on the hemisphere  $\mathcal{S}_{SH}$  centered at the South pole.*

*Proof.* This follows from Proposition 12, which implies that an orbit of the hyperbolic Kepler problem is sent to an orbit of the spherical/hyperbolic Hooke problem up to a time parametrization. Thus the conclusion of the corollary follows. □

We now show that any confocal family of centered spherical/hyperbolic conic sections is transformed into a confocal family of focused hyperbolic conic sections by this series of conformal transformations.

**Proposition 13.** *A family of confocal focused hyperbolic conic sections on  $\mathcal{H}_S$ , expressed in the Poincaré disc  $\mathcal{D}$  are transformed into a family of confocal centered spherical/hyperbolic conic sections in the stereographic chart/Poincaré disc in the plane  $\{z = 0\} \cong \mathbb{C}$  via the complex square mapping  $\mathbb{C} \rightarrow \mathbb{C} : z \mapsto z^2$ .*

*Proof.* We start with a family of confocal focused hyperbolic conic section on  $\mathcal{H}_S$ . Choose a parameter  $0 < a < 1$ , and suppose that a family of such hyperbolic conic sections has common centers at  $(0, \frac{a}{\sqrt{1-a^2}}, -\frac{1}{\sqrt{1-a^2}})$ .

We take a new set of orthogonal coordinates in the Minkowski space  $\mathbb{R}^{2,1}$  as

$$u = x, \quad v = \frac{y + az}{\sqrt{1 - a^2}}, \quad w = \frac{ay + z}{\sqrt{1 - a^2}},$$

The pseudo-Riemannian metric defined by (3.17) is expressed in these new coordinates as

$$du^2 + dv^2 - dw^2.$$

In this coordinates, the two-sheeted hyperboloid is given by the equation

$$\mathcal{H} = \{(u, v, w) \in \mathbb{R}^{2,1} \mid u^2 + v^2 - w^2 = -1\}.$$

The plane  $\hat{V} := \{w = -1\}$  is tangent to the hyperboloid  $\mathcal{H}$  at the the point  $(u, v, w) = (0, 0, -1)$ . We equip  $\hat{V}$  with the norm  $\|\cdot\|_a$  defined as

$$\|(\tilde{u}, \tilde{v})\|_a^2 = \tilde{u}^2 + \frac{\tilde{v}^2}{1 - a^2}$$

for  $(\tilde{u}, \tilde{v}) \in \hat{V}$ . We now consider the family of confocal centered ellipses in  $\hat{V}$  with foci at  $(0, -a, -1)$  and  $(0, a, -1)$  (with respect to  $\|\cdot\|_a$ ) given by the equation

$$\frac{\tilde{u}^2}{\frac{B^2 - a^2}{1 - a^2}} + \frac{\tilde{v}^2}{B^2} - 1 = 0, \tag{3.23}$$

where  $B > a$  is a positive parameter.

We now project this family of confocal centered ellipses in  $\hat{V}$  to the hyperboloid by the central projection. Let  $(u, v, w) \in \mathcal{H}_S$  be the centrally projected point of  $(\tilde{u}, \tilde{v}, -1)$ . Then we have

$$\tilde{u} = -\frac{u}{w}, \quad \tilde{v} = -\frac{v}{w},$$

and the transformed expression of the family of confocal ellipses is given by

$$\frac{u^2(1-a^2)}{w^2(B^2-a^2)} + \frac{v^2}{w^2B^2} - 1 = 0. \quad (3.24)$$

As an implication of the projective correspondence of the hyperbolic Kepler problem and the planer Kepler problem, the central projection projects the hyperbolic conic sections to conic sections in the plane and projects foci to foci when they are centered. Thus, the projected conic sections on  $\mathcal{H}_S$  is again confocal.

In the original coordinates  $(x, y, z)$  in  $\mathbb{R}^{2,1}$ , the equation (3.24) can be written as

$$\frac{x^2(1-a^2)^2}{(ay+z)^2(B^2-a^2)} + \frac{(y+az)^2}{(ay+z)^2B^2} - 1 = 0.$$

We now rewrite this in the coordinates  $(q_1, q_2)$  in the Poincaré disc  $\mathcal{D}$  with the stereographic projection

$$x = \frac{2q_1}{1-q_1^2-q_2^2}, \quad y = \frac{2q_2}{1-q_1^2-q_2^2}, \quad z = -\frac{1+q_1^2+q_2^2}{1-q_1^2-q_2^2},$$

which transforms the equation of the confocal focused hyperbolic conic sections in the Poincaré disc  $\mathcal{D}$  into

$$\frac{4(1-a^2)q_1^2}{(B^2-a^2)(2aq_2-q_1^2-q_2^2-1)^2} + \frac{(-2q_2+a(q_1^2+q_2^2+1))^2}{B^2(2aq_2-q_1^2-q_2^2-1)^2} - 1 = 0.$$

We now apply the complex square mapping. Set

$$q_1 + iq_2 = (z_1 + iz_2)^2.$$

and the above equation is now

$$\frac{4(1-a^2)^2(z_1^2-z_2^2)^2}{(B^2-a^2)(-z_1^4-2z_1^2z_2^2-z_2^4+4az_1z_2-1)^2} + \frac{-4z_1z_2+a(z_1^4+2z_1^2z_2^2+z_2^4+1))^2}{B^2(-z_1^4-2z_1^2z_2^2-z_2^4+4az_1z_2-1)^2} - 1 = 0.$$

Suppose that  $(z_1, z_2) \in \mathcal{D}$  corresponds to the point  $(x, y, z) \in \mathcal{S}_{SH}$  via stereographic projection:

$$z_1 = -\frac{x}{z}, \quad z_2 = -\frac{y}{z}.$$

Then the above equation can be equivalently written as

$$\frac{4(1-a^2)^2(-1+z)^4(x^2-y^2)^2}{(B+a)(B-a)(z^4-4z^3+(-4xya+6)z^2+(8xya-4)z+x^4+2x^2y^2+y^4-4axy+1)^2} + \frac{(z^4a-4z^3a+(-4xy+6a)z^2+(8xy-4a)z+(x^4+2x^2y^2+y^4+1)a-4xy)^2}{B^2(z^4-4z^3+(-4xya+6)z^2+(8xya-4)z+x^4+2x^2y^2+y^4-4axy+1)^2} - 1 = 0. \quad (3.25)$$

In order to see that this equation determines spherical conic sections with common centers at the “South pole” and common foci, we project them to the plane  $V = \{z = -1\}$  by the central projection and examine their images therein. In the gnomonic chart  $V$ , the above equation is expressed with coordinates  $(\tilde{x}, \tilde{y}, -1) \in V$  as

$$x = \frac{\tilde{x}}{\sqrt{\tilde{x}^2 + \tilde{y}^2 + 1}}, \quad y = \frac{\tilde{y}}{\sqrt{\tilde{x}^2 + \tilde{y}^2 + 1}}, \quad z = -\frac{1}{\sqrt{\tilde{x}^2 + \tilde{y}^2 + 1}}.$$

By using Maple, this can be factorized into

$$\begin{aligned} & 4((4\tilde{x}^2 + 4\tilde{y}^2 + 8)\sqrt{\tilde{x}^2 + \tilde{y}^2 + 1} + \tilde{x}^4 + (2\tilde{y}^2 + 8)\tilde{x}^2 + \tilde{y}^4 + 8\tilde{y}^2 + 8)(1 + \tilde{x}^2 + \tilde{y}^2) \\ & \times \left( -\frac{(-a^2 + B)(B + 1)\tilde{x}^2}{2} + a\tilde{y}(B - 1)(B + 1)\tilde{x} - \frac{(-a^2 + B)(B + 1)\tilde{y}^2}{2} - B^2 + a^2 \right) \\ & \times \left( -\frac{(a^2 + B)(B - 1)\tilde{x}^2}{2} + a\tilde{y}(B - 1)(B + 1)\tilde{x} - \frac{(a^2 + B)(B + 1)\tilde{y}^2}{2} - B^2 + a^2 \right) = 0 \end{aligned}$$

The factors in the first line only takes positive value. Thus, we only consider the last two factors:

$$G_1 := -\frac{(-a^2 + B)(B + 1)\tilde{x}^2}{2} + a\tilde{y}(B - 1)(B + 1)\tilde{x} - \frac{(-a^2 + B)(B + 1)\tilde{y}^2}{2} - B^2 + a^2$$

and

$$G_2 := -\frac{(a^2 + B)(B - 1)\tilde{x}^2}{2} + a\tilde{y}(B - 1)(B + 1)\tilde{x} - \frac{(a^2 + B)(B + 1)\tilde{y}^2}{2} - B^2 + a^2.$$

In the rotated coordinates  $\tilde{X} = \frac{\tilde{x} + \tilde{y}}{\sqrt{2}}$ ,  $\tilde{Y} = \frac{\tilde{x} - \tilde{y}}{\sqrt{2}}$ , they can be rewritten into

$$G_1 = \frac{\tilde{X}^2}{\frac{2(B^2 - a^2)}{(a-1)(B+1)(B+a)}} + \frac{\tilde{Y}^2}{\frac{-2(B^2 - a^2)}{(a+1)(B+1)(B-a)}} - 1$$

and

$$G_2 = \frac{\tilde{X}^2}{\frac{2(B^2 - a^2)}{(a-1)(B-1)(B-a)}} + \frac{\tilde{Y}^2}{\frac{-2(B^2 - a^2)}{(a+1)(B-1)(B+a)}} - 1.$$

Notice that  $G_1 = 0$  contains no real points, since the coefficients of  $\tilde{X}^2, \tilde{Y}^2$  are both negative. Hence, only  $G_2 = 0$  determines centered conic sections in  $V$ . We now compute the positions of their foci by taking the affine change of the norm on  $V$  into account. Suppose that the foci of  $G_2 = 0$  are located at

$(\tilde{X}, \tilde{Y}) = (\pm c, 0)$ , then the norm  $\|\cdot\|_c$  in  $V$  which depends on the positions of foci is necessarily defined as

$$\|(\tilde{X}, \tilde{Y})\|_c^2 = \frac{\tilde{X}^2}{1+c^2} + \tilde{Y}^2.$$

This means we have the following equation in terms of  $c$ :

$$\frac{c^2}{1+c^2} = \frac{2(B^2-a^2)}{(a-1)(B-1)(B-a)} - \frac{-2(B^2-a^2)}{(a+1)(B-1)(B+a)}.$$

By solving this with respect to  $c$ , we obtain

$$c = \pm \frac{2\sqrt{a}}{1-a}$$

which depends only on  $a$ . Therefore, the equation  $G_2 = 0$  determines a family of confocal central conic sections in  $V$ . From this fact and the projective correspondence of the spherical Kepler problem and the planer Kepler problem, we conclude that the equation (3.25) determines confocal centered spherical conic sections on  $\mathcal{S}_{SH}$ .

Should we start from a family of confocal centered hyperbolae in  $\hat{V}$  instead of ellipses, then we get the same type of results in a similar way. we thus conclude that a family of confocal focused hyperbolic conic sections are transformed into a family of confocal centered spherical conic sections.

Analogously, one can show that a family of confocal focused hyperbolic conic sections are transformed into a family of confocal centered hyperbolic conic sections.  $\square$

Combining these results, we obtain the following proposition.

**Proposition 14.** *The hyperbolic Kepler billiards with a combination of branches of confocal conic sections focused at the “South pole”  $(0, 0, -1)$  on the hyperboloid model as reflection wall are conformally transformed into the hemispherical/hyperbolic Hooke billiards with the corresponding combination of confocal conic sections reflection wall centered at the “South pole” on the hemisphere/hyperboloid. Therefore their integrabilities are equivalent by Theorem 1.*

# Chapter 4

## Boltzmann's Billiard Systems

In [7], Boltzmann considered the following mechanical billiard model: the model is defined via the central force problem in  $\mathbb{R}^2$  with a force function  $U_{\alpha,\beta} := \frac{\alpha}{2r} - \frac{\beta}{2r^2}$ , in which  $r$  is the distance of the moving particle to the origin and  $\alpha, \beta \in \mathbb{R}$  are parameters, with a line in  $\mathbb{R}^2$  with distance  $\gamma > 0$  to the center as a wall of reflection. We suppose that trajectories of the billiard system are defined in the region  $y \geq \gamma$ . See Section 1.3 for prior works on Boltzmann's billiards. In this chapter, we summarize our results for Boltzmann's billiard systems.

All numerical results presented in this chapter are generated by MATLAB.

### 4.1 New Canonical Coordinates for Central Force Problem

In this section, we construct new canonical coordinates for general central force problems, which will be used in the next section to show the symplectic property for the billiard mapping.

Consider a central problem in the plane with a general force function  $U = U(r)$ . Its kinetic energy is given by

$$K = \frac{1}{2}(\dot{r}^2 + r^2\dot{\phi}^2)$$

in polar coordinates. The conjugate momenta are defined as

$$p_r = \frac{\partial K}{\partial \dot{r}} = \dot{r}, \quad p_\phi = \frac{\partial K}{\partial \dot{\phi}} = C,$$

where  $C := r^2\dot{\phi}$  is the angular momentum. In the coordinates  $(r, \phi, p_r, p_\phi)$ , the Hamiltonian is given by

$$H = \frac{1}{2} \left( p_r^2 + \frac{p_\phi^2}{r^2} \right) - U(r).$$

We will now find new canonical local coordinates which we denote by  $(Q_1, Q_2, P_1, P_2)$ . Let  $S = S(r, \phi, P_1, P_2)$  be a generating function of the canonical transformation, where  $P_1$  and  $P_2$  are new conjugate momenta which must be constant. The time-independent Hamilton-Jacobi equation

$$H\left(r, \phi, \frac{\partial S}{\partial \phi}, \frac{\partial S}{\partial r}\right) = E,$$

where  $E$  is the total energy, leads

$$\frac{1}{2} \left( \left( \frac{\partial S}{\partial r} \right)^2 + \left( \frac{1}{r} \cdot \frac{\partial S}{\partial \phi} \right)^2 \right) - U(r) = E. \quad (4.1)$$

We now use the method of separation to solve the above partial differential equation. Assume that the function  $S$  is separable into

$$S(r, \phi) = S_r(r) + S_\phi(\phi),$$

where  $S_r, S_\phi$  are only dependent on  $r, \phi$  respectively. After substituting this into the equation (4.1), we have

$$\frac{1}{2} \left( \left( \frac{\partial S_r}{\partial r} \right)^2 + \left( \frac{1}{r} \cdot \frac{\partial S_\phi}{\partial \phi} \right)^2 \right) - U(r) = E. \quad (4.2)$$

Also, realize that in the above equation only the term  $\frac{1}{r} \cdot \frac{\partial S_\phi}{\partial \phi}$  in the LHS is dependent on  $\phi$ , thus this must be constant. We write,

$$\frac{\partial S_\phi}{\partial \phi} = \kappa \quad (4.3)$$

where  $\kappa$  is constant. To determine what  $\kappa$  is, we use the property of the generating function:

$$\frac{\partial S}{\partial \phi} = p_\phi = C.$$

Thus, we have  $\kappa = C$ .

Substituting this to the equation (4.2), we yet obtain

$$\frac{\partial S_r}{\partial r} = \sqrt{2(E + U(r)) - \frac{C^2}{r^2}}. \quad (4.4)$$

Note that we here assumed  $\dot{r}(= \partial S/\partial r) \geq 0$ . From the equations (4.3),(4.4), the generating function can be determined as

$$S = C\phi + \int^r \sqrt{2(E + U(r)) - \frac{C^2}{r^2}}.$$

We set two constants  $E$  and  $C$  as new momenta

$$P_1 = E, \quad P_2 = C,$$

then we get

$$Q_1 = \frac{\partial S}{\partial P_1} = \frac{\partial S}{\partial E}, \quad Q_2 = \frac{\partial S}{\partial P_2} = \frac{\partial S}{\partial C}.$$

Using them, the new coordinates  $Q_1$  and  $Q_2$  can be computed as

$$Q_1 = \int^r \frac{dr}{\sqrt{2(H + U(r)) - \frac{C^2}{r^2}}} \quad (4.5)$$

and

$$Q_2 = \phi - C \int^r \frac{dr}{r^2 \sqrt{2(H + U(r)) - \frac{C^2}{r^2}}}. \quad (4.6)$$

To compute the equation of motion for the new coordinates, we use the following equations:

$$dt = \frac{dr}{\sqrt{2(H + U(r)) - \frac{C^2}{r^2}}},$$

and

$$d\phi = \frac{C dr}{r^2 \sqrt{2(H + U(r)) - \frac{C^2}{r^2}}}$$

for the case  $\dot{r} \geq 0$  (see also Section 4.3.1 for the derivations and the details.) By taking the time derivative of these components, we obtain,

$$\dot{Q}_1 = 1, \quad \dot{Q}_2 = 0.$$

The case  $\dot{r} < 0$  can be treated similarly. The physical meaning of these new coordinates is as follows:  $Q_1$  represents the time  $\tilde{t}$  of the passage from the pericenter, and  $Q_2$  represents the argument of pericenter  $g$  (the angle of the pericenter from a fixed direction).

In this way, we obtain the new canonical coordinate system ( $P_1(= H)$ ,  $P_2(= C)$ ,  $Q_1(= \tilde{t})$ ,  $Q_2(= g)$ ) which will be used in the following section.

## 4.2 Symplectic Property of the Billiard Mapping

We here investigate symplectic property of the billiard mapping. A main assertion by Boltzmann in [7] is that the billiard mapping preserves a measure. It is equivalent to say that the billiard mapping preserves and explicit symplectic 2-form which gives a Liouville measure. Later in this paper, Boltzmann remarked that this preservation holds for more general force function  $U = U(r)$ , and with any curve  $\mathcal{C} : r = \psi(\theta)$ . In our discussion, we assume that  $U$  and  $\mathcal{C}$  are both  $C^1$ .

In the following, we explain the method of symplectic reduction. We start with Hamiltonian symplectic geometry. Recall the followings: A symplectic manifold is a pair  $(M, \omega)$  with a smooth manifold  $M$  with a closed and non-degenerate 2-form  $\omega$ . A vector field  $X$  on  $M$  is called a Hamiltonian vector field if  $\omega(X, \cdot) = -dH$  for a smooth  $C^1$ -function  $H$ . In a natural mechanical system such as our central force problems, the symplectic manifold is the cotangent bundle of the configuration space, equipped with a canonical symplectic form, and the Hamiltonian function is the total energy.

Now we take quotients of symplectic manifolds under group actions that is called symplectic reduction. Let  $G$  be a Lie group acting on a symplectic manifold  $(M, \omega)$ . We say that the action is Hamiltonian if for every  $\xi \in T_e G$  associated vector field  $X_\xi$  given by

$$(X_\xi)_x = \left. \frac{d}{dt} \right|_{t=0} \exp(t\xi) \cdot x$$

is Hamiltonian. We denote this associated Hamiltonian by  $\{H_\xi\}$ . For a regular value  $c$  of the functions  $\{H_\xi\}$ . We take the level set  $H_\xi^{-1}(c)$  that is submanifold of  $M$  with codimension 1. The quotient space  $H_\xi^{-1}(c)/G_\xi$  where  $G_\xi := \{\exp(t\xi)\}$  is a 1-parameter subgroup of  $G$  is a symplectic with a symplectic structure induced by  $\omega$ . This can be checked from the facts that  $\omega$  is invariant under  $G$  and  $H_\xi$  is a constant of motion (*i.e.*  $\{H, H_\xi\} = 0$ ).

We now go back to our central force problem with the Hamiltonian

$$H(p, q) = \frac{\|p\|^2}{2} - U(r), \quad (p, q) \in \mathbb{R}^2 \times (\mathbb{R}^2 \setminus O), r = \|q\|.$$

Their canonical symplectic form is

$$\omega = dp_1 \wedge dq_1 + dp_2 \wedge dq_2.$$

This symplectic form is invariant under  $SO(2)$  action. The angular momentum  $C$  whose vector field is the generator of  $SO(2)$  action, is a conserved

quantity. We may thus apply the symplectic reduction and get the reduced Hamiltonian

$$H_r(p, q; C) = \frac{p_r^2}{2} - U(r) + \frac{C^2}{r^2},$$

with the reduced symplectic form  $dr \wedge dp_r$ . The reduced energy level  $\{H_r = h\}$  now projects into the Hill's region  $\left\{-U(r) + \frac{C^2}{r^2} \leq h\right\}$  in the reduced configuration space  $\mathbb{R}_+$ . We assume that this projection is not the full  $\mathbb{R}_+$  and we consider a connected component of this projection that is not merely a point, that is, a closed interval  $[a_h, b_h]$  not containing 0 but which can tend to  $\infty$ . (Analogously we may consider the case that the interval has a boundary point 0 and the other boundary point is finite.) We assume in addition that the boundary points of this component depend continuously on  $h$  and  $C$ . We localize our system near this component for energy close to  $h$  and for angular momentum close to  $C$ . In this way, we get the localized system defined on the localized phase space, that preserves the symplectic structure of the original system.

We now use the coordinates  $(H, C, \tilde{t}, g)$  that we constructed in the previous section. Note that for general  $U(r)$  and for a fixed orbit, pericenters and apocenters are not unique. Therefore this canonical variables  $(H, C, \tilde{t}, g)$  is defined on a covering space on the localized phase space. We remember that the localized phase space is a symplectic therefore its covering space is also symplectic. This symplectic form is written as

$$dH \wedge d\tilde{t} + dC \wedge dg.$$

By fixing  $H$ , we get the reduced symplectic form  $dC \wedge dg$ . This symplectic property can be checked in the other way. Indeed since  $\partial_{\tilde{t}}, \partial_g$  are respectively the Hamiltonian vector fields of  $H$  and  $C$ , the symplectic form has to take the form

$$dH \wedge d\tilde{t} + dC \wedge dg + f(H, C, \tilde{t}, g)dH \wedge dC;$$

now since  $\{H, C\} = 0$  we conclude that  $f(H, C, \tilde{t}, g) = 0$ . Consequently, the reduced symplectic form by fixing  $H$  is simply  $dC \wedge dg$ .

We now add the wall of reflection. We study the reflection at a point in  $\mathcal{C}$ . Without loss of generality, we may take an auxiliary new Cartesian coordinate system such that this point is at the origin and the tangent line to  $\mathcal{C}$  at this point is the first axis in the new coordinate system. We consider the symplectic involution  $(p_1, p_2, q_1, q_2) \mapsto (p_1, -p_2, q_1, -q_2)$  in the new coordinate system which keeps the point of reflection invariant and transform the momentum as  $(p_1, p_2) \mapsto (p_1, -p_2)$  which agrees with the law of reflection at this point.

Consequently, since all the transformations are symplectic, we conclude that the symplectic form is conserved. Since  $H$  is invariant along the orbit of the central force problem as well as under reflection at  $\mathcal{C}$ , we conclude that the reduced form  $dC \wedge dg$  is preserved under reflection. This is the first assertion of Boltzmann.

Note that these argument holds only when  $H$  and  $C$  are independent. When  $H$  and  $C$  are dependent, then the orbit is circular and there are no pericenter directions. The situation is similar to the problem of polar coordinates at the origin and they form a set of positive codimension, so this set can be thought of as having measure zero.

### 4.3 Computation of the Billiard Mapping

#### 4.3.1 Solutions for the Central Force Problem: Kepler Problem with Centrifugal Force

As the first step of computing billiard maps, we solve the central force problem in the plane with the force function  $U = \frac{\alpha}{2r} - \frac{\beta}{2r^2}$ .

We recall the analysis of Boltzmann in [7]. He passes from Cartesian to polar coordinates  $(r, \phi)$  and writes down the equations of the preservation of the energy  $E$  and the angular momentum  $C$  of the mechanical system as

$$\dot{r}^2 + r^2 \dot{\phi}^2 = 2 \cdot E + \frac{\alpha}{r} - \frac{\beta}{r^2}, \quad (4.7)$$

$$r^2 \dot{\phi} = C, \quad (4.8)$$

in which a dot denotes the derivative of the quantity with respect to time. We shall only consider bounded orbits, so we set  $E < 0$ .

Note that here  $E$  is always conserved in the billiard system since the kinetic energy does not change at reflections, while  $C$  changes from orbit arcs to orbit arcs when a reflection at the wall takes place.

Boltzmann then writes “from here it follows that”

$$\dot{r} = \sqrt{2 \cdot E + \frac{\alpha}{r} - \frac{C^2 + \beta}{r^2}},$$

thus

$$dt = \frac{dr}{\sqrt{2 \cdot E + \frac{\alpha}{r} - \frac{C^2 + \beta}{r^2}}}.$$

This deduction is problematic, as in general  $x^2 = a$  does not imply  $x = \sqrt{a}$ , as well as the computations that follow. Along an arc containing either an pericenter or an apocenter, the quantity  $\dot{r}$  changes its signs.

From (4.8), it follows that

$$dt = \frac{r^2 d\phi}{C}.$$

By equating these equations for  $dt$ , we have

$$d\phi = \frac{C dr}{r\sqrt{2 \cdot Er^2 + \alpha r - C^2 - \beta}}.$$

Also, this formula is problematic, as it uses the previous formula. Indeed, the LHS has the same sign as  $C$ , which is positive resp. negative when the corresponding orbit is oriented counterclockwise resp. clockwise. On the other hand, when an arc contains a peri- or apo-center, the monotonicity of  $r$  changes while the monotonicity of  $\phi$  does not change.

We now restrict our system to the case that these formulas are valid. Namely, we consider an arc between a pericenter and the consecutive apocenter. In this case, one can rewrite the above equation as

$$d\phi = \frac{dr/r^2}{\sqrt{\frac{2E}{C^2} + \frac{\alpha}{C^2 r} - \frac{C^2 + \beta}{C^2 r^2}}} = \sqrt{\frac{C^2}{C^2 + \beta}} \cdot \frac{dr/r^2}{\sqrt{-\left(\frac{1}{r_{min}} - \frac{1}{r}\right)\left(\frac{1}{r_{max}} - \frac{1}{r}\right)}},$$

assuming that  $C^2 + \beta > 0$ . Here,  $r_{min}$  and  $r_{max}$  are respectively distances of the pericenter and apocenter to the center of the system. We have

$$r_{min} = \frac{-\alpha + \sqrt{\alpha^2 + 8E(C^2 + \beta)}}{4E},$$

$$r_{max} = \frac{-\alpha - \sqrt{\alpha^2 + 8E(C^2 + \beta)}}{4E}.$$

We now set  $\rho = 1/r$  so that  $d\rho = -dr/r^2$ , and we get

$$d\phi = \sqrt{\frac{C^2}{C^2 + \beta}} \cdot \frac{-d\rho}{\sqrt{-(\rho_{min} - \rho)(\rho_{max} - \rho)}},$$

naturally,  $\rho_{min} = 1/r_{min}$  and  $\rho_{max} = 1/r_{max}$ . Note that  $\rho_{min} \geq \rho_{max}$ .

Finally, we change the integration variable as  $\chi = \rho - \frac{1}{2}(\rho_{max} - \rho_{min})$  and set  $\chi_0 = \frac{1}{2}(\rho_{min} - \rho_{max})$ , then we get

$$d\phi = \sqrt{\frac{C^2}{C^2 + \beta}} \cdot \frac{-d\chi}{\sqrt{\chi_0^2 - \chi^2}}.$$

If  $C \geq 0$  so that the particle moves in the counterclockwise direction, then the integration from the pericenter to another point on the orbit arc between the pericenter and the successive apocenter becomes

$$\begin{aligned} \phi - \varepsilon &= \int_{r_{min}}^r \frac{C dr}{r \sqrt{2 \cdot E r^2 + \alpha r - C^2 - \beta}} \\ &= \sqrt{\frac{C^2}{C^2 + \beta}} \cdot \int_{\chi_0}^{\chi} \frac{-d\chi}{\sqrt{\chi_0^2 - \chi^2}} \\ &= \sqrt{\frac{C^2}{C^2 + \beta}} \cdot \arccos \frac{\chi}{\chi_0} \\ &= \sqrt{\frac{C^2}{C^2 + \beta}} \cdot \arccos \frac{2 \frac{C^2 + \beta}{r} - \alpha}{\sqrt{\alpha^2 + 8 \cdot E(C^2 + \beta)}}, \end{aligned}$$

where  $\varepsilon$  denotes the argument of a pericenter, which means the angle that the pericenter makes from the x-axis. In the third equality we used  $\arccos 1 = 0$ . Recall that  $0 \leq \arccos x \leq \pi$  for  $-1 \leq x \leq 1$ .

For  $C \leq 0$ , the particle moves in the clockwise direction. Considering that the sign of the left hand side will be changed for this case, we get

$$\phi - \varepsilon = -\sqrt{\frac{C^2}{C^2 + \beta}} \cdot \arccos \frac{2 \frac{C^2 + \beta}{r} - \alpha}{\sqrt{\alpha^2 + 8 \cdot E(C^2 + \beta)}}.$$

By combining these two cases, they can be rewritten in a uniform way as

$$\phi - \varepsilon = \frac{C}{\sqrt{C^2 + \beta}} \cdot \arccos \frac{2 \frac{C^2 + \beta}{r} - \alpha}{\sqrt{\alpha^2 + 8 \cdot E(C^2 + \beta)}}. \quad (4.9)$$

This equation appears in Boltzmann's paper. However there is a typo in the formula in [7]

Remind that we still have to consider the case

$$\dot{r} = -\sqrt{2 \cdot E + \frac{\alpha}{r} - \frac{C^2 + \beta}{r^2}},$$

when the distance from the center decreases with time.

In this case, the sign of the LHS of (4.9) will be switched, and we have

$$\phi - \varepsilon = -\frac{C}{\sqrt{C^2 + \beta}} \cdot \arccos \frac{2\frac{C^2 + \beta}{r} - \alpha}{\sqrt{\alpha^2 + 8 \cdot E(C^2 + \beta)}}. \quad (4.10)$$

As Boltzmann has not considered this case, at least in his computation of Jacobian, his analysis was largely incomplete.

We may then solve the problem further from (4.9) and (4.10). To be consistent with modern convention in celestial mechanics, we denote the angle which the particle makes from the x-axis by  $\theta$  and denote the angle of (one of) the pericenter makes from the x-axis by  $g$ .

From

$$\theta - g = \pm \frac{C}{\sqrt{C^2 + \beta}} \cdot \arccos \frac{2\frac{C^2 + \beta}{r} - \alpha}{\sqrt{\alpha^2 + 8 \cdot E(C^2 + \beta)}},$$

we get

$$\pm \frac{\sqrt{C^2 + \beta}}{C} (\theta - g) = \arccos \frac{2\frac{C^2 + \beta}{r} - \alpha}{\sqrt{\alpha^2 + 8 \cdot E(C^2 + \beta)}}.$$

By taking cosine in both sides we get

$$\cos \left( \sqrt{\frac{C^2 + \beta}{C^2}} (\theta - g) \right) = \frac{2\frac{C^2 + \beta}{r} - \alpha}{\sqrt{\alpha^2 + 8 \cdot E(C^2 + \beta)}}. \quad (4.11)$$

Solving this equation for  $r$  in the case of  $\alpha > 0$ , we get

$$r = \frac{p}{e \cos(\omega(\theta - g)) + 1}, \quad (4.12)$$

here,  $p = \frac{2(C^2 + \beta)}{\alpha}$ ,  $\omega = \sqrt{\frac{C^2 + \beta}{C^2}}$ , and  $e = \sqrt{1 + \frac{8E(C^2 + \beta)}{\alpha^2}}$ . Figure 4.2, 4.3 illustrate the orbits for  $p = 1, e = 0.8, \omega = 1.1$  and  $p = 1, e = 0.2, \omega = 10.1$ , respectively.

Note that for the repulsive case  $\alpha < 0$ , we necessarily have  $E > 0$ , and in this case we get

$$r = \frac{p}{e \cos(\omega(\theta - g)) - 1}, \quad (4.13)$$

where  $p = \frac{2(C^2 + \beta)}{-\alpha}$ ,  $\omega = \sqrt{\frac{C^2 + \beta}{C^2}}$  and  $e = \sqrt{1 + \frac{8E(C^2 + \beta)}{\alpha^2}}$ , from (4.11). Note that in this case, we have the corresponding billiard system only in the region  $y \leq \gamma$  not in  $y \geq \gamma$ .

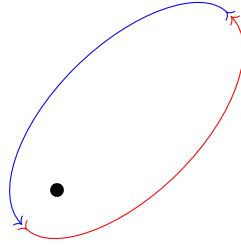


Figure 4.1:  $r$ -increasing direction (in red) and decreasing direction (in blue) for an ellipse

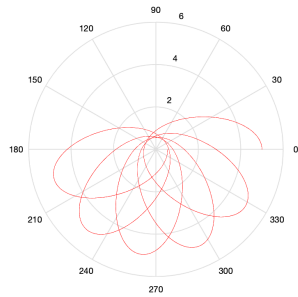


Figure 4.2: Orbit for  $p = 1, e = 0.8, \omega = 1.1$

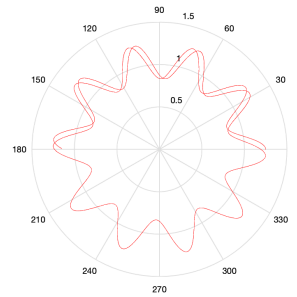


Figure 4.3: Orbit for  $p = 1, e = 0.2, \omega = 10.1$

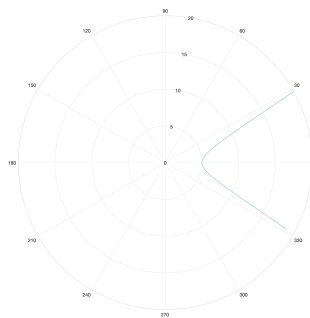


Figure 4.4: Orbit for  $\alpha < 0$

Indeed, since we must have positive radius, we find solutions only in the case  $e > 1$ . For  $e > 1$ , we have unbounded hyperbolic orbits look like those shown in Figure 4.4. Notice that  $r \rightarrow \infty$  when  $e \cos(\omega(\theta - g)) \rightarrow 1$ .

We now consider the other cases when  $C^2 + \beta = 0$  or  $C^2 + \beta < 0$ . By differentiating the equation (4.7) with respect to  $t$ , we have

$$\ddot{r} - \frac{C^2 + \beta}{r^3} = -\frac{\alpha}{2r^2}.$$

Taking the Clairaut variable  $\rho = 1/r$  and using  $C^2 \frac{d^2 \rho}{d\theta^2} = -r^2 \ddot{r}$ , the above equation is transformed into

$$\frac{d^2 \rho}{d\theta^2} + \frac{C^2 + \beta}{C^2} \rho = \frac{\alpha}{2C^2}. \quad (4.14)$$

When  $C^2 + \beta = 0$ , the equation reduces to

$$\frac{d^2 \rho}{d\theta^2} = \frac{\alpha}{2C^2}.$$

So, the orbit takes the form

$$\frac{1}{r} = \rho = \frac{\alpha}{2C^2} \theta^2 + k_1 \theta + k_2$$

which determines a spiral.

When  $C^2 + \beta < 0$ , we get that the general solution in the form

$$\frac{1}{r} = \rho = k \cos \omega(\theta - g) + \frac{\alpha}{2C^2},$$

where  $\omega = \sqrt{\frac{C^2 + \beta}{C^2}}$ . Note that in this case  $\omega$  is purely-imaginary and thus, the  $\cos$  appearing in the above formula is a  $\cosh$ . We may again put it into the form

$$r = \frac{p}{1 + e \cos \omega(\theta - g)},$$

where  $p = \frac{2C^2}{\alpha}$  and  $e = \frac{2kC^2}{\alpha}$ . Note that  $e$  may be either positive, negative, or zero.

We first discuss the case  $\alpha < 0$ . In this case we have  $p < 0$ . When  $e \geq 0$ , there are no solutions. When  $-1 \leq e < 0$ , the value of  $\theta$  is restricted to  $\theta < \theta_1 \leq \theta_2 < \theta$  with two limiting values  $\theta_1, \theta_2$  such that  $r \rightarrow \infty$  when  $\theta \rightarrow \theta_1 - 0$  or  $\theta \rightarrow \theta_2 + 0$ , and  $r \rightarrow 0$  when  $\theta \rightarrow \pm\infty$ , thus the orbit is an unbounded spiral. When  $e < -1$ , we have  $r < \frac{p}{1+e}$  and  $r \rightarrow 0$  when

$\theta \rightarrow \pm\infty$ , thus the orbit is a bounded spiral which is biasymptotic to the origin.

Secondly, we discuss the case  $\alpha > 0$ . In this case  $p > 0$ . When  $e > 0$ , we see that  $r \rightarrow 0$  when  $\theta \rightarrow \pm\infty$ , so the orbit is a spiral which is biasymptotic to the origin. When  $e = 0$ , the orbit is a circle. When  $-1 < e < 0$ ,  $\theta$  is confronted between two limiting values, and the orbit is unbounded and has two asymptotic directions. There are no solutions when  $e \leq -1$ .

### 4.3.2 Computation of General Boltzmann's Billiard Mapping

The billiard system is defined by adding a wall of reflection to the central force problem. In this section, we assume  $\alpha > 0$  and  $C^2 + \beta > 0$ . We define an arc as part of an orbit with starting and ending points on the reflection wall, and no other points hit the wall in between. The billiard mapping that sends a reflection point and a reflection velocity to the next extends to a mapping that maps an arc to another arc which then extends to a mapping of orbits. We shall analyze this mapping.

In polar coordinates, the wall of reflection  $\{y = \gamma > 0\}$  is represented by the equation

$$r \sin \theta = \gamma.$$

We now compute the billiard mapping that maps an orbit to the orbit to which a given orbit is reflected after reaching a point  $(r_*, \theta_*) = (\gamma / \sin \theta_*, \theta_*)$  on the wall, *i.e.*,  $(r_*, \theta_*)$  is the reflection point between the first orbit and the proceeding second orbit. Once fixing the energy, an orbit is characterized by the coordinates  $(g, C)$ , where  $C$  is the angular momentum and  $g$  is the argument of pericenter (the angular coordinates of the pericenters). Define the billiard mapping  $S$  as  $S(g_1, C_1) = (g_2, C_2)$ , where  $(g_1, C_1)$  and  $(g_2, C_2)$  correspond to the consecutive two arcs before and after the reflection. The derivatives

$$\frac{dr}{d\theta}(r_*, \theta_*) = \frac{p \cdot e \cdot \omega \cdot \sin \omega(\theta_* - g_{1,2})}{(1 + e \cos \omega(\theta_* - g_{1,2}))^2}$$

will be denoted as  $r'_{1,2}$  in the two orbits respectively. The derivatives

$$\frac{d\theta}{dt}(r_*, \theta_*)$$

will be denoted as  $\dot{\theta}_{1,2}$  in the two orbits respectively. We also write the corresponding  $p, e, \omega$  in the two orbits as  $p_{1,2}, e_{1,2},$  and  $\omega_{1,2}$ .

We get the following equations from the law of reflection.

$$\begin{cases} r_* = \frac{\gamma}{\sin \theta_*} = \frac{p_1}{1 + e_1 \cos \omega_1(\theta_* - g_1)} = \frac{p_2}{1 + e_2 \cos \omega_2(\theta_* - g_2)} \\ (r'_1 \sin \theta_* + r_* \cos \theta_*) \dot{\theta}_1 = -(r'_2 \sin \theta_* + r_* \cos \theta_*) \dot{\theta}_2 \\ (r'_1 \cos \theta_* - r_* \sin \theta_*) \dot{\theta}_1 = (r'_2 \cos \theta_* - r_* \sin \theta_*) \dot{\theta}_2 \\ \dot{\theta}_1 = \frac{C_1}{r_*^2}, \quad \dot{\theta}_2 = \frac{C_2}{r_*^2} \end{cases}$$

From these, one deduces that

$$C_2 = \frac{C_1(-2r_* \cos^2 \theta_* - 2r'_1 \sin \theta_* \cos \theta_* + r_*)}{r_*}$$

$$r'_2 = \frac{-r_* r'_1 \tan^2 \theta_* - 2r_*^2 \tan \theta_* + r'_1 r_*}{r_* \tan^2 \theta_* - 2r'_1 \tan \theta_* - r_*}$$

and then

$$p_2 = \frac{2(C_2^2 + \beta)}{\alpha}, \quad \omega_2 = \sqrt{\frac{(C_2^2 + \beta)}{C_2^2}}, \quad e_2 = \sqrt{1 + \frac{8E(C_2^2 + \beta)}{\alpha^2}}.$$

Consequently, we obtain

$$e_2 \cos \omega_2(\theta_* - g_2) = \frac{p_2 - r_*}{r_*}, \quad e_2 \sin \omega_2(\theta_* - g_2) = \frac{p_2 r'_2}{\omega_2 r_*^2}$$

From these one may solve  $g_2$  as

$$g_2 = \theta_* - \frac{\text{sign} \left( \frac{p_2 r'_2}{e_2 \omega_2 r_*^2} \right) \arccos \left( \frac{p_2 - r_*}{e_2 r_*} \right)}{\omega_2}. \quad (4.15)$$

Remember that, when  $\omega \neq 1$ , there are multiple pericenters and apocenters. We choose the closest pericenter from the current reflection point, that is defined in (4.15) as the next argument of pericenter. In order to complete this inductive step, we finally compute the next reflection point  $(r_{**}, \theta_{**})$  from

$$e_2 \cos \omega_2(\theta_{**} - g_2) = \frac{p_2 - r_{**}}{r_{**}}, \quad r_{**} \sin \theta_{**} = \gamma. \quad (4.16)$$

Remember that  $0 \leq \theta_{**} \leq \pi$ . The equation (4.16) can have multiple solutions and one of them must be the current reflection point  $(r_*, \theta_*)$ . Therefore, we add the following condition to determine next reflection point  $(r_{**}, \theta_{**})$  corresponding to the current one  $(r_*, \theta_*)$ :

$$r \cdot \sin \theta = \frac{p \sin \theta}{e \cos(\omega(\theta - g)) - 1} \geq \gamma \quad (4.17)$$

for all  $\theta$  such that  $\theta_* \leq \theta \leq \theta_{**}$  if  $C > 0$  (for all  $\theta$  such that  $\theta_{**} \leq \theta \leq \theta_*$  if  $C < 0$ ).

### 4.3.3 Solutions for the Central Force Problem: Cotes' Spiral Case

We now consider the case  $\alpha = 0, C \neq 0$ , in this special case, solution curves of the central force problem with a force function  $\beta/r^2$  are known as *Cotes' spiral* [14, Chapter IV].

By differentiating the equation (4.7) with respect to  $t$ , we have

$$\ddot{r} - \frac{C^2 + \beta}{r^3} = -\frac{\alpha}{2r^2}$$

(remembering that  $C$  is a constant of motion). Taking the Clairaut variable  $\rho = 1/r$  and having  $C^2 \frac{d^2 \rho}{d\theta^2} = -r^2 \ddot{r}$ , the above equation is transformed into

$$\frac{d^2 \rho}{d\theta^2} + \frac{C^2 + \beta}{C^2} \rho = \frac{\alpha}{2C^2}. \quad (4.18)$$

By substituting  $\alpha = 0$ , the equation (4.18) can be written into

$$\frac{d^2 \rho}{d\theta^2} + \left( \frac{C^2 + \beta}{C^2} \right) \rho = 0.$$

We discuss different subcases.

When  $C^2 + \beta > 0$ , the general solution of the equation is written as

$$\frac{1}{r} = \rho = k \cos \omega(\theta - \psi),$$

where  $k \in \mathbb{R}$  and  $\psi \in [0, 2\pi)$ . When  $C^2 + \beta = 0$ , the general solution reduces to the form

$$\frac{1}{r} = \rho = k_1 \theta + k_2.$$

When  $C^2 + \beta < 0$ , the general solution is

$$\frac{1}{r} = \rho = k_1 \exp(i\omega(\theta - \psi)) + k_2 \exp(-i\omega(\theta - \psi)),$$

with a purely imaginary  $\omega$ .

To make further analysis observe that

$$h := \left( \frac{d\rho}{d\theta} \right)^2 + \left( \frac{C^2 + \beta}{C^2} \right) \rho^2$$

is a first integral of the equation. Drawing its level sets in the phase space with coordinates  $(\frac{d\rho}{d\theta}, \rho)$  we see that the level sets are hyperbolae and bifurcates at zero-level  $\{h = 0\}$  through a degeneration into a pair of lines and then switching of major axis.

When  $h < 0$ , the hyperbola has a major axis, the  $\rho$ -axis, and thus, admits a parametrization with hyperbolic functions. The corresponding solution in polar form is

$$\frac{1}{r} = \rho = k \cos \omega(\theta - \psi).$$

Similarly, when  $h > 0$ , we get

$$\frac{1}{r} = \rho = k \cdot i \cdot \sin \omega(\theta - \psi).$$

Finally, when  $h = 0$  we have

$$\frac{1}{r} = \rho = k \exp(\pm i\omega(\theta - \psi)).$$

We thus get the five classes of Cotes' spirals as orbits of the problem with  $\alpha = 0$ .

#### 4.3.4 Computation of the Billiard Mapping: Cotes' Spiral Case

Analogously, we will also compute the billiard mapping for the special case  $\alpha = 0$ . We again consider bounded orbits, thus we assume  $E < 0$ . The doubled total energy is written as

$$\dot{r}^2 + \frac{C^2 + \beta}{r^2} = 2E,$$

and it leads to

$$h = \left(\frac{d\rho}{d\theta}\right)^2 + \left(\frac{C^2 + \beta}{C^2}\right)\rho^2 = \frac{2E}{C^2}.$$

From these equations and  $E < 0$ , we always have  $C^2 + \beta < 0$  and  $h := \left(\frac{d\rho}{d\theta}\right)^2 + \left(\frac{C^2 + \beta}{C^2}\right)\rho^2 < 0$ . Therefore, orbits are given in the form

$$\frac{1}{r} = \rho = k \cos \omega(\theta - \psi).$$

here  $\omega = \sqrt{\frac{C^2 + \beta}{C^2}}$ ,  $k = \sqrt{\frac{2E}{\omega^2 C^2}}$  and  $\psi$  denotes the angle of the apocenter direction. As in the case  $\alpha > 0$ , we consider the billiard mapping  $(\psi_1, C_1) \mapsto (\psi_2, C_2)$ . Let  $(r_*, \theta_*)$  be the collision point between the first orbit and the second one. The derivatives

$$\frac{dr}{d\theta}(r_*, \theta_*) = \frac{\omega \sin \omega(\theta_* - \psi_{1,2})}{k \cos^2 \omega(\theta_* - \psi_{1,2})}$$

will be denoted as  $r'_{1,2}$  in the two orbits respectively. The derivatives

$$\frac{d\theta}{dt}(r_*, \theta_*)$$

will be denoted as  $\dot{\theta}_{1,2}$  in the two orbits respectively. We also write the corresponding  $p, e, \omega$  in the two orbits as  $p_{1,2}, e_{1,2}$ , and  $\omega_{1,2}$ . To compute the next collision point, we use following equations

$$\begin{cases} r_* = \frac{\gamma}{\sin \theta_*} = \frac{1}{k_1 \cos \omega_1(\theta_* - \psi_1)} = \frac{1}{k_2 \cos \omega_2(\theta_* - \psi_2)} \\ (r'_1 \sin \theta_* + r_* \cos \theta_*) \dot{\theta}_1 = -(r'_2 \sin \theta_* + r_* \cos \theta_*) \dot{\theta}_2 \\ (r'_1 \cos \theta_* - r_* \sin \theta_*) \dot{\theta}_1 = (r'_2 \cos \theta_* - r_* \sin \theta_*) \dot{\theta}_2 \\ \dot{\theta}_1 = \frac{C_1}{r_*^2}, \quad \dot{\theta}_2 = \frac{C_2}{r_*^2}. \end{cases}$$

From these one deduces that

$$C_2 = \frac{C_1(-2r_* \cos^2 \theta_* - 2r'_1 \sin \theta_* \cos \theta_* + r_*)}{r_*},$$

$$r'_2 = \frac{-r_* r'_1 \tan^2 \theta_* - 2r_*^2 \tan \theta_* + r'_1 r_*}{r_* \tan^2 \theta_* - 2r'_1 \tan \theta_* - r_*},$$

and then

$$\omega_2 = \sqrt{\frac{C_2^2 + \beta}{C_2^2}},$$

$$k_2 = \sqrt{\frac{2E}{\omega_2^2 C_2^2}}.$$

Consequently, we obtain

$$\frac{1}{r_*} = k_2 \cos \omega_2(\theta_* - \psi_2), \quad -\frac{1}{r_*^2} r'_2 = -k_2 \omega_2 \sin \omega(\theta_* - \psi_2).$$

From these, one may solve  $\psi_2$  as

$$\psi_2 = \theta_* - \frac{\text{sign}\left(-\frac{r'_2}{r_* k_2(-i\omega)}\right) \text{arccosh}\left(\frac{1}{k_2 r_*}\right)}{-i\omega_2}.$$

The second orbit is thus determined by  $(C_2, \psi_2)$ . In order to complete this inductive step, we finally compute the next collision point  $(r_{**}, \theta_{**})$  from

$$\frac{1}{r_{**}} = k_2 \cos \omega_2 (\theta_{**} - \psi_2), \quad r_{**} \sin \theta_{**} = \gamma. \quad (4.19)$$

Remember that  $0 \leq \theta_{**} \leq \pi$ .

## 4.4 Numerical Results of Boltzmann's Billiard Trajectories

We here present some numerical results of the Boltzmann's billiard mapping computed in section 4.3.2. In our simulations, we set  $\alpha = 4$ ,  $E = -0.5$ ,  $\gamma = 0.5$ , and vary the parameter  $\beta \geq 0$ . Figures in this section illustrate numerically computed trajectories of the billiard mapping *i.e.* the evolving values of  $(g, C) \in [0, 2\pi) \times [C_{min}, C_{max}]$  at each reflection.

For  $\beta = 0$ , our simulation shows periodic behavior of a trajectory as we illustrated in Figure 4.5, which is compatible with the integrability of the system for this parameter setting. For small  $\beta$ , for example  $\beta = 0.5$  the system remains quasi-periodicity and seems not to be transitive, see figure 4.6. For a bigger value of  $\beta$ , the periodicity may be broken, and chaotic behavior may appear, as we illustrated for the case  $\beta = 2.6$  in Figure 4.7. In this case, we can expect that a single orbit densely covers the whole energy hypersurface in state space (for fixed  $H = E$ ). Therefore, there is a chance to show the ergodicity of the billiard system for big enough  $\beta$ . However, chaotic behavior does not always show up for large  $\beta$ . More interestingly, Figure 4.8 shows both quasi-periodic (Subfig. a) and chaotic (but not transitive) behavior (Subfig. b) for the same parameter setting ( $\beta = 2.4$ ) but with different initial values. Also, Subfig. c indicates the existence of period two periodic orbit for the same parameter setting.

## 4.5 Koopman Operator and Eigenvalue Problem

For any measure-preserving map  $S$  on a probability measure space  $(X, \mu, \Sigma)$ , the Koopman operator can be defined as the transfer operator on  $L^2(X) :=$

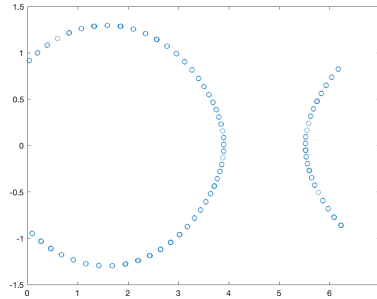


Figure 4.5: Periodic behavior of the mapping trajectory for  $\beta = 0$

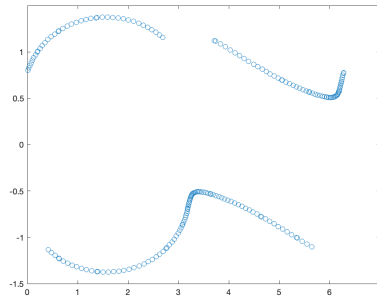


Figure 4.6: (Quasi-)periodic behavior of the mapping trajectory for  $\beta = 0.5$

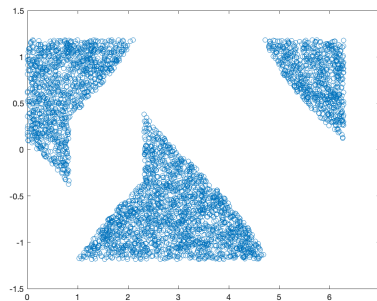
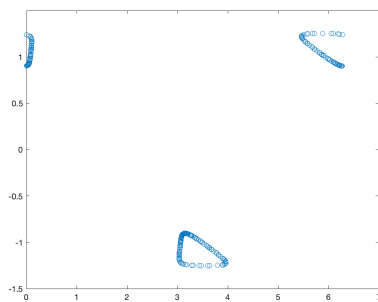
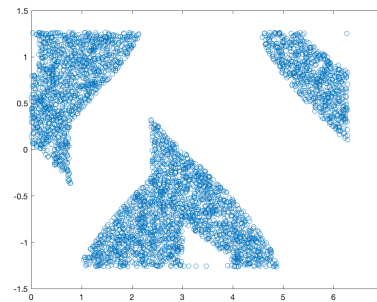


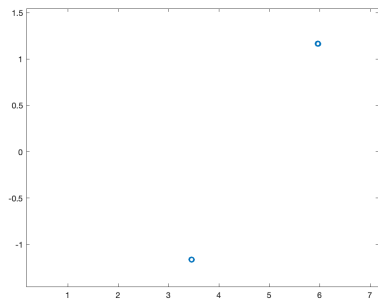
Figure 4.7: Transitive behavior of the mapping trajectory for  $\beta = 2.6$



a. Trajectory with initial value  $(g_0, C_0) = (0.1, 1.1)$



b. Trajectory with initial value  $(g_0, C_0) = (0.2, 1.0)$



c. Periodic trajectory with initial value  $(g_0, C_0) = (3.45, -1.16)$

Figure 4.8: (Quasi-)periodic and chaotic behavior for  $\beta = 2.4$

$L^2(X, \mathbb{C})$  by

$$Kf := f \circ S, \quad f \in L^2(X). \quad (4.20)$$

From the preservation of measure (i.e.  $\mu(A) = \mu(S^{-1}(A)), \forall A \in \Sigma$ ), one can see the Koopman operator  $K : L^2(X) \rightarrow L^2(X)$  preserves norm. Therefore, this operator is unitary and has its spectrum on the unit circle. The spectrum of the Koopman operator carries essential information from the mapping  $S$  (e.g., ergodicity, weakly mixing, invariant sets). The following proposition connects the ergodic property of the original mapping  $S$  and the eigenvalue problem of the corresponding Koopman operator.

**Proposition 15.** *Let  $S$  be a measure-preserving map on a probability measure space  $((X, \mu, \Sigma))$  and let  $K : L^2(X) \rightarrow L^2(X)$  be the corresponding Koopman operator.  $K$  has eigenvalue 1. Moreover, the map  $S$  is ergodic if and only if eigenvalue 1 is simple.*

See [15, Proposition 7.15] for the proof.

In the following sections, we solve the eigenvalue problem of Koopman operator numerically by approximating the problem with Galerkin method.

### 4.5.1 Approximation of Koopman Eigenvalue Problem with Galerkin Method

We here explain the approximation procedure of the Koopman eigenvalue problem using Galerkin method with piecewise constant basis functions.

#### Galerkin Method and Midpoint Quadrature with Uniform Weights

Consider the original eigenvalue problem of the Koopman operator on  $L^2(X)$

$$Ku = \lambda u, \quad u \in L^2(X),$$

then we transform it into the equivalent equation

$$\langle Ku, v \rangle = \lambda \langle u, v \rangle, \quad \forall v \in L^2(X),$$

where  $\langle \cdot, \cdot \rangle$  is the inner product of the Hilbert space  $L^2(X)$ . Now we set the finitely many basis functions  $\{f_1, \dots, f_N\}$  in  $L^2(X)$ . We look for approximate eigenfunctions in the form  $u = \sum_{n=1}^N \alpha_n f_n$  and we restrict the above equation to the space which is spanned by the base functions. Then it can be rewritten as

$$\sum_{n=1}^N \alpha_n \langle f_n \circ S, f_m \rangle = \lambda \sum_{n=1}^N \alpha_n \langle f_n, f_m \rangle, \quad \forall m \in \{1, \dots, N\}.$$

This can be transformed in the matrix form

$$\begin{pmatrix} \langle f_1 \circ S, f_1 \rangle & \cdots & \langle f_N \circ S, f_1 \rangle \\ \vdots & \ddots & \vdots \\ \langle f_1 \circ S, f_N \rangle & \cdots & \langle f_N \circ S, f_N \rangle \end{pmatrix} \begin{pmatrix} \alpha_1 \\ \vdots \\ \alpha_N \end{pmatrix} = \lambda \begin{pmatrix} \langle f_1, f_1 \rangle & \cdots & \langle f_N, f_1 \rangle \\ \vdots & \ddots & \vdots \\ \langle f_1, f_N \rangle & \cdots & \langle f_N, f_N \rangle \end{pmatrix} \begin{pmatrix} \alpha_1 \\ \vdots \\ \alpha_N \end{pmatrix} \quad (4.21)$$

For the computation of each entry of the matrices above, we divide the domain  $X$  of the mapping  $S$  into finitely many disjoint sections  $\Omega_1, \dots, \Omega_N$  so that  $X = \sqcup_{n=1}^N \Omega_n$ . Suppose that our basis functions  $f_n$  are the characteristic functions of each region  $\Omega_n$  i.e.  $f_n(x) = 1$  if  $x \in \Omega_n$  and  $f_n(x) = 0$  otherwise. Then the matrix in the left hand side of (4.21) can be written as

$$\begin{aligned} \langle f_n \circ S, f_m \rangle &= \int_X f_n(S(x)) \cdot f_m(x) dx \\ &= \int_{\Omega_m} f_n(S(x)) dx \\ &\approx \sum_{\ell=1}^L w_\ell^{(m)} f_n(S(x_\ell)) \end{aligned} \quad (4.22)$$

In the last line, we approximated the integral with the weighted summation of  $f_n(S(x_\ell))$  over  $L$  nodes in  $\Omega_m$  which is chosen by the midpoint rule.

If we set the same weight  $w^{(m)} = w_\ell^{(m)}$  at all nodes  $\{x_\ell\}_{\ell=1}^L$  in  $\Omega_m$ , then we can simplify the above form as

$$\begin{aligned} \langle f_n \circ S, f_m \rangle &\approx \sum_{\ell=1}^L w_\ell^{(m)} f_n(S(x_\ell)) \\ &= w^{(m)} \cdot \#\{\ell \mid S(x_\ell) \in \Omega_n\} \\ &= |\Omega_m| \cdot \frac{\#\{\ell \mid S(x_\ell) \in \Omega_n\}}{L}, \end{aligned} \quad (4.23)$$

where  $|\Omega_m|$  is the measure of  $\Omega_m$ . In the last equation, we used

$$|\Omega_m| = \int_{\Omega_m} dx = \sum_{\ell \text{ s.t. } x_\ell \in \Omega_m} w_\ell^{(m)} = \#\{\ell \mid x_\ell \in \Omega_m\} \cdot w^{(m)} = L \cdot w^{(m)}.$$

The matrix in the left hand side of (4.21) becomes

$$\begin{aligned}
 \langle f_n, f_m \rangle &= \int_{\Omega} f_n(x) \cdot f_m(x) dx \\
 &= \int_{\Omega_n} f_n(x) dx \\
 &\approx \sum_{\ell=1}^L w_{\ell}^{(m)} f_n(x_{\ell}) \\
 &= w^{(m)} \cdot \#\{\ell \mid x_{\ell} \in \Omega_n\} \\
 &= \begin{cases} |\Omega_n| & \text{if } n = m \\ 0 & \text{otherwise.} \end{cases}
 \end{aligned}$$

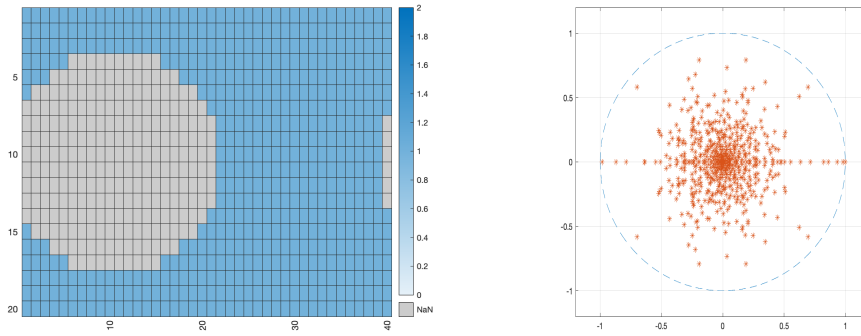
We call the matrix eigenvalue problem (4.21) approximated in the above way the discretized Koopman eigenvalue problem.

We now set  $X = [0, 2\pi) \times [C_{min}, C_{max}]$  and  $X \ni x = (g, C)$  and let  $S$  be the Boltzmann's billiard mapping computed in Section 4.3 and consider the approximated eigenvalue problem of the corresponding Koopman operator.

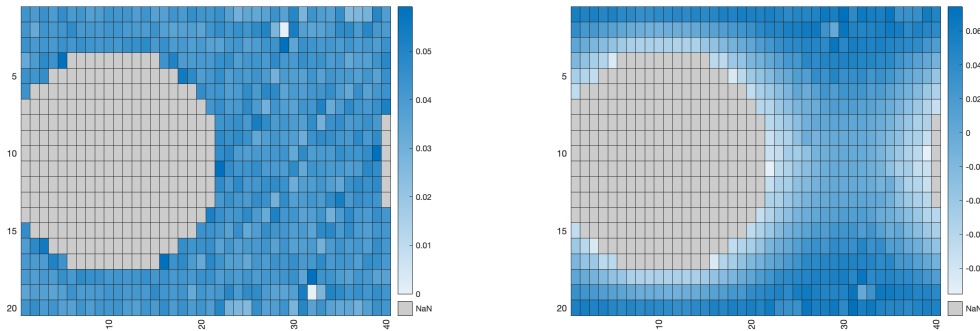
In the following numerical computations, we divided the  $(g, C)$ -coordinate space  $[0, 2\pi) \times [C_{min}, C_{max}]$  into  $N = 800$  partial sets. The number  $L = 25$  represents the number of the test nodes in each section used to approximate integrals, which appear in the equations (4.22) and (4.23). We note that the billiard mapping  $S$  is not defined on the whole space  $[0, 2\pi) \times [C_{min}, C_{max}]$ , therefore we need to restrict the divided space into the subset of all partitions where the corresponding orbits of the underlying mechanical system have at least two intersection points with the reflection wall  $y = \gamma$  so that the reflection occurs at the wall. In our computations, we set  $\alpha = 4.0, E = -0.5, \gamma = 0.5$ , and vary the parameter  $\beta$ .

In Figure 4.9, Subfig. a shows the restricted region in a divided space  $[0, 2\pi) \times [C_{min}, C_{max}]$  where the billiard mapping is well-defined for  $\alpha = 4.0, \beta = 0.0$ , and Subfig. b shows the all eigenvalues of the discretized Koopman eigenvalue problem, Subfig. c,d,e, and f show the level sets of all independent eigenfunctions (taking multiplicity also into account) corresponding to the three closest eigenvalues from 1. Figure. 4.10, Figure. 4.11 and Figure. 4.12 show the same information on the discretized Koopman eigenvalue problem as Figure. 4.9 but for the different parameter setting  $\beta = 0.5, \beta = 2.4$ , and  $\beta = 2.6$ , respectively.

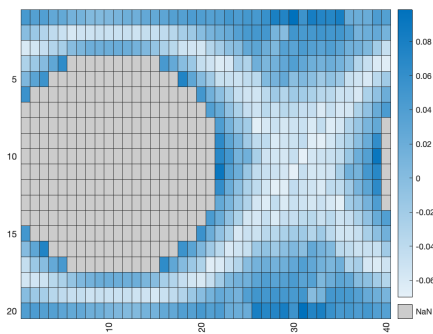
**Galerkin method and Gauss-Legendre quadrature** The Gauss-Legendre quadrature approximates the integral of the function  $f$  in the domain  $[-1, 1]$



a. Allowed regions (in blue) in  $[0, 2\pi) \times [C_{min}, C_{max}]$  b. All Eigenvalues

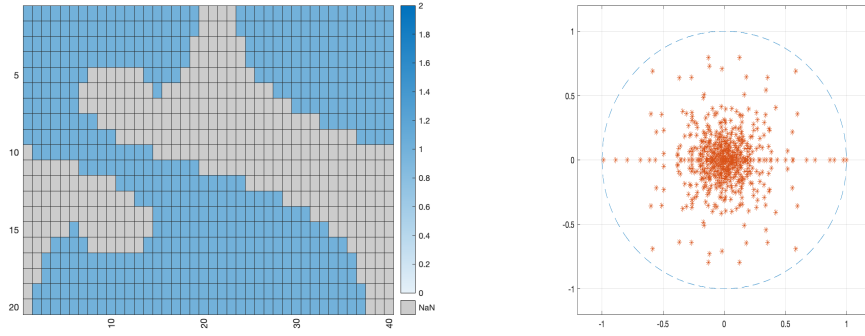


c. Eigenfunction for eigenvalue 1.00 d. Eigenfunction for eigenvalue 0.98

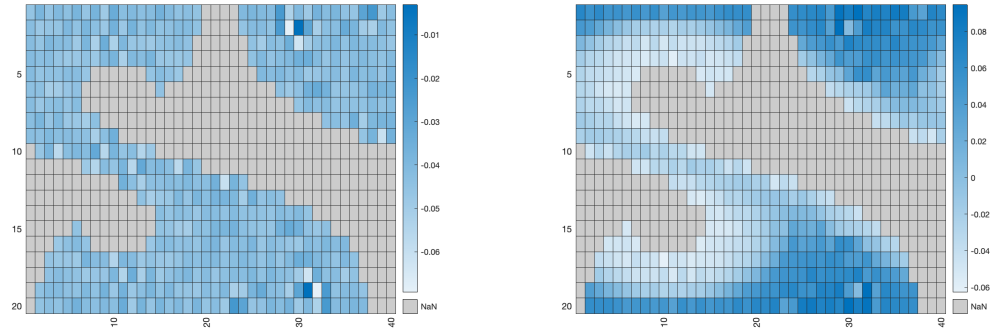


e. Eigenfunction for eigenvalue 0.93

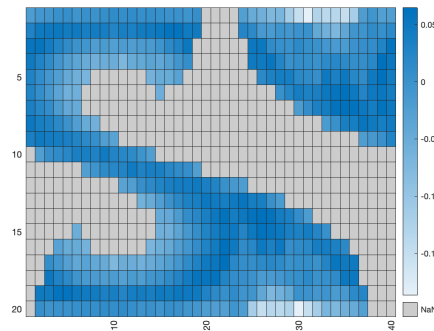
Figure 4.9: Allowed regions in  $(g, C)$ -coordinates space  $[0, 2\pi) \times [C_{min}, C_{max}]$ . Eigenvalues and eigenfunctions of approximated Koopman operator for  $\alpha = 4.0, \beta = 0.0, N = 800, L = 25$ , uniform weights.



a. Allowed regions (in blue) in  $[0, 2\pi) \times [C_{min}, C_{max}]$  b. All eigenvalues

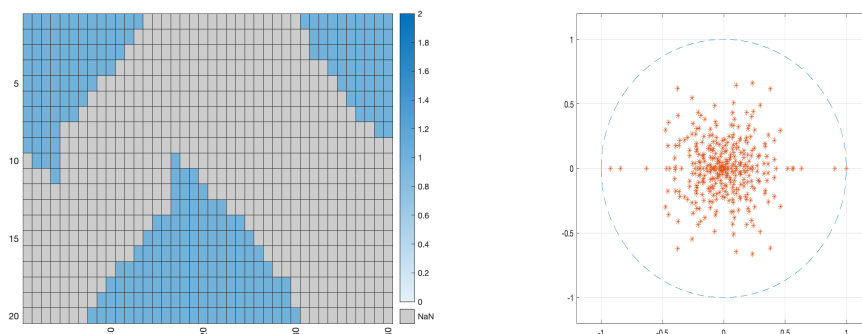


c. Eigenfunction for eigenvalue 1.00 d. Eigenfunction for eigenvalue 0.98

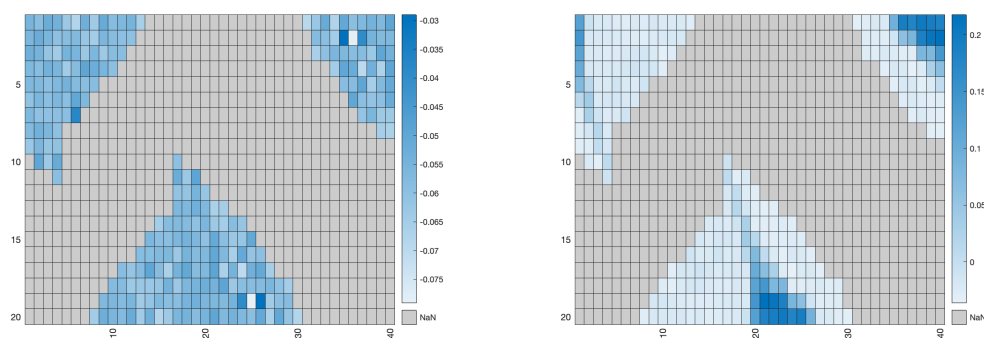


e. Eigenfunction for eigenvalue 0.90

Figure 4.10: Allowed regions in  $(g, C)$ -coordinates space  $[0, 2\pi) \times [C_{min}, C_{max}]$ . Eigenvalues and eigenfunctions of approximated Koopman operator for  $\alpha = 4.0, \beta = 0.5, N = 800, L = 25$ , uniform weights.

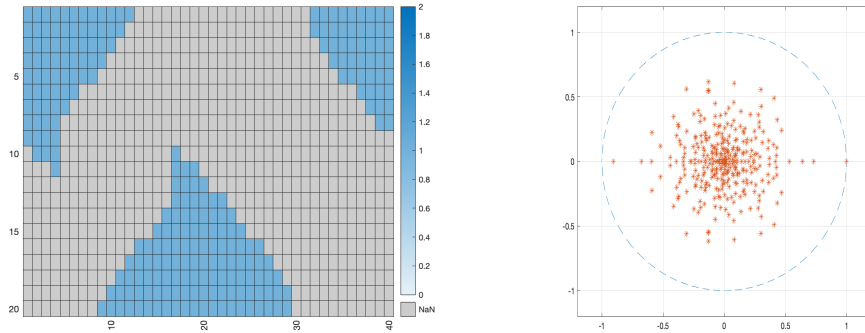


a. Allowed regions (in blue) in  $[0, 2\pi) \times [C_{min}, C_{max}]$  b. All eigenvalues

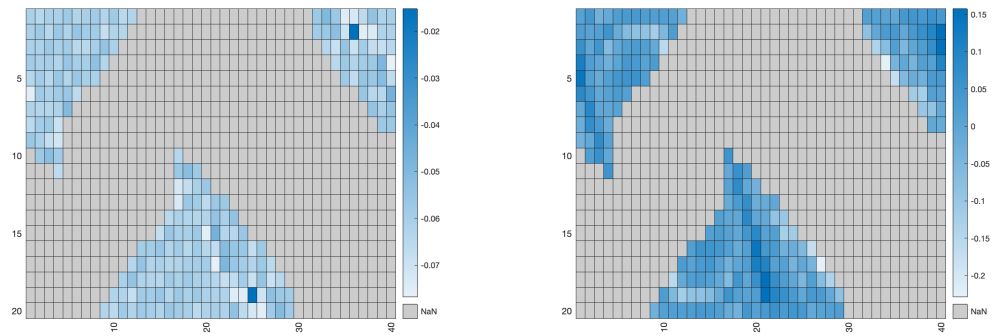


c. Eigenfunction for eigenvalue 1.00 d. Eigenfunction for eigenvalue 0.91

Figure 4.11: Allowed regions in  $(g, C)$ -coordinates space  $[0, 2\pi) \times [C_{min}, C_{max}]$ . Eigenvalues and eigenfunctions of approximated Koopman operator for  $\alpha = 4.0, \beta = 2.4, N = 800, L = 25$ , uniform weights.



a. Allowed regions (in blue) in  $[0, 2\pi) \times [C_{min}, C_{max}]$  b. All eigenvalues



c. Eigenfunction for eigenvalue 1.00 e. Eigenfunction for eigenvalue 0.73

Figure 4.12: Allowed regions in  $(g, C)$ -coordinates space  $[0, 2\pi) \times [C_{min}, C_{max}]$ . Eigenvalues and eigenfunctions of approximated Koopman operator for  $\alpha = 4.0, \beta = 2.6, N = 800, L = 25$ , uniform weights.

with the sum of the values of the function at the Gauss points  $\{x_k\}$ , with the appropriate weights  $\{w_k\}$ , as

$$\int_{-1}^1 f(x)dx \approx \sum_{k=1}^K w_k f(x_k).$$

The Gauss node points can be defined as the roots of Legendre polynomials

$$P_K(x) = \frac{1}{2^K K!} \frac{d^K}{dx^K} (x^2 - 1)^K,$$

and the weights are obtained as follows:

$$w_k = \frac{2}{(1 - x_k^2)[P'_K(x_k)]^2}.$$

The Gauss-Legendre quadrature can be extended to integration over surface:

$$\int_{-1}^1 \int_{-1}^1 f(x, y) dx_1 dx_2 \approx \sum_{k_1=1}^K \sum_{k_2=1}^K w_{k_1 k_2} f(x_k, x_l),$$

where  $w_{k_1 k_2} = w_{k_1} w_{k_2}$ . In this way, we approximate each entry of the matrices in (4.21), then we get

$$\begin{aligned} \langle f_n \circ S, f_m \rangle &= \int_X f_n(S(x)) \cdot f_m(x) dx \\ &= \int_{\Omega_m} f_n(S(x)) dx \\ &\approx \sum_{k_1=1}^K \sum_{k_2=1}^K w_{k_1 k_2}^{(m)} f_n(S(x_{k_1 k_2})) \\ &= \sum_{\ell=1}^{L=K \times K} w_\ell^{(m)} f_n(S(x_\ell)) \\ &= \sum_{\ell \text{ s.t. } S(x_\ell) \in \Omega_n} w_\ell^{(m)}, \end{aligned} \tag{4.24}$$

and

$$\begin{aligned}
\langle f_n, f_m \rangle &= \int_X f_n(x) \cdot f_m(x) dx \\
&= \int_{\Omega_m} f_n(x) dx \\
&\approx \sum_{\ell=1}^L w_\ell^{(m)} f_n(x_\ell) \\
&= \sum_{\ell \text{ s.t. } x_\ell \in \Omega_n} w_\ell^{(m)}.
\end{aligned} \tag{4.25}$$

Remember that  $f_n(x_\ell) = 1$  if  $x_\ell \in \Omega_n$  and  $f_n(x_\ell) = 0$  otherwise.

We again set  $X = [0, 2\pi) \times [C_{min}, C_{max}]$  and  $x = (g, C)$  and consider the approximated eigenvalue problem of the corresponding Koopman operator with the Galerkin method using Gauss-Legendre quadrature.

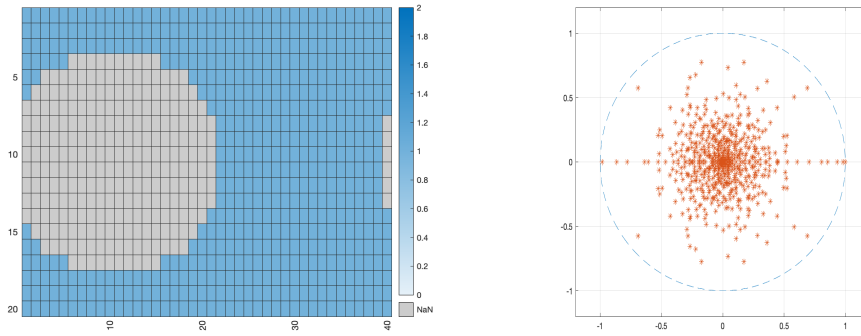
In the following numerical computations, we divided the  $(g, C)$ -coordinate space  $[0, 2\pi) \times [C_{min}, C_{max}]$  into  $N = 800$  partial sets. Recall that we need to restrict the space  $[0, 2\pi) \times [C_{min}, C_{max}]$  into the subset where the billiard mapping is well-defined. In our computations, we set  $\alpha = 4.0, E = -0.5, \gamma = 0.5$ , and vary the parameter  $\beta$ . The number  $L = 25$  represents the number of Gauss nodes in each partition used to approximate integrals, which appear in the equations (4.24) and (4.25).

In the following figures, we illustrate the numerical results on the discretized eigenvalue problem (4.21) approximated by Galerkin method with Gauss-Legendre quadrature as is described above.

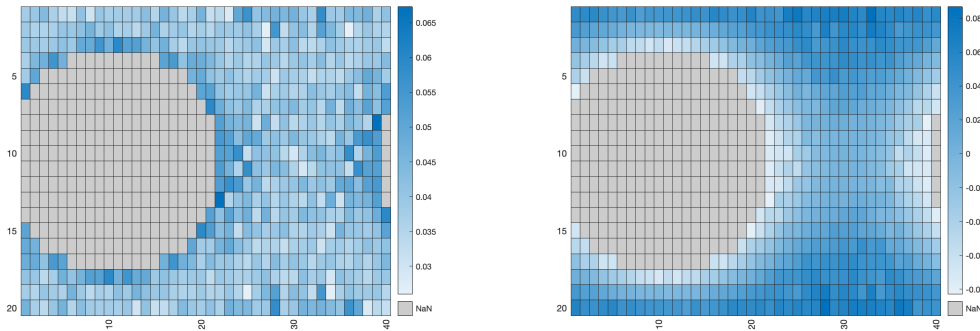
In Figure 4.13, Subfig. a shows the restricted region in a divided phase space  $[0, 2\pi) \times [C_{min}, C_{max}]$  ( $N = 800$ ) where the billiard mapping is well-defined for  $\alpha = 4.0, \beta = 0.0$ , and Subfig. b shows the all eigenvalues of the discretized Koopman eigenvalue problem, Subfig. c,d,e, and f show the level sets of all independent eigenfunctions corresponding to the three closest eigenvalues from 1. Figure 4.14, Figure 4.15 and Figure 4.16 show the same information on the discretized Koopman eigenvalue problem as Figure 4.13 but for different parameter values  $\beta = 0.5, \beta = 2.4$  and  $\beta = 2.6$ , respectively.

## 4.5.2 Discussion on Ergodicity based on Numerical Results

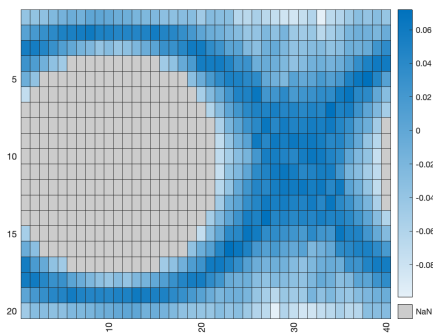
Based on the numerical results we presented, in this section, we discuss ergodicity and other dynamical properties of Boltzmann's billiard systems. For the Kepler case ( $\beta = 0$ ), as one can see in Figure 4.9 and Figure 4.13, our numerical study indicates there is large multiplicity for the eigenvalue 1. Also,



a. Allowed regions (in blue) in  $[0, 2\pi) \times [C_{min}, C_{max}]$  b. All eigenvalues

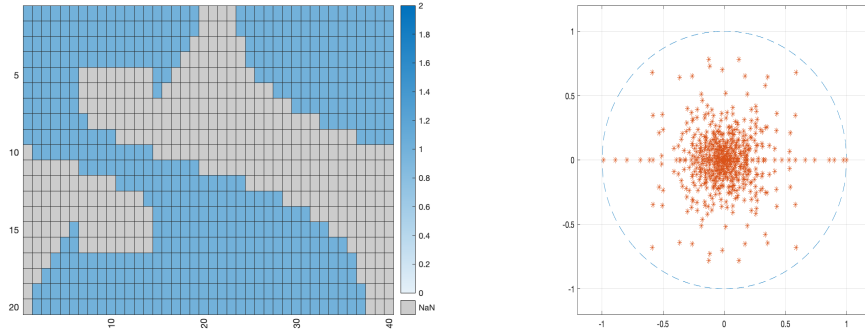


c. Eigenfunction for eigenvalue 1.00 f. Eigenfunction for eigenvalue 0.98

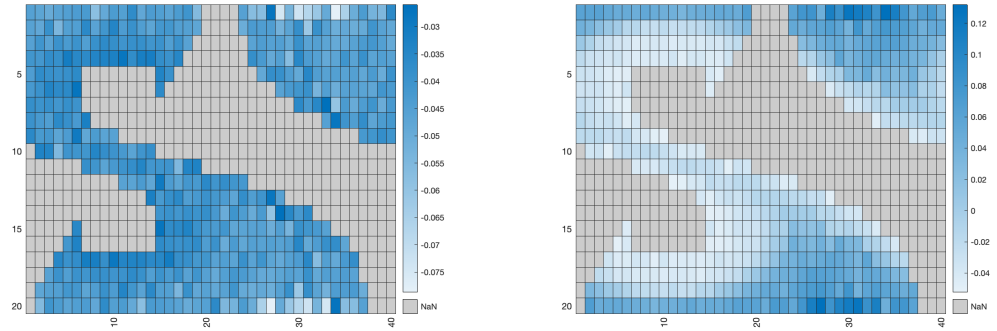


e. Eigenfunction for eigenvalue 0.93

Figure 4.13: Allowed regions in  $(g, C)$ -coordinates space  $[0, 2\pi) \times [C_{min}, C_{max}]$ . Eigenvalues and eigenfunctions of approximated Koopman operator for  $\alpha = 4.0, \beta = 0.0, N = 800, L = 25$ , Gauss-Legendre quadrature.

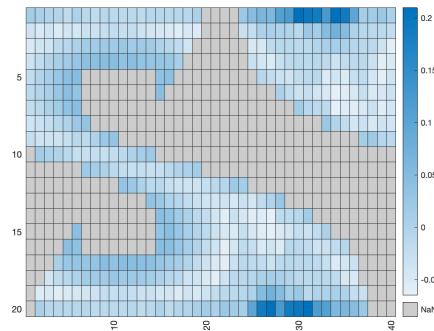


a. Allowed regions (in blue) in  $[0, 2\pi) \times [C_{min}, C_{max}]$  b. All eigenvalues



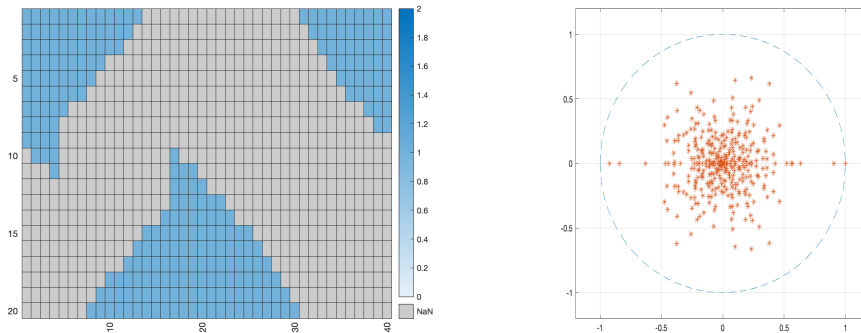
c. Eigenfunction for eigenvalue 1.00

d. Eigenfunction for eigenvalue 0.97

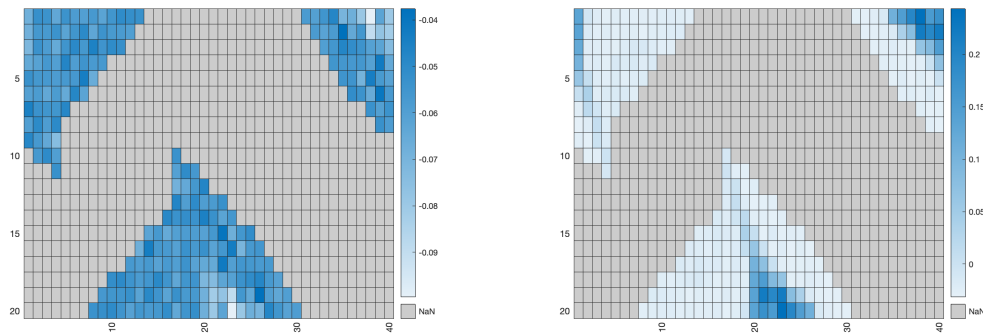


e. Eigenfunction for eigenvalue 0.90

Figure 4.14: Allowed regions in  $(g, C)$ -coordinates space  $[0, 2\pi) \times [C_{min}, C_{max}]$ . Eigenvalues and eigenfunctions of approximated Koopman operator for  $\alpha = 4.0, \beta = 0.5, N = 800, L = 25$ , Gauss-Legendre quadrature.

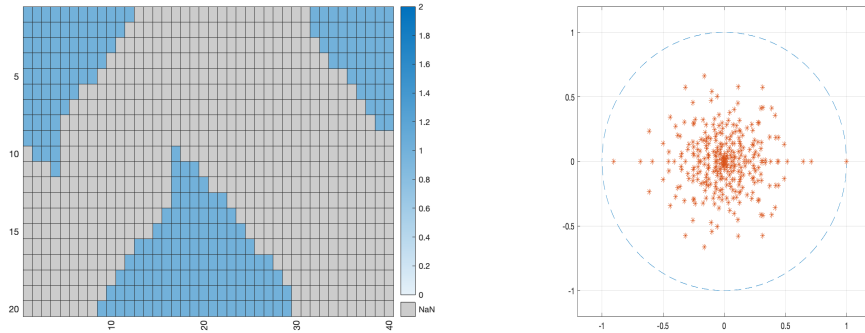


a. Allowed regions (in blue) in  $[0, 2\pi) \times [C_{min}, C_{max}]$  b. All eigenvalues

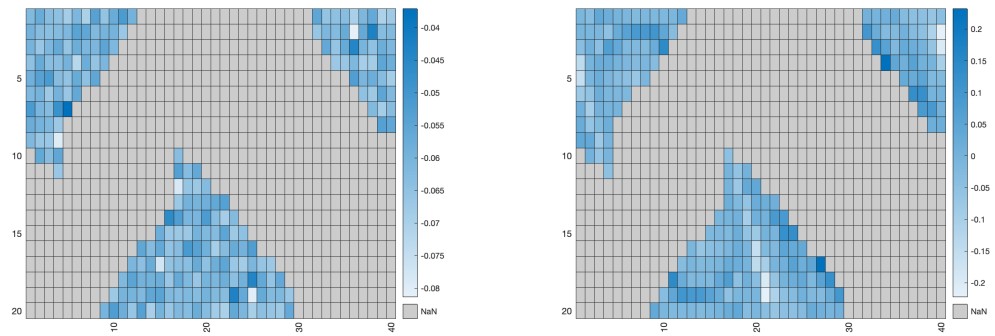


c. Eigenfunction for eigenvalue 1.00 d. Eigenfunction for eigenvalue 0.91

Figure 4.15: Allowed regions in  $(g, C)$ -coordinates space  $[0, 2\pi) \times [C_{min}, C_{max}]$ . Eigenvalues and eigenfunctions of approximated Koopman operator for  $\alpha = 4.0, \beta = 2.4, N = 800, L = 25$ , Gauss-Legendre quadrature.



a. Allowed regions (in blue) in  $[0, 2\pi) \times [C_{min}, C_{max}]$  b. All eigenvalues



c. Eigenfunction for eigenvalue 1.00 e. Eigenfunction for eigenvalue 0.71

Figure 4.16: Allowed regions in  $(g, C)$ -coordinates space  $[0, 2\pi) \times [C_{min}, C_{max}]$ . Eigenvalues and eigenfunctions of approximated Koopman operator for  $\alpha = 4.0, \beta = 2.6, N = 800, L = 25$ , Gauss-Legendre quadrature.

these figures indicate that the level sets of eigenfunctions corresponding to eigenvalue 1 or close value from 1 form each periodic trajectory as an invariant subset. These results are compatible with the integrability of the billiard system for  $\beta = 0$ , as it has been shown in [23].

For small values of  $\beta$ , our numerical results (Figure 4.10 and Figure 4.14) indicate that there is still a large multiplicity for the eigenvalue 1 and the level sets of its eigenfunctions show many invariant subsets of the system, which means the system is far from ergodic. This observation can be interpreted as the KAM stability of the integrable Boltzmann's billiard system ( $\beta = 0$ ) under the small perturbation by the additional centrifugal force  $\beta/r^2$  in a force function with  $\beta \simeq 0$ , which is again compatible with the KAM applicability shown in [19].

For large values of  $\beta$ , we can expect both chaotic behavior and regular behavior. As one can see from the level sets of eigenfunction depicted in Figure 4.11 and Figure 4.15, for  $\beta = 2.4$ , there exists small regions which are foliated by (quasi-)periodic trajectories and the left region is a large indecomposable invariant subset which is covered by a single chaotic trajectory. Our particular interest is the case  $\beta = 2.6$  Figure 4.12 and Figure 4.16, indicates the ergodicity of the system for this parameter setting as one can see the discretized eigenvalue problem has only one simple eigenvalue in the neighborhood of 1. On the other hand, this Galerkin approximation might not be able to capture the true eigenfunctions corresponding to eigenvalue 1 with high oscillation terms. This means that the system might have invariant subsets which are finely distributed in the phase space, which indeed also implies the system is *nearly* ergodic.

Based on the above observations, we make the following conjecture on the ergodicity of Boltzmann's billiard system.

**Conjecture 3.** *There exist parameter values of  $\alpha, \beta, \gamma$  such that the corresponding Boltzmann's billiard system with some fixed energy is ergodic.*



# Bibliography

- [1] A. Albouy. Projective dynamics and classical gravitation. *Regul. Chaot. Dyn.*, 13(6):525–542, 2008.
- [2] A. Albouy. There is a projective dynamics. *Eur. Math. Soc. Newsl.*, 89:37–43, 2013.
- [3] V. Arnold. *Mathematical Methods of Classical Mechanics*. Springer-Verlag, New York, 1978.
- [4] M. Bialy and A. Mironov. The Birkhoff-Poritsky conjecture for centrally-symmetric billiard tables. *arXiv:2008.03566*, to appear in *Ann. Math.*
- [5] G. Birkhoff. The restricted problem of three bodies. *Rend. Circ. Mat. Palermo*, 39:265–33, 1915.
- [6] G. Birkhoff. On the periodic motions of dynamical systems. *Acta Math.*, 50(1):359–379, 1927.
- [7] L. Boltzmann. Lösung eines mechanischen Problems. *Wiener Berichte*, 58:1035–1044, 1868. *Wissenschaftliche Abhandlungen*, 1:97–105.
- [8] L. Bunimovich. On billiards close to dispersing. *Mat. Sb.*, 136(1):49–73, 1974.
- [9] L. Bunimovich. On the ergodic properties of nowhere dispersing billiards. *Comm. Math. Phys.*, 65(3):295–312, 1979.
- [10] K. Cieliebak, U. Frauenfelder, and O. van Koert. Periodic orbits in the restricted three-body problem and Arnold’s  $J^+$ -invariant. *Regul. Chaot. Dyn.*, 22(4):408–434, 2017.
- [11] K. Cieliebak, U. Frauenfelder, and L. Zhao.  $J^+$ -invariants for planar two-center Stark-Zeeman systems. *Ergodic Theory Dynam. Systems*, 1–35, 2022.

- 
- [12] A. Cannas da Silva. *Lectures on Symplectic Geometry. Lecture Notes in Mathematics*, volume 1764. Springer-Verlag, Berlin, 2001.
- [13] R. De la Llave. A tutorial on KAM theory. *Smooth ergodic theory and its applications (Seattle, WA, 1999)*. Amer. Math. Soc., Providence, 175–292, 2001.
- [14] S. Earnshaw. *Dynamics: Or an Elementary Treatise on Motion*. J. & JJ. Deighton, Cambridge, 1832.
- [15] T. Eisner, B. Farkas, M. Haase, and R. Nagel. *Operator Theoretic Aspects of Ergodic Theory*, volume 272. Springer, Cham, 2015.
- [16] L. Euler. De motu corporis ad duo centra virium fixa attracti. *Nov. Comm. Acad. Imp. Petropolitanae*, 152–184, 1767.
- [17] Y. N. Fedorov. An ellipsoidal billiard with a quadratic potential. *Funct. Anal. Appl.*, 35(3):199–208, 2001.
- [18] J. Féjoz. Introduction to KAM theory, with a view to celestial mechanics. *Variational methods in imaging and geometric control (Radon Series on Computational and Applied Mathematics, 18)*, 2016.
- [19] G. Felder. Poncelet property and quasi-periodicity of the integrable Boltzmann system. *Lett. Math. Phys.*, 111(1):1–19, 2021.
- [20] S. Feldt and J. S. Olafsen. Inelastic gravitational billiards. *Phys. Rev. Lett.*, 94(22):224102, 2005.
- [21] A. T. Fomenko and V. V. Vedyushkina. Billiards and integrability in geometry and physics. new scope and new potential. *Moscow Univ. Math. Bull.*, 74(3):98–107, 2019.
- [22] G. Gallavotti. *Nonequilibrium and Irreversibility*. Springer, Berlin, 2014.
- [23] G. Gallavotti and I. Jauslin. A theorem on ellipses, an integrable system and a theorem of Boltzmann. *arXiv:2008.01955*, 2020.
- [24] A. A. Glutsyuk. On two-dimensional polynomially integrable billiards on surfaces of constant curvature. *Dokl. Math.*, 98(1):382–385, 2018.
- [25] A. A. Glutsyuk. On polynomially integrable Birkhoff billiards on surfaces of constant curvature. *J. Eur. Math. Soc.*, 23(3):995–1049, 2020.

- [26] E. Goursat. Les transformations isogonales en Mécanique. *Comptes Rendus des Séances de l'Académie des Sciences, Paris*, 108:446–448, 1889.
- [27] G. H. Halphen. Sur les lois de Kepler. *Bulletin de la Société Philomatique de Paris*, 7(1):89–91, 1878.
- [28] C. G. J. Jacobi. Vorlesungen über Dynamik. *Verlag von Georg Reimer, Berlin*, 1886.
- [29] V. Kaloshin and A. Sorrentino. On the local Birkhoff conjecture for convex billiards. *Ann. Math.*, 188(1):315–380, 2018.
- [30] I. F. Kobtsev. An elliptic billiard in a potential force field: classification of motions, topological analysis. *Sb. Math.*, 211(7):987, 2020.
- [31] H. J. Korsch and J. Lang. A new integrable gravitational billiard. *J. Phys. A: Math. Gen.*, 24(1):45–52, 1991.
- [32] V. V. Kozlov and D. V. Treshchëv. *Billiards. A Genetic Introduction to the Dynamics of Systems with Impacts. Translation of Mathematical Monographs*, volume 89. American Mathematical Society, Providence, 1991.
- [33] I. Kubo. Perturbed billiard systems, I. The ergodicity of the motion of a particle in a compound central field. *Nagoya Math. J.*, 61:1–57, 1976.
- [34] J. L. Lagrange. Recherches sur le mouvement d'un corps qui est attiré vers deux centres fixes, Second mémoire, VIII. *Miscellanea Taurinensia*, t. IV(1):67–121, 1766–1769. Œuvres complètes, tome 2, 67–121.
- [35] L. D. Landau and E. M. Lifshitz. *Course of Theoretical Physics, Vol. 1*. Pergamon Press, Oxford, 1976.
- [36] T. Levi-Civita. Sur la résolution qualitative du problème restreint des trois corps. *ICM report*, 1904.
- [37] T. Levi-Civita. Sur la régularisation du problème des trois corps. *Acta. Math.*, 42:204–219, 1920.
- [38] C. Maclaurin. *A treatise of fluxion*, volume 2. Ruddimans, Edinburgh, 1742.
- [39] D. Ó. Mathúna. *Integrable Systems in Celestial Mechanics*. Birkhäuser, Basel, 2008.

- [40] R. McGehee. Double collisions for a classical particle system with non-gravitational interactions. *Comm. Math. Helv.*, 56(1).
- [41] A. Nersessian and G. Pogosyan. Relation of the oscillator and Coulomb systems on spheres and pseudospheres. *Phy. Rev. A*, 63(2):020103, 2001.
- [42] D. A. Poet and R. R. W. Poet. Confocal conic billiards. *Phys. Lett. A*, 271(4):277–284, 2000.
- [43] H. Poritsky. The billiard ball problem on a table with a convex boundary—an illustrative dynamical problem. *Ann. Math.*, 51:446–470, 1950.
- [44] J. Pöschel. A lecture on the classical KAM theorem. *Proc. Symp. Pure Math.*, 69:707–732.
- [45] S. E. Pustovoitov. Topological analysis of a billiard in elliptic ring in a potential field. *Fundamentalnaya i Prikladnaya Matematika*, 22(6):201–225, 2019.
- [46] S. E. Pustovoitov. Topological analysis of a billiard bounded by confocal quadrics in a potential field. *Sb. Math.*, 212(2):211–233, 2021.
- [47] P. Serret. *Théorie Nouvelle Géométrie et Mécanique des Lignes à Double Courbure*. Mallet-Bachelier, Paris, 1860.
- [48] Y. G. Sinai. Dynamical systems with elastic reflections. Ergodic properties of dispersing billiards. *Usp. Mat. Nauk.*, 25(2):141–192, 1970.
- [49] S. Tabachnikov. Exact transverse line fields and projective billiards in a ball. *Geom. Funct. Anal. GAFA*, 7(3):594–608, 1997.
- [50] S. Tabachnikov. Introducing projective billiards. *Erg. Th. Dyn. Sys.*, 17(4):957–976, 1997.
- [51] S. Tabachnikov. Projectively equivalent metrics, exact transverse line fields and the geodesic flow on the ellipsoid. *Comment. Math. Helv.*, 74(2):306–321, 1999.
- [52] S. Tabachnikov. Ellipsoids, complete integrability and hyperbolic geometry. *Moscow Math. J.*, 2(1):183–196, 2002.
- [53] S. Tabachnikov. *Geometry and Billiards*. American Mathematical Society, Providence, 2005.
- [54] A. Takeuchi and L. Zhao. Conformal transformations and integrable mechanical billiards. *arXiv:2110.03376*, 2021.

- 
- [55] A. Takeuchi and L. Zhao. Projective integrable mechanical billiards. *arXiv:2203.12938*, 2022.
- [56] P. J. Topalov and V. S. Matveev. Geodesic equivalence and integrability. *MPIM Preprint Series*, 74, 1998.
- [57] H. Varvoglis, C. H. Vozikis, and K. Wodnar. The two fixed centers: an exceptional integrable system. *Cel. Mech. Dyn. Astron.*, 89(4):343–356, 2004.
- [58] A. P. Veselov. Confocal surfaces and integrable billiards on the sphere and in the Lobachevsky space. *J. Geom. Phys.*, 7(1):81–107, 1990.
- [59] J. Waldvogel. Quaternions for regularizing celestial mechanics: the right way. *Cel. Mech. Dyn. Astron.*, 102(1):149–162, 2008.
- [60] S. Wojciechowski. Integrable one-particle potentials related to the Neumann system and the Jacobi problem of geodesic motion on an ellipsoid. *Phys. Lett. A*, 107(3):106–111, 1985.
- [61] L. Zhao. Projective dynamics and an integrable Boltzmann billiard model. *Comm. Contem. Math.*, 2150085, 2021.



# Eidesstattliche Erklärung

Hiermit erkläre ich an Eides statt, dass ich die vorliegende Arbeit selbstständig und nur unter Zuhilfenahme der ausgewiesenen Hilfsmittel angefertigt habe. Sämtliche Stellen der Arbeit, die im Wortlaut oder dem Sinn nach anderen gedruckten oder im Internet veröffentlichten Werken entnommen sind, habe ich durch genaue Quellenangaben kenntlich gemacht.

Karlsruhe, den 21.07.2022